NORTHWESTERN UNIVERSITY

E. coli RNA helicase DbpA and its role in assembly of the large subunit of the ribosome.

A DISSERTATION

SUBMITTED TO THE GRADUATE SCHOOL

IN PARTIAL FULLFILLMENT OF THE REQUIREMENTS

for the degree

DOCTOR OF PHILOSOPHY

Field of Biochemistry, Molecular Biology and Cellular Biology

By

Lisa Marie Sharpe Elles

EVANSTON, ILLINOIS

December 2008

ABSTRACT

E. coli RNA helicase DbpA and its role in assembly

of the large subunit of the ribosome.

Lisa Marie Sharpe Elles

Assembly of the large and small subunits of the *E. coli* ribosome is a complicated process that involves transcription, processing, and modifying of the ribosomal RNA, the binding of ribosomal proteins, and the folding of the particles into complex structures. A number of ribosome assembly factors, including maturation factors, GTPases, and DEAD-box proteins, have been recently identified to associate transiently with the growing ribosome and assist assembly. Understanding the molecular mechanisms of these factors is important for understanding how ribosomes are made.

E. coli DEAD-box protein A (DbpA) is an RNA-stimulated ATPase and helicase that has been implicated in the assembly of the 50S subunit of the ribosome. Although biochemically well-characterized, the molecular function was still undefined. Therefore, in order to identify a phenotype for DbpA, eleven single-point mutations in the conserved ATPase motifs (I, II, III, and VI) were designed to disrupt function of DbpA without affecting binding to its RNA substrate. *In vitro* biochemical assays of the purified mutant proteins revealed significantly reduced ATPase and helicase activities but wild type affinities for the 23S rRNA substrate. Interestingly, only one of the eleven mutants, R331A, resulted in a slow growth phenotype that was found to be due to a decrease in functional 70S ribosomes and accumulation of an inactive

45S particle. Analysis of this 45S particle revealed that it contains incompletely processed and undermodified 23S rRNA and reduced levels of five late assembly L-proteins. These five L-proteins are located in the same region that DbpA binds to, which is consistent with the absence of a conformational rearrangement necessary for their binding at this site. In addition, 45S particles could stimulate DbpA to hydrolyze ATP nearly as well as 23S rRNA, suggesting that the DbpA binding site in the particles is accessible in contrast to mature 50S subunits, which are not able to stimulate DbpA activity. Therefore, the 45S particles accumulate due to the inactivity of the R331A mutant, although the exact stage that this occurs is still unknown. In summary, these data support the hypothesis that DbpA participates in a conformational rearrangement necessary for maturation of the 50S subunit.

ACKNOWLEDGEMENTS

Throughout my graduate career, I have been fortunate to have met so many wonderful people who helped me learn about science and grow as a person. First of all, I would like to thank my advisor, Olke Uhlenbeck for his guidance and support over the years. I have enjoyed the many stories and scientific conversations. The Uhlenbeck lab has been a great environment for education as well as fun experiences. Thank you to each of the lab members, past and present, for all the support and laughter. Especially; Jared, who always made me smile, Merideth, for always listening, Irina, for caring, Sarah, for all the fabulous intellectual conversations and common sense, and last but not least, Ivy, for being a teacher, a mentor, and a friend from the very beginning.

I am grateful for the members of my committee, Erik Sontheimer, Andreas Matouschek, and Jon Widom for their time, insight, and knowledge.

I would also like to thank Debbie Klos and Elizabeth Truesdell, my classmates, who were a source of comfort and laughter through many days. You are both wonderful people and I am lucky to have met you.

Most importantly, I would like to thank my family. It has been easier, knowing that you were always on my side and there when I needed you. Mom and dad you have always been supportive throughout everything I have done. Chris, thank you for your love, encouragement, and inspiration, I could not have made it without you!

Dedicated to my family-

Mom, Dad, Becky, Amy and Chris, you were there for me through it all!

ABBREVIATIONS

AMPPNP	Adenylyl imidodiphosphate
AMV RT	Avian myeloblastosis virus reverse transcriptase
ATP	Adenosine triphosphate
BSA	Bovine serum albumin
CTD	Carboxy terminal domain
C-terminal	Carboxy terminal
DNA	Deoxyribonucleic acid
DNase	Deoxyribonuclease
dNTP	Deoxynucleotide triphosphte
DTT	Dithiothreitol
E. coli	*Escherichia Coli*
EDTA	Ethylenediaminetetraacetic acid
ESI-TOF MS	Eelectrospray ionization time-of-flight mass spectrometry
FPLC	Fast protein liquid chromatography
HEPES	4-(2-hydroxyethyl)-1-piperazineethanesulfonic acid
IPTG	Isopropyl-beta-D-thiogalactopyranoside
mRNA	Messenger RNA
Ni-NTA	Nickel-nitrilotriacetic acid
N-terminal	Amino terminal
NTP	Nucleotide triphosphate
L-protein	Large subunit protein

PAGE	Polyacrylamide gel electrophoresis
PTC	Peptidyl transferase center
PVDF	Polyvinylidene Fluoride
r-protein	Ribosomal protein
RNase	Ribonuclease
RNA	Ribonucleic acid
RPM	Revolutions per minute
rRNA	Ribosomal RNA
RRM	RNA recognition motif
rrn	Ribosomal RNA operon
SDS	Sodium dodecyl sulfate
S-protein	Small subunit protein
TBE	Tris-borate-EDTA
TCA	Trichloroacetic acid
TE	Tris-EDTA
TLC	Thin layer chromatography
TP50	Total proteins from 50S subunits
TP30	Total proteins from 30S subunits
tRNA	Transfer RNA
v/v	Volume/volume
w/v	Weight/volume

TABLE OF CONTENTS

LIST OF TABLES

LIST OF FIGURES

CHAPTER 1

Introduction

1.1. The *E. coli* 70S ribosome

The 70S bacterial ribosome is a complex macromolecular machine consisting of two ribonucleoprotein subunits, each of which performs distinct functions in the mechanism of mRNA-encoded protein synthesis. Crystal structures of the 70S ribosome reveal that the larger 50S subunit is more structurally complex than the smaller 30S subunit (Ban et al. 2000; Schluenzen et al. 2000; Wimberly et al. 2000; Harms et al. 2001; Yusupov et al. 2001; Schuwirth et al. 2005). The overall architecture of each subunit is primarily defined by the tertiary structure of the large ribosomal RNA (rRNA) molecules, consisting of many short helices packed together in a defined manner by tertiary interactions (Figure 1.1). Several small and globular ribosomal proteins (r-proteins) are scattered about the surfaces of the subunits and sometimes extend into the interiors (Figure 1.1). In the small subunit the secondary structure of the 16S rRNA is divided into four domains which pack adjacently to each other in the tertiary structure, and comprise the 5' (body), central (platform), 3' major (head) and 3' minor domains (Figure 1.2) (Schluenzen et al. 2000; Wimberly et al. 2000; Yusupov et al. 2001). Each of the 21 small subunit proteins (S-proteins) bind to different sites on the 16S rRNA but rarely contact more than one domain (Wimberly et al. 2000; Yusupov et al. 2001). In contrast to the small subunit, the 23S and 5S rRNAs in the large subunit, form seven secondary structure domains that are highly intertwined in the tertiary structure (Figure 1.3) (Ban et al. 2000; Harms et al. 2001; Yusupov et al. 2001). This results in a single large hemispherical folded RNA domain that projects three

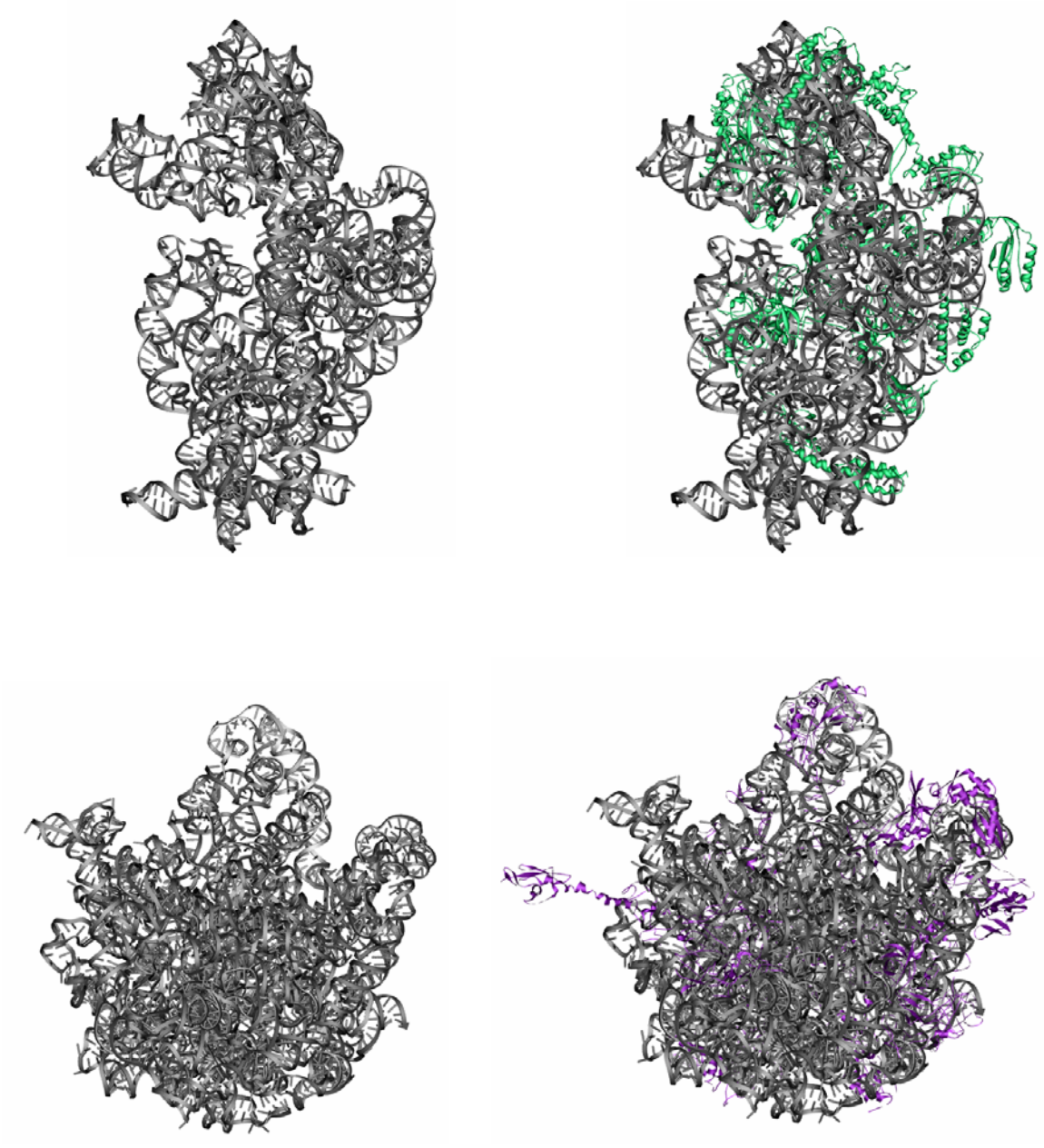

Figure 1.1 30S and 50S subunit crystal structures

30S (top) and 50S (bottom) subunits, RNA only (left) and with colored r-proteins (right). 16S, 23S and 5S rRNA is colored grey, S-proteins are green and L-proteins are purple. PDB: 2AW7 and 2AW4.

Figure 1.2 Secondary and tertiary structure of 16S rRNA

E. coli 16S rRNA secondary structure (left) and tertiary structure (right). Domains are color-coded similarly on both structures with the 5' domain (5') in blue, central domain (C) in purple, 3' major domain (3M) in red and the3' minor domain (3'm) in yellow (Yusupov et al. 2001).

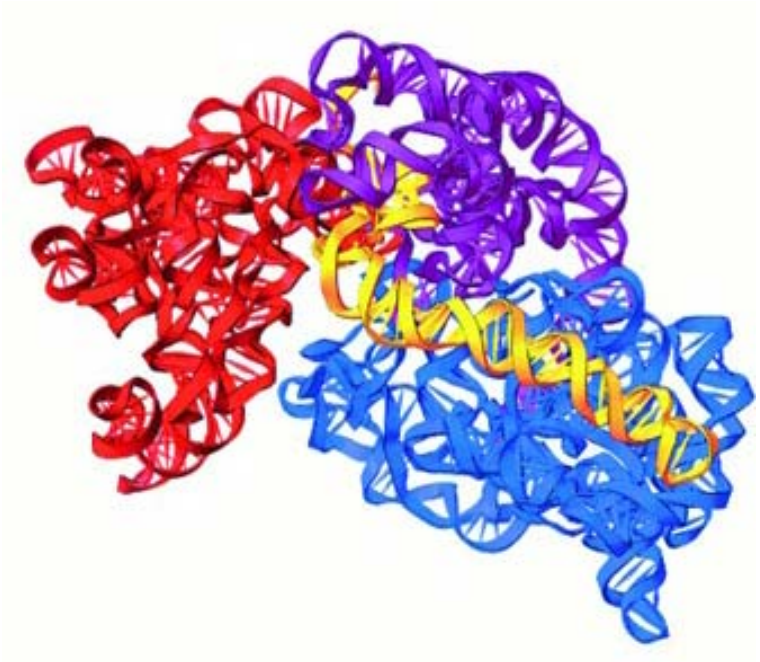

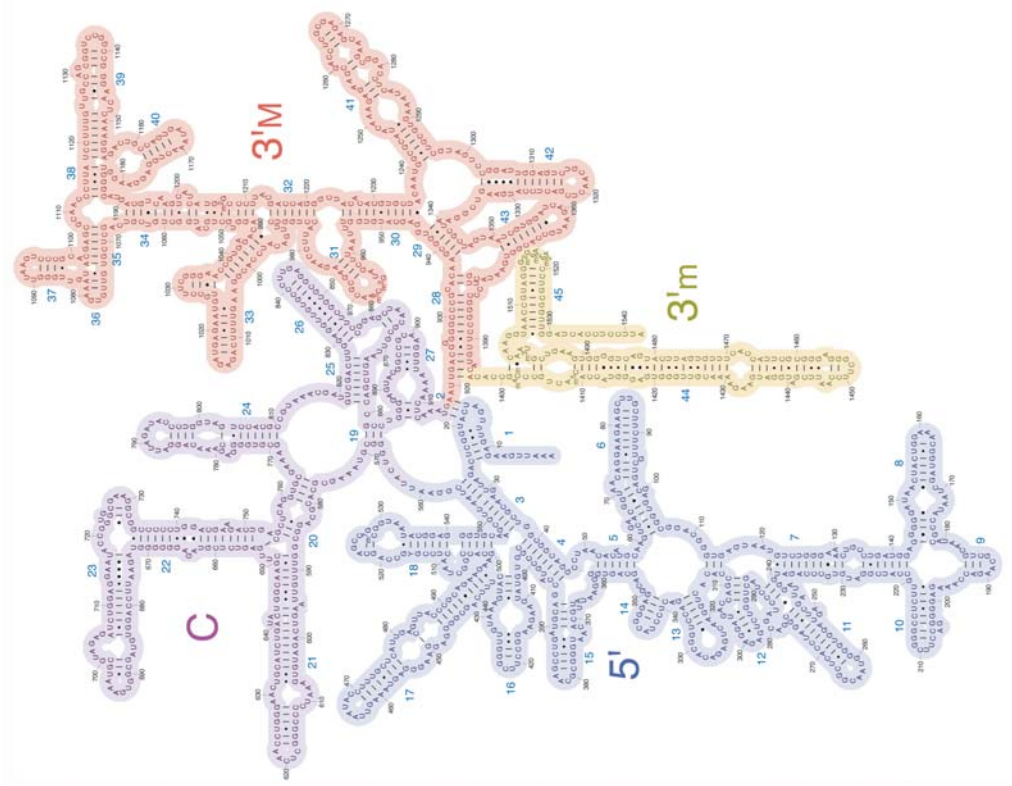
3'M
3'm
C
5'

Figure 1.3 Secondary and tertiary structure of 23S rRNA

E. coli 23S rRNA secondary structure (top) and tertiary structure (bottom). Domains are color-coded similarly on both structures (Yusupov et al. 2001).

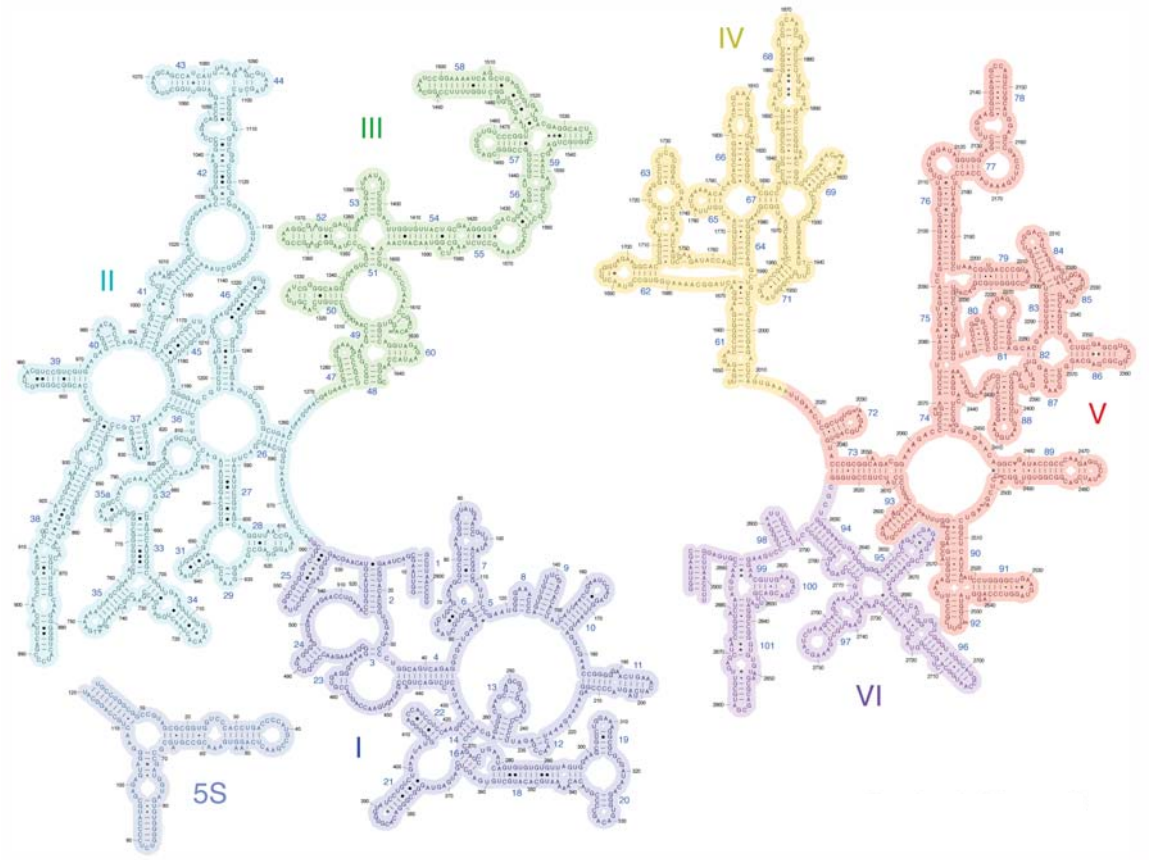
IV
III
II
V
VI
I
5S

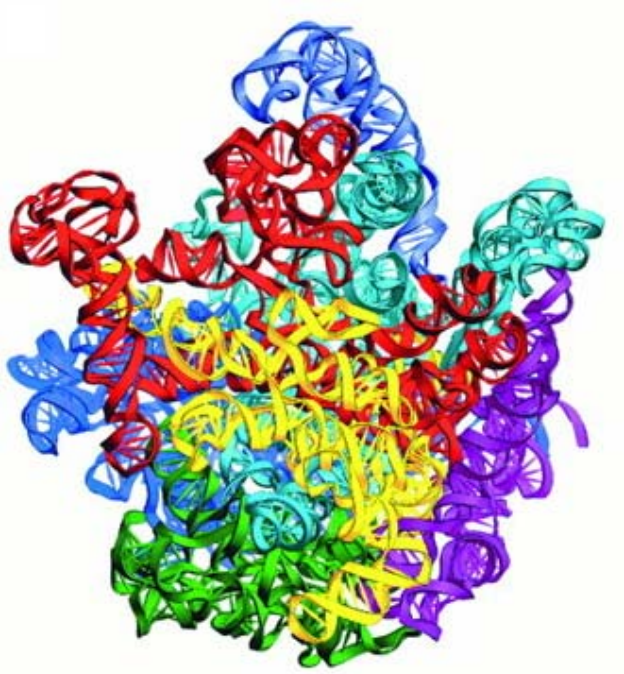

molecular stalks formed by domains II, IV, V, VI and VII (5S rRNA) (Yusupov et al. 2001). A majority of the 33 large subunit r-proteins (L-proteins) are also intricately interwoven, each making contacts with helices from more than one secondary structure rRNA domain (Ban et al. 2000). In addition to the increased size and number of components in the 50S subunit, this intertwining of the rRNA domains and the L-proteins makes the large subunit more structurally complex than the small subunit.

The intricate structure of the ribosomal subunits suggests that their synthesis and assembly must also be complex. Nevertheless, the entire assembly process is remarkably rapid, taking only about 2 minutes to form an active ribosome in logarithmically growing *E. coli* at 37 °C, which is close to the amount of time required for transcription of the entire rRNA operon (Lindahl 1975; Gotta et al. 1991). Because the cell devotes nearly 40% of its metabolic energy towards synthesizing ribosomes, the process must also be extremely accurate so that misfolded inactive ribosomes rarely form (Nierhaus 1991). This rapid and accurate assembly of such a large ribonucleoprotein is especially astonishing given the large number of components involved and the complexities of each. In addition to the proper synthesis, folding, and binding of the 54 r-proteins, the extremely large rRNA molecules must also be synthesized and folded correctly. Folding of the rRNA is thought to occur in multiple steps with the initial small hairpins and short helices forming rapidly during transcription, followed by the formation of helices between distal sequences (Weeks 1997). The resulting secondary structure then rapidly collapses into a more compact molecule that is a mixture of conformations. The rRNA then slowly rearranges during the formation of multiple tertiary interactions that position the helices in their unique final arrangement. Binding of r-proteins can occur throughout this process and may help guide the rRNA folding to its native conformation (Moazed et al. 1986; Talkington et al. 2005). It is likely

that the folding of a molecule as large as rRNA does not occur in a single pathway, but is best described as a set of parallel pathways with multiple transient intermediates (Pan et al. 1997). The stable folding intermediates that form can differ substantially from the final structure and present kinetic barriers that must be resolved to further proceed along the folding pathway (Talkington et al. 2005). It has been proposed that different kinds of RNA chaperones participate in the folding pathway possibly by resolving these misfolded structures and thus allowing assembly to proceed (Herschlag 1995; Woodson 2000). Therefore, ribosome assembly can generally be described as an assembly landscape, which involves a series of rRNA conformational changes and r-protein binding events (Talkington et al. 2005; Williamson 2005).

An illustration of some of the challenges in understanding ribosome assembly concerns a region of the peptidyl transferase center (PTC) which is depicted in Figure 1.4. In the PTC, protein L16 makes contacts with helices 38, 39, 42, 43, and 44 from domain II, helix 89 from domain V and helix 4 from 5S rRNA (Nishimura et al. 2004). As seen in Figure 1.4, L16 binds to these rRNA helices and holds them together in the correct conformation within the 50S subunit, acting as "molecular glue" (Nishimura et al. 2004). Association of L16 during assembly must be a complex process because domain II is transcribed well before domain V and 5S rRNA is not transcribed until 23S rRNA is complete. This leads to several questions about how this region is formed. When do the helices in domain II contact domain V and 5S rRNA? When does L16 bind during assembly of this region of the rRNA? Is L16 responsible for the arrangement of these rRNA helices or is the binding site arranged prior to L16 binding? As depicted by the intricacies of L16 binding within this small region of the 50S subunit, it is clear that rRNA folding and ribosome assembly is a complex process that relies on the coordination of multiple sequential steps.

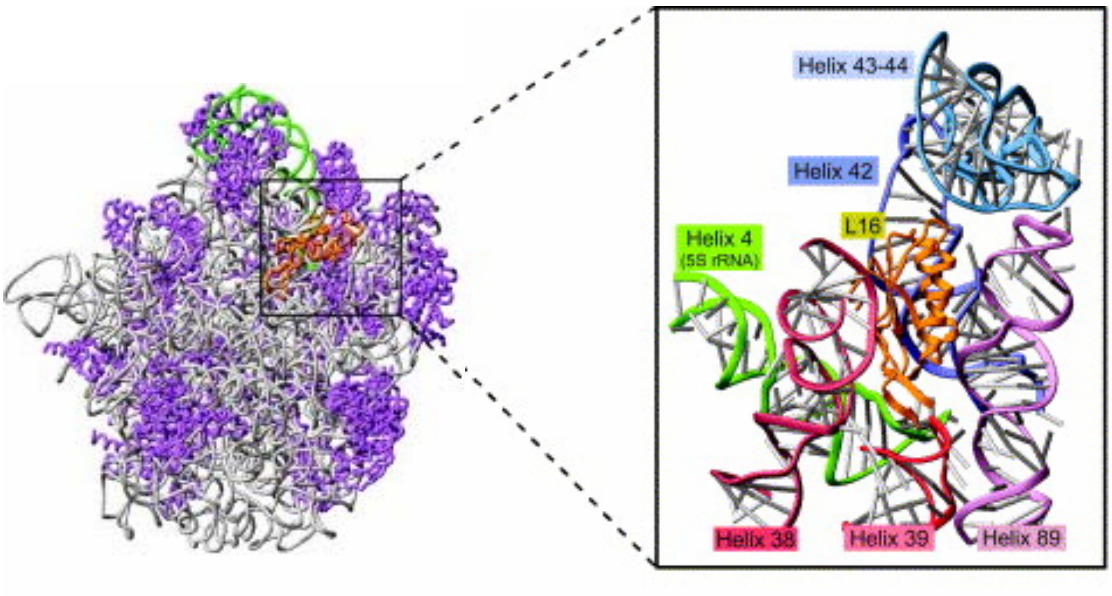

Figure 1.4 Close-up of the L16 binding site

A close-up view of the L16 binding site in the 50S subunit crystal structure in which L16 contacts helices from domain II, domain V, and 5S rRNA (Nishimura et al. 2004).

This chapter reviews what is known about the process of bacterial ribosome assembly. Because 30S subunit assembly has been studied in much greater detail and is the subject of recent reviews (Culver 2003; Williamson 2005), the focus here is the assembly of the 50S subunit. Ribosome biogenesis *in vivo* proceeds via the assembly gradient, which involves the coupling of rRNA transcription, cleavage of the rRNA at specific sites (termed processing), covalent modification of individual nucleotides, folding of the rRNA and the sequential association of r-proteins (Spillmann et al. 1977). Biochemists have determined *in vitro* reconstitution protocols, which involve long incubations of fully processed and modified rRNA with total r-proteins in non-physiological buffers and at elevated temperatures, which are required in order to obtain fully active 30S subunits and partially active 50S subunits (Traub and Nomura 1968; Nierhaus and Dohme 1974). Although there are significant differences between *in vivo* and *in vitro* assembly, precursor particles identified in biogenesis and intermediates formed during reconstitution have similar sedimentation values and r-protein composition (Homann and Nierhaus 1971; Dohme and Nierhaus 1976). Therefore, reconstitution experiments have been useful in determining rRNA folding intermediates and the order of r-protein binding. Recently, several non-ribosomal proteins that do not covalently modify the rRNA have been identified as factors that assist ribosome assembly *in vivo*. Although in most cases the exact role of these assembly factors is unknown, a likely possibility is that they transiently stabilize or rearrange rRNA structures. One of the factors of particular interest to this thesis is the DEAD-box protein, DbpA which binds to and is stimulated by a specific hairpin of 23S rRNA.

1.2. Ribosomal RNA transcription and cleavage

Ribosome biogenesis begins with the initiation of rRNA transcription from seven nearly identical operons found in the *E. coli* genome (Srivastava and Schlessinger 1990). Each operon named, *rrnA, B, C, D, E, G, or H* has a similar arrangement, beginning with two promoters located upstream of the gene for 16S rRNA followed by the 23S rRNA gene and one or two copies of the 5S rRNA gene (Figure 1.5). The seven operons differ from one another in the number and type of tRNA genes located in the spacer regions between the 16S and 23S genes and following the 5S gene (Srivastava and Schlessinger 1990) (Figure 1.5). Processing of the rRNA involves different endo- or exoribonucleases which cleave at various sites in the extra sequences surrounding the mature 16S, 23S and 5S rRNA. Initial cleavages are made by RNase III which recognizes double stranded stems that form between residues flanking both the mature 16S and 23S rRNA genes (Figure 1.6) (Dunn and Studier 1973; Young and Steitz 1978; Bram et al. 1980; King et al. 1984). Once cleaved by RNase III, the pre-16S rRNA (17S rRNA) contains an additional 115 nucleotides at the 5' end and 33 nucleotides at the 3'end and the pre-5S rRNA (9S) has 85 extra nucleotides at the 5' end and a 3' end that extends to the operon terminator site (Figure 1.6) (Young and Steitz 1978; Singh and Apirion 1982; Roy et al. 1983). RNase III makes several cuts in pre-23S rRNA resulting in molecules that are 3 or 7 nucleotides longer at the 5' end and 7 or 9 nucleotides longer at the 3' end, (Figure 1.6) (Young and Steitz 1978; Singh and Apirion 1982; Roy et al. 1983; Sirdeshmukh and Schlessinger 1985b). Processing of the 5' end of 17S rRNA is completed by a two-step sequential cleavage involving the endoribonucleases RNase E and RNase G (Li et al. 1999b), while cleavage at the 3' end is performed by an unidentified endoribonuclease (Figure 1.6) (Hayes and Vasseur 1976; Li et al. 1999b). Mature 16S rRNA was observed in a RNase III-deficient mutant, which suggests that

RNase III cleavage is dispensable for 5' and 3' end processing of 17S rRNA (King and Schlessinger 1983; Sirdeshmukh and Schlessinger 1985b). However, in this same strain only pre-23S rRNA was formed, indicating that pre-23S processing is dependent on the initial RNase III cleavages (King et al. 1984; Sirdeshmukh and Schlessinger 1985b). After RNase III cleavage, processing at the 3' end of pre-23S rRNA can be performed by several different exoribonucleases with only RNase T making the final cleavage of residues close to the mature 3' end (Figure 1.6) (Li et al. 1999a). Subsequent processing at the 5' end of pre-23S rRNA occurs independent of the 3' end processing but the endoribonuclease is still unknown (Sirdeshmukh and Schlessinger 1985a; Srivastava and Schlessinger 1988; Li et al. 1999a). Following RNase III cleavage, pre-5S rRNA is rapidly cleaved by the endoribonuclease RNase E at both ends and followed by RNase T cleavage at the 5' and an unknown enzyme cleavage at the 3' end producing mature 5S rRNA (Misra and Apirion 1979; Roy et al. 1983; Li and Deutscher 1995).

Processing of the rRNA begins before transcription is complete, continues throughout transcription and is finalized on the mature translating ribosome. The complete 30S transcript is not observed in wild type cells and even in RNase III deficient mutant strains it is short-lived (Nikolaev et al. 1973), demonstrating that RNase III cleavage is rapid. Although these initial RNase III cleavage events occur early in assembly, the final rRNA maturation events are presumed to happen later. Consistent with this, pre-16S and pre-23S sequences have been observed in mature subunits and polysomes (Mangiarotti et al. 1974; Dahlberg et al. 1978; Sirdeshmukh and Schlessinger 1985b). Additionally, maturation of 16S and 23S *in vitro* is more efficient under the conditions of protein synthesis and in polysomes (Dahlberg et al. 1978; Sirdeshmukh and Schlessinger 1985a; Srivastava and Schlessinger 1988; Li et al. 1999a; Li et al. 1999b). The fact that pre-23S rRNA is found and matured in polysomes is not surprising

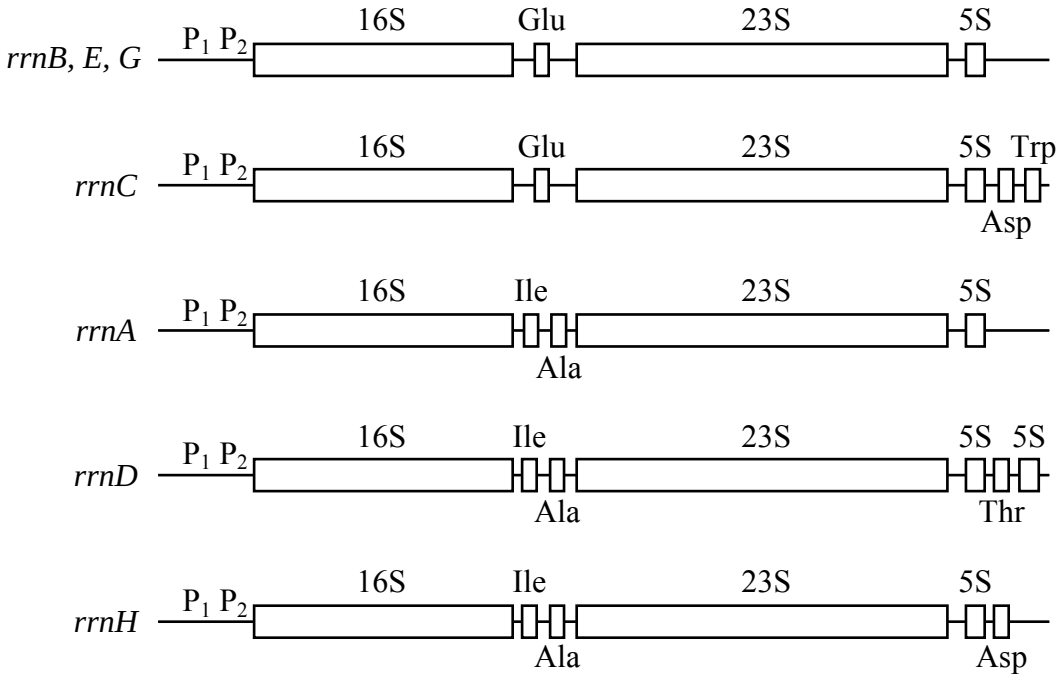

Figure 1.5 Ribosomal RNA operons

E. coli rRNA is transcribed from seven different operons (*rrn A-E, G,* and *H*) containing the genes for 16S, 23S, and 5S rRNA as well as six different tRNA genes. Figure modified from (Srivastava and Schlessinger 1990).

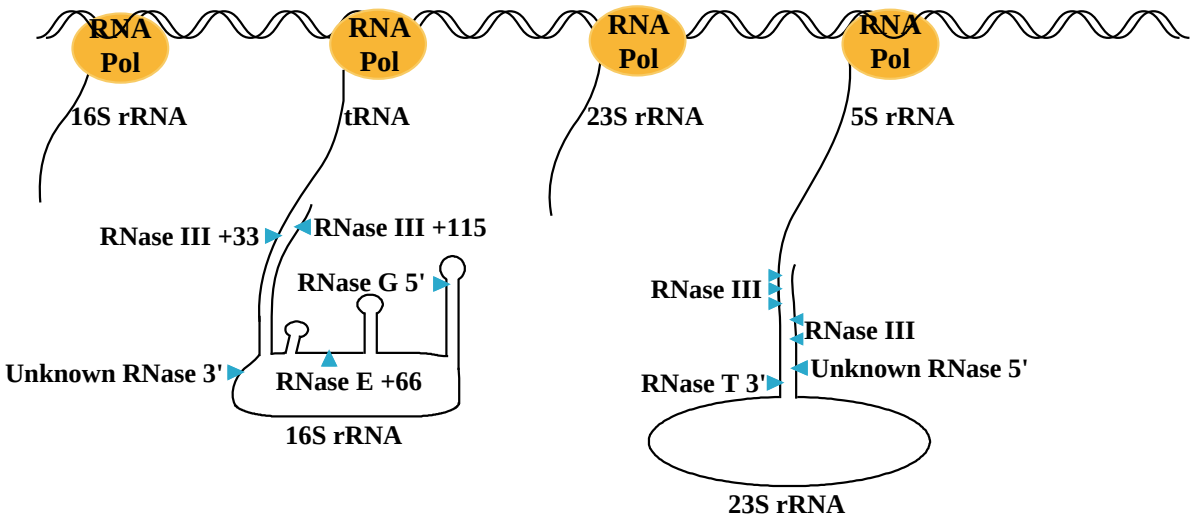

Figure 1.6 Co-transcriptional cleavage of rRNA

As the rRNA is transcribed, it is cleaved by processing enzymes at specific sites in the sequence, forming mature 16S and 23S rRNA. Figures are modified from (Li et al. 1999a; Li et al. 1999b).

because mature 23S rRNA is not required for ribosome function (King et al. 1984). In contrast, the inactivity of reconstituted ribosomes containing pre-16S rRNA demonstrates that mature 16S rRNA is required for ribosome function (Wireman and Sypherd 1974). Furthermore, crystal structures reveal that the 5' and 3' ends of 23S rRNA are base paired and not near the ribosome active site while the 16S rRNA ends are unpaired and far from each other with the 3' end anti-Shine Delgarno sequence binding to mRNA. In the absence of processing, additional base-paired nucleotides at the ends of pre-23S rRNA are not likely to disrupt activity while base-pairing of pre-16S ends could prevent mRNA binding. The identification of pre-rRNA in ribosomal subunits and observation of processing steps occurring late in ribosome assembly further demonstrates that maturation of rRNA is coupled to biogenesis.

1.3. Modified nucleotides in ribosomal RNA

As rRNA is transcribed and cleaved, specific nucleotides in 16S and 23S rRNA are covalently modified by 2'-O-methylations, conversion of uridine to pseudouridine and other base modifications (Decatur and Fournier 2002). *E. coli* ribosomes contain a total of 36 modifications, 11 in 16S rRNA and 25 in 23S rRNA. There are 10 methylations and one pseudouridine in 16S rRNA, compared with 14 methylations, 10 pseudouridines, one dihydrouridine and one unknown modification, proposed to be a 2-thiocytidine, found in 23S rRNA (Andersen et al. 2004; Ofengand and del Campo 2004). The majority of these modified nucleotides are located in the conserved regions of the rRNA and are clustered around active sites in the ribosome, specifically near the PTC, the tRNA binding sites, the decoding center, at the beginning of the exit channel and in intersubunit bridges (Figure 1.7 and 1.8) (Smith et al. 1992; Brimacombe et al. 1993; Decatur and Fournier 2002). The clustering of rRNA

Figure 1.7 Modification sites in 16S rRNA

Locations of rRNA modifications on the 16S rRNA secondary (left) and tertiary (right) structures are color-coded to represent pseudouridines (red triangles), 2'-O-methylations (green circles) and base methylations (orange squares) (Decatur and Fournier 2002).

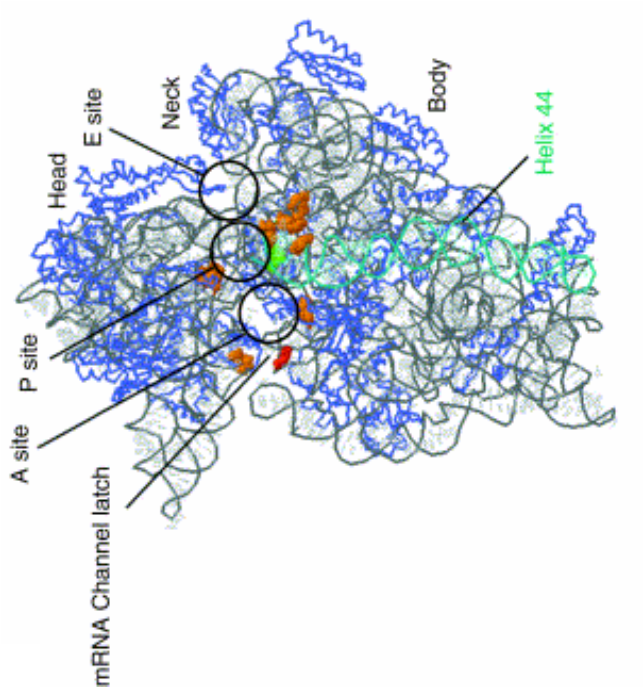
Head
E site
Neck
Body
Helix 44
P site
A site
mRNA Channel latch

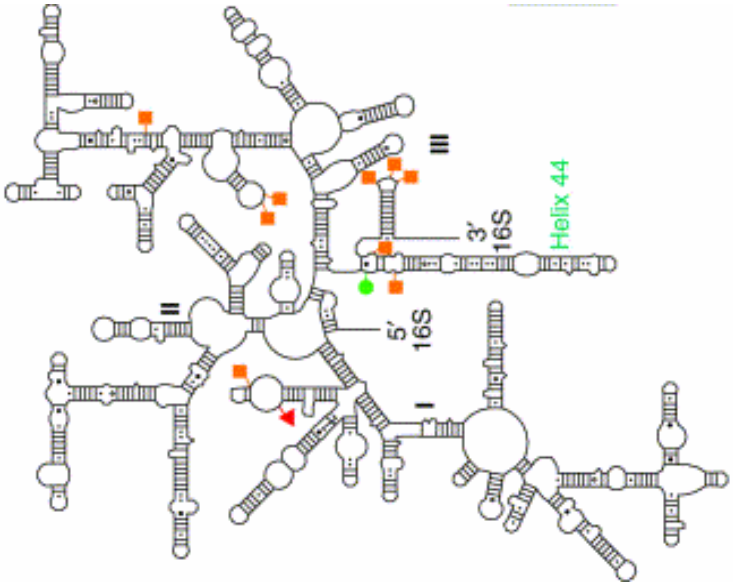
III
3'
16S
Helix 44
II
5'
16S
I

Figure 1.8 Modification sites in 23S rRNA

Locations of rRNA modifications on the 23S rRNA secondary (left) and tertiary (right) structures are color-coded to represent pseudouridines (red triangles), 2'-O-methylations (green circles), and base methylations (orange squaraes) (Decatur and Fournier 2002).

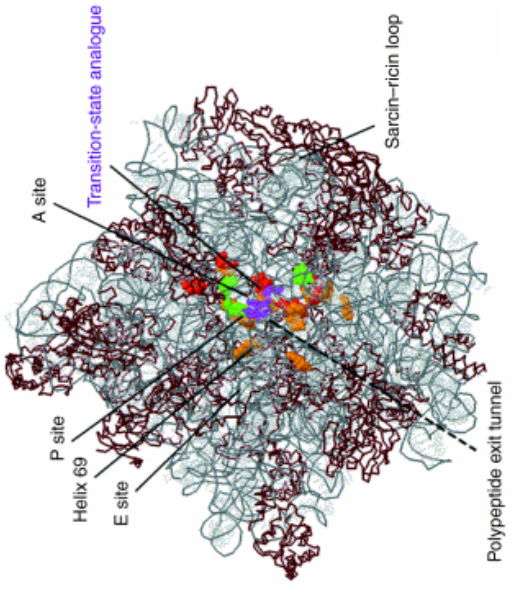
A site
Transition-state analogue
Sarcin–ricin loop
P site
Helix 69
E site
Polypeptide exit tunnel

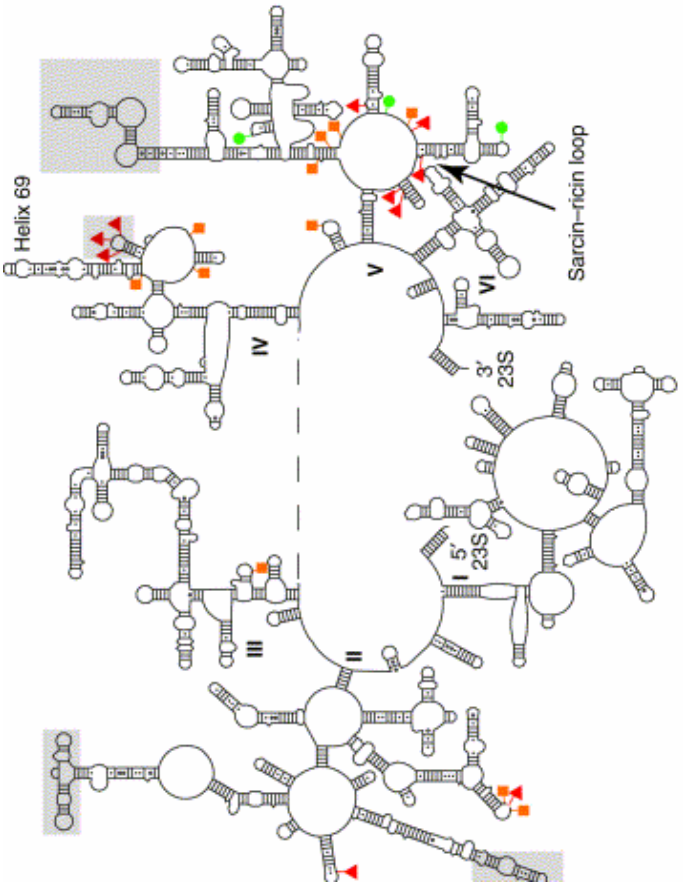
Helix 69
Sarcin–ricin loop
V
VI
IV
3' 23S
5' 23S
I
III
II

modifications near ribosomal active sites suggests that they are important for ribosomal function and may also be required for proper folding and assembly of these highly critical sites (Decatur and Fournier 2002; Ofengand and del Campo 2004).

Bacterial rRNA modifications are introduced by site-specific enzymes usually modifying a single or few nucleotides within the same region (Decatur and Fournier 2002). Seven pseudouridine synthases that make the 11 uridine modifications and a little more than half of the proposed 24 methyltransferases have been identified (Ofengand and del Campo 2004; Kaczanowska and Rydén-Aulin 2007; Wilson and Nierhaus 2007) (Table 1.1). Many of the modifying enzymes act early in assembly during transcription, while others recognize sites in preribosomal complexes formed later in assembly (Ofengand and del Campo 2004). For example, the pseudouridine synthase, RluA, and the methyltransferase, RlmD, both modify 23S rRNA transcripts *in vitro* and therefore are presumed to act early in assembly (Wrzesinski et al. 1995; Agarwalla et al. 2002) whereas the methyltransferase, RsmC, prefers reconstituted 30S subunits over 16S rRNA *in vitro*, suggesting that the modification occurs late in assembly, prior to completion of the 30S subunit (Tscherne et al. 1999). The substrates of the other known methyltransferases and pseudouridine synthases have been determined and reviewed extensively elsewhere (Ofengand and del Campo 2004; Wilson and Nierhaus 2007).

Most of the rRNA modifications are dispensable for growth *in vivo* since wild type growth rates are observed when the genes for individual modifying enzymes are deleted or mutated suggesting that they do not disrupt activity(Ofengand and del Campo 2004). There are however, at least three modifying enzymes, RluD, $RlmA^{I}$ and RrmJ, which display significant defects in growth rate and altered ribosome profiles when their genes are deleted *in vivo*. The pseudouridine synthase RluD is responsible for the conversion of three uridines to

pseudouridine, Ψ1911, m^5Ψ1915, Ψ1917 in helix 69 of 23S rRNA (Huang et al. 1998; Raychaudhuri et al. 1998). Deletion of *rluD* results in slow growth and severe ribosome profile defects that can be restored by addition of wild type RluD but not active site mutants of RluD (Raychaudhuri et al. 1998; Gutgsell et al. 2001; Gutgsell et al. 2005). This suggests that the three pseudouridines in helix 69 made by RluD are important for proper folding of 23S rRNA and assembly of the 50S subunit. RluD presumably acts late in assembly since the purified enzyme efficiently modifies 50S subunits from the deletion strains but does not modify 23S rRNA (Vaidyanathan et al. 2007). The second modifying enzyme that displays a severe growth defect when deleted is the $RlmA^I$ methyltransferase which is responsible for the methylation of G745 at position N1 in helix 35 of 23S rRNA (Gustafsson and Persson 1998). Mutants of $RlmA^I$ accumulate ribosomal subunits and produce 70S ribosomes that have decreased elongation rates (Gustafsson and Persson 1998). These defects disappeared when a plasmid encoding wild type *rlmA*^{I} was introduced to the mutant strain (Gustafsson and Persson 1998). In contrast to RluD, this methyltransferase most likely acts early in assembly since it can modify 23S rRNA transcripts *in vitro* (Hansen et al. 2001). Additionally, $RlmA^I$ can methylate any rRNA substrates that contain helicies 33, 34, and 35 only in the absence of neighboring modifications Ψ746 or m^5U747, further demonstrating that it acts early in assembly (Hansen et al. 2001). A third modifying enzyme that displays a growth defect is, RrmJ methyltransferase, which is responsible for the 2'-O-methylation of U2552 in hairpin 92 of 23S rRNA (Bügl et al. 2000; Caldas et al. 2000b). An *rrmJ* deletion strain displays severely reduced growth rates in rich and minimal media, accumulation of ribosomal subunits, and a decrease in 70S ribosomes (Bügl et al. 2000; Caldas et al. 2000b; Hager et al. 2002). On sucrose gradients run in 1 mM Mg^{2+}, the accumulated 50S subunits are separated from a 40S particle which is deficient in several late

Table 1.1 *E. coli* rRNA modifications

Site	Modification	Synthetase
16S rRNA		
516	Ψ	RsuA
527	m^7G	RsmG
966	m^2A	RsmA
967	m^5C	RsmB
1207	m^2G	RsmC
1402	m^4Cm	
1407	m^5C	RsmF
1498	m^3U	RsmE
1516	m^2G	
1518	$m^6{}_2A$	RsmA
1519	$m^6{}_2A$	RsmA
23S rRNA		
745	m^1G	$RlmA^I$
746	Ψ	RluA
747	m^5U	RumB
955	Ψ	RluC
1618	m^6A	$RlmF^a$
1835	m^2G	RlmG
1911	Ψ	RluD
1915	$m^5Ψ$	RluD
1917	Ψ	RluD
1939	m^5U	RlmD
1962	m^5C	
2030	m^6A	
2069	m^7G	
2251	Gm	RlmB
2445	m^2G	RlmL
2449	hU	
2457	Ψ	RluE
2498	Cm	
2501	s^2C*	
2503	m^2A	$RlmN^b$
2504	Ψ	RluC
2552	Um	RrmJ
2580	Ψ	RluC
2604	Ψ	RluF
2605	Ψ	RluB

Data are from (Kaczanowska and Rydén-Aulin 2007) and (Wilson and Nierhaus 2007) unless otherwise indicated. * Proposed 2-thiocytidine (Andersen et al. 2004). a; (Sergiev et al. 2008) and b; (Toh et al. 2008).

assembly proteins (Bügl et al. 2000; Hager et al. 2002). Interestingly, only 50S subunits and not the 40S particle or 23S rRNA from the deletion strain can be methylated by RrmJ *in vitro* (Bügl et al. 2000; Caldas et al. 2000a). This suggests that RrmJ acts late in assembly similar to RluD but in contrast to $RlmA^I$. As mentioned above, the function of individual modifications is not well defined and while RluD appears to be important for producing the three Ψs, the other two enzymes, $RlmA^I$ and RrmJ, may have alternative roles in assembly in addition to covalent modification rRNA as will be further described below.

1.4. Ribosomal proteins and assembly precursors

Biogenesis of the ribosomal subunits *in vivo* involves ordered binding of ribosomal proteins during the transcription, processing and folding of the rRNA. Determining the order of protein binding *in vivo* has been difficult because assembly of 30S and 50S subunits occurs rapidly and only low concentrations of precursor particles are present at a given time during growth. However, precursor particles which are similar in size and r-protein composition have been identified by several methods including pulse-labeling rRNA or r-proteins (McCarthy et al. 1962; Mangiarotti et al. 1968; Forget and Varricchio 1970; Hayes and Hayes 1971; Lindahl 1975), using zonal centrifugation to separate the small amounts of natural precursors from large quantities of ribosomes (Homann and Nierhaus 1971; Nierhaus et al. 1973), or disrupting assembly by the use of cold sensitive mutants (Guthrie et al. 1969) or antibiotics such as chloramphenicol (Osawa et al. 1969). Using these methods, two particles, $p_1$30S and $p_2$30S, were identified as precursors in small subunit assembly (Figure 1.9) (Mangiarotti et al. 1968; Osawa et al. 1969; Nierhaus et al. 1973; Lindahl 1975). The larger of the two precursors, $p_2$30S, is nearly 30S in sedimentation value and S-protein composition. While the smaller $p_1$30S

Biogenesis versus reconstitution

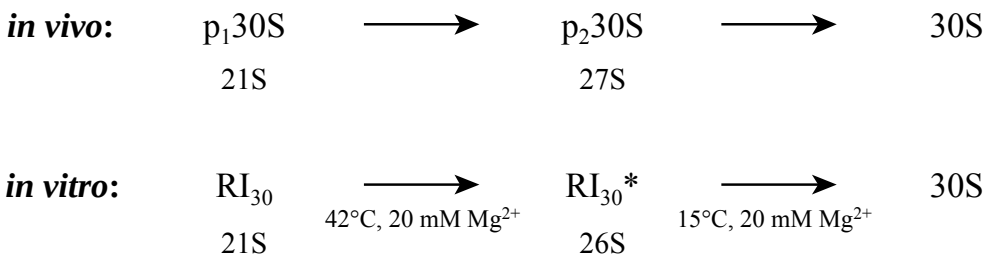

Figure 1.9 30S subunit assembly precursors and reconstitution intermediates

The *in vivo* assembly precursors and *in vitro* reconstitution intermediates of the 30S subunit (Nierhaus 1991).

sediments at 21S and is missing 11 of 21 S-proteins (Nierhaus et al. 1973; Nierhaus 1991). Those proteins present in the $p_1$30S particles are early assembly proteins and with a few exceptions are similar to the group of early S-proteins identified by r-protein pulse-labeling studies *in vivo* (Pichon et al. 1975).

Assembly of the more complex large subunit is characterized by three intermediate particles, beginning with the rapid appearance of $p_1$50S followed by $p_2$50S and $p_3$50S in succession (Figure 1.10) (Mangiarotti et al. 1968; Osawa et al. 1969; Hayes and Hayes 1971; Nierhaus et al. 1973; Lindahl 1975). The r-protein content and sedimentation values of these particles correspond to the order in which they appear, with the first, $p_1$50S, being the smallest (34S) and the last, $p_3$50S, being nearly mature with a sedimentation value of 50S and a full complement of L-proteins (Nierhaus et al. 1973; Lindahl 1975). Some of the early binding L-proteins as determined by r-protein pulse-labeling studies *in vivo* (Pichon et al. 1975) are similarly found in the first precursor, although the overall assembly order is less well correlated to the assembly order determined by examination of precursor particles (Nierhaus et al. 1973; Spillmann et al. 1977). In addition to missing proteins, the intermediate 30S and 50S particles contain rRNA that is not fully processed (Lindahl 1975) and is undermethylated (Hayes and Hayes 1971). Finding unprocessed an undermodified rRNA in partially assembled precursor particles further defines assembly as a process involving concurrent steps of transcription, cleavage, modification, folding, and protein binding.

1.5. *In vitro* reconstitution

Much of what is known about the order of ribosome assembly was determined from *in vitro* experiments in which, 30S and 50S subunits are reconstituted by combining mature rRNA

Biogenesis versus reconstitution

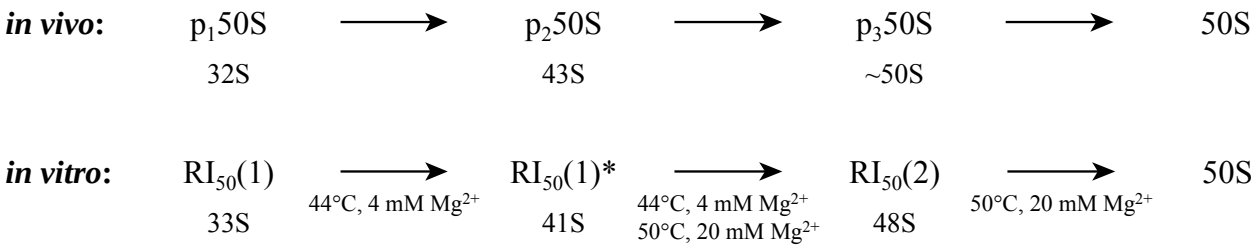

Figure 1.10 50S subunit assembly precursors and reconstitution intermediates

The *in vivo* assembly precursors and *in vitro* reconstitution intermediates of the 30S subunit (Nierhaus 1991).

and a mixture of r-proteins. Reconstitution of the 30S subunit involves the incubation of native 16S rRNA and total proteins derived from 30S subunits (TP30) in 20 mM Mg^{2+} buffer at 42 °C resulting in a particle that is nearly fully active in protein synthesis (Traub and Nomura 1969) (Figure 1.9). Active 30S subunits can also be reconstituted using unmodified 16S rRNA prepared by *in vitro* transcription (Krzyzosiak et al. 1987) and using individually purified recombinant S-proteins, underscoring the idea that all of the necessary assembly information for small subunit assembly is contained in the primary sequences of the components (Culver and Noller 1999).

An *in vitro* assembly map depicting the order of protein binding during assembly was deduced in a series of reconstitution experiments with various combinations of S-proteins (Mizushima and Nomura 1970; Held et al. 1974) (Figure 1.11A). Further confirmation and updates to the *in vitro* assembly map were made by comparing the kinetics of reconstitution by footprinting studies (Powers et al. 1993) or by mass spectrometry (Talkington et al. 2005) (Figure 1.11A and 1.11B). The 30S subunit *in vitro* assembly map as seen in Figure 1.11A depicts the general order of addition of S-proteins onto the 16S rRNA and the interdependencies of each component. The arrows at the top of the map point from the 16S rRNA to the S-proteins that bind directly to the rRNA early in assembly, while the arrows in between components indicate a strong or weak dependence on the presence of an r-protein. Pulse-chase *in vitro* reconstitution experiments monitored by quantitative mass spectrometry demonstrated that S-proteins bind 16S rRNA in an order that reflects the 5' to 3' transcription of the rRNA (Figure 1.11B) (Talkington et al. 2005; Williamson 2005). Therefore, as seen in Figure 1.11B and 1.11C, the proteins that bind early associate with the 5' minor domain and those that bind later associate with the 3' domains. During reconstitution two intermediate particles are formed, RI_{30}

Figure 1.11 30S subunit *in vitro* assembly map and S-protein binding rates

(A) The 30S subunit *in vitro* assembly map depicting the order of S-protein binding. The bar at the top represents 16S rRNA with arrows pointing to the proteins that bind early in assembly. In between proteins, arrows indicate a strong (thick arrows) or weak (thin arrows) dependence on the presence of an S-protein. The dotted box around S18 and S6 indicates that they bind as a heterodimer. All of the proteins in the large dotted box must be bound for S11 and S18/S6 to bind (Held et al. 1974). The 30S subunit *in vitro* assembly map according to S-protein binding rates (B) and their corresponding positions on the *T. thermophilus* crystal structure (C). Red, 20 to $\geq$30 min^{-1}; orange, 8.1-15 min^{-1}; green, 1.2-2.2 min^{-1}; blue, 0.38-0.73 min^{-1}; purple, 0.1-0.26 min^{-1} (Talkington et al. 2005).

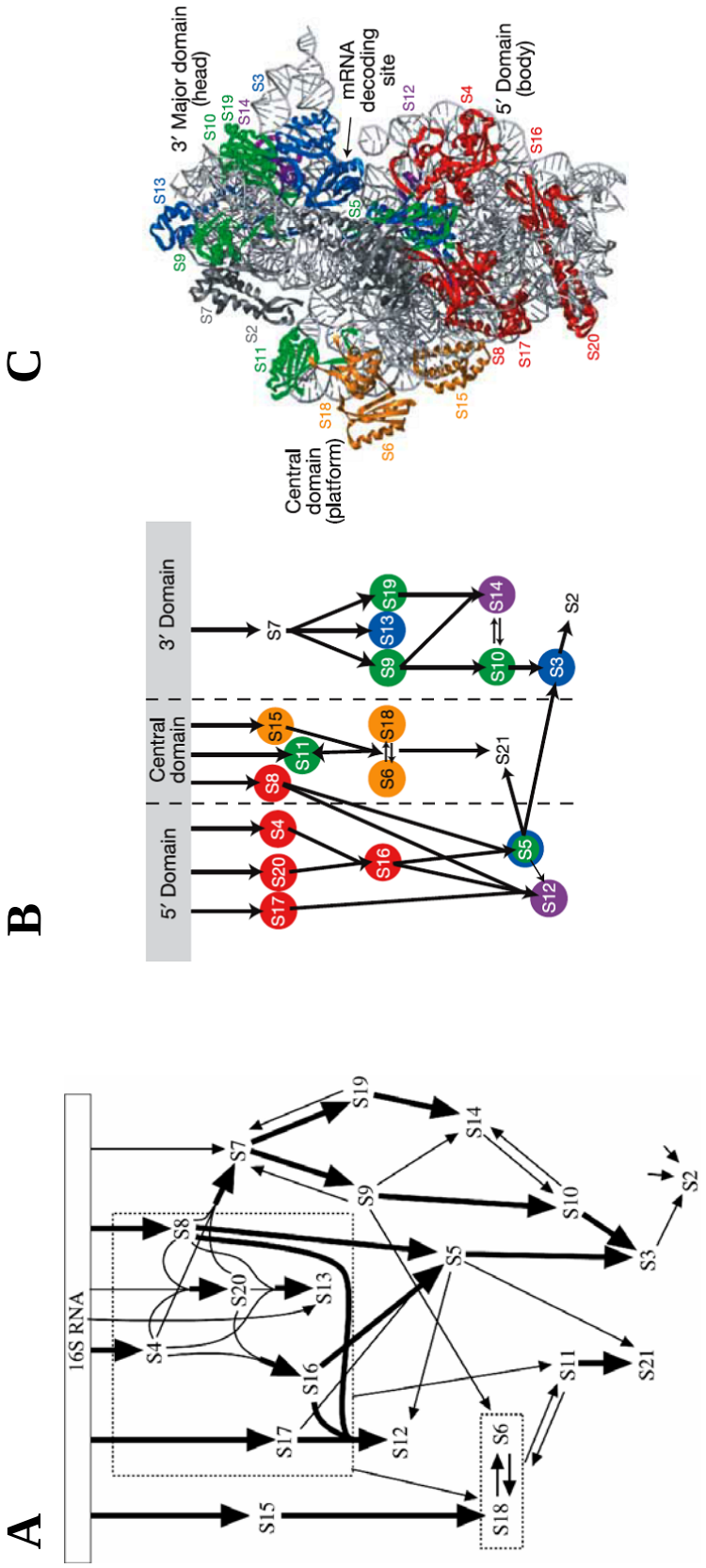
A
16S RNA
S15
S17
S4
S20
S8
S7
S19
S9
S13
S16
S12
S18
S6
S5
S14
S10
S3
S2
S11
S21
B
5′ Domain
Central domain
3′ Domain
C
3′ Major domain (head)
mRNA decoding site
5′ Domain (body)
Central domain (platform)

and RI_{30}*, which both contain the same 15 early binding S-proteins but differ in sedimentation value (21S vs. 26S) and therefore also in conformation (Traub and Nomura 1969; Homann and Nierhaus 1971; Held and Nomura 1973) (Figure 1.9). The first intermediate, RI_{30} is formed upon the incubation of 16S rRNA and S-proteins at 0 °C and can only be converted to RI_{30}* upon heat activation at 42 °C (Traub and Nomura 1969) (Figure 1.9). The conformational change that forms RI_{30}* is required before the second set of S-proteins can bind and form 30S subunits (Traub and Nomura 1969).

The structure of the large subunit of the ribosome is more complex than the small subunit and therefore, it is not surprising that it requires a more complicated *in vitro* reconstitution process. One-step reconstitution experiments similar to the 30S subunit procedure were unsuccessful in forming 50S subunits (Nierhaus and Dohme 1974). Instead, initial 50S subunit reconstitution experiments involved partial reconstitution of core particles, those that had been stripped of several L-proteins by washing the subunits at high ionic strength and then reformed using the complementary "split" L-proteins that were removed (Hosokawa et al. 1966). Eventually a two-step reconstitution procedure involving the incubation of native 23S rRNA, 5S rRNA, and the total proteins derived from 50S subunits (TP50) at two different sets of conditions was developed (Figure 1.10) (Nierhaus and Dohme 1974; Dohme and Nierhaus 1976). Reconstitution experiments have also been performed with in vitro-transcribed *E. coli* 23S rRNA. However, the particles are virtually inactive unless the rRNA contains seven of the 25 rRNA covalent modifications or specific osmolytes are added to the reaction during incubation (Green and Noller 1996; Semrad and Green 2002). The first step of the two-step reconstitution which results in a nearly complete particle, involves incubation of all components in 4 mM Mg^{2+} buffer at 44 ºC for 20 minutes and is followed by a second incubation at 50 ºC for 90 minutes in

20 mM Mg^{2+} buffer (Nierhaus and Dohme 1974). Reconstitution of 50S subunits progresses via three intermediates; $RI_{50}(1)$ which forms at 0 °C and is converted to $RI_{50}(1)$* upon heat activation at 44 °C and $RI_{50}(2)$, which is matured to 50S upon a second heat activation of 50 °C (Figure 1.10) (Dohme and Nierhaus 1976; Herold and Nierhaus 1987). As seen with 30S precursors and intermediates, the 50S subunit *in vitro* reconstitution intermediates are similar to the precursors isolated *in vivo* (Figure 1.10). Analysis of the sedimentation coefficients and protein content of each reconstitution intermediate revealed that the first pair and second pair of particles contain the same L- proteins and therefore differ only in S-value and conformation (Dohme and Nierhaus 1976). These two conformational changes, $RI_{50}(1) \rightarrow RI_{50}(1)$* and $RI_{50}(2) \rightarrow$ 50S, are the rate limiting steps at each incubation temperature (Dohme and Nierhaus 1976). Only six of the 22 early L-proteins associated with the first conformational change are essential for $RI_{50}(1)$* formation (Spillmann et al. 1977). *In vitro*, these early assembly proteins all bind near the 5' end of 23S rRNA (Chen-Schmeisser and Garrett 1976) and all except one remain on the core particles formed after washing with high concentrations of LiCl (Nierhaus and Dohme 1974). *In vivo*, these six proteins are also among the early binding proteins found in kinetic labeling studies (Pichon et al. 1975) and on the $p_1$50S precursor (Nierhaus et al. 1973) suggesting that reconstitution and early assembly begin down the same pathway. Eight late assembly proteins are associated with the second conformational change and are among the first to be split off of mature 50S subunits in low levels of LiCl (Nierhaus and Montejo 1973). However, these eight proteins are less well correlated to those that assemble late *in vivo* (Nierhaus and Montejo 1973; Pichon et al. 1975) suggesting that although reconstitution and assembly begin similarly, the pathways may diverge later on (Spillmann et al. 1977).

An *in vitro* assembly map for 50S subunits was determined from reconstitution

experiments in the presence of subsets of L-proteins (Roth and Nierhaus 1980; Rohl and Nierhaus 1982; Herold and Nierhaus 1987) and L-protein binding experiments to full or fragmented 23S rRNA (Figure 1.12) (Chen-Schmeisser and Garrett 1976; Spierer and Zimmermann 1976; Spierer et al. 1979). Similar to the 30S subunit, the 50S subunit *in vitro* assembly map as depicts the general order and interdependencies of L-protein binding to 23S and 5S rRNA. Additionally, the L-proteins needed to form the first reconstitution intermediate, $RI_{50}(1)$, are separated from those that are added in the second step to form $RI_{50}(2)$ as indicated by the horizontal line found near the bottom of the map. At the top of the map is a bar representing 23S rRNA which is divided into its major sub-fragments, 13S, 8S, and 12S (Chen-Schmeisser and Garrett 1976; Rohl and Nierhaus 1982). Arrows pointing from the 23S rRNA to L-proteins indicates the general positions and identity of the primary binding proteins, those which bind directly to the rRNA. Black or orange arrows indicate a weak or strong dependence of one protein on the presence of the other protein or rRNA fragment. Additional features of the 50S subunit *in vitro* assembly map include indications of the specific proteins involved in binding of 5S rRNA (green triangle) and those essential for $RI_{50}(1)$* formation (blue boxes) (Figure 1.12). The *in vitro* assembly map correlates well with other 50S subunit data (Rohl and Nierhaus 1982). For example, proteins split off by increasing LiCl concentrations reflect the reverse order of assembly (Spillmann et al. 1977) and are grouped accordingly on the *in vitro* assembly map (Rohl and Nierhaus 1982; Herold and Nierhaus 1987). Proteins translated from the same operon are also grouped on the *in vitro* assembly map in clusters.

1.6. The Assembly Gradient

Ribosome biogenesis *in vivo* proceeds via the "assembly gradient" in which the

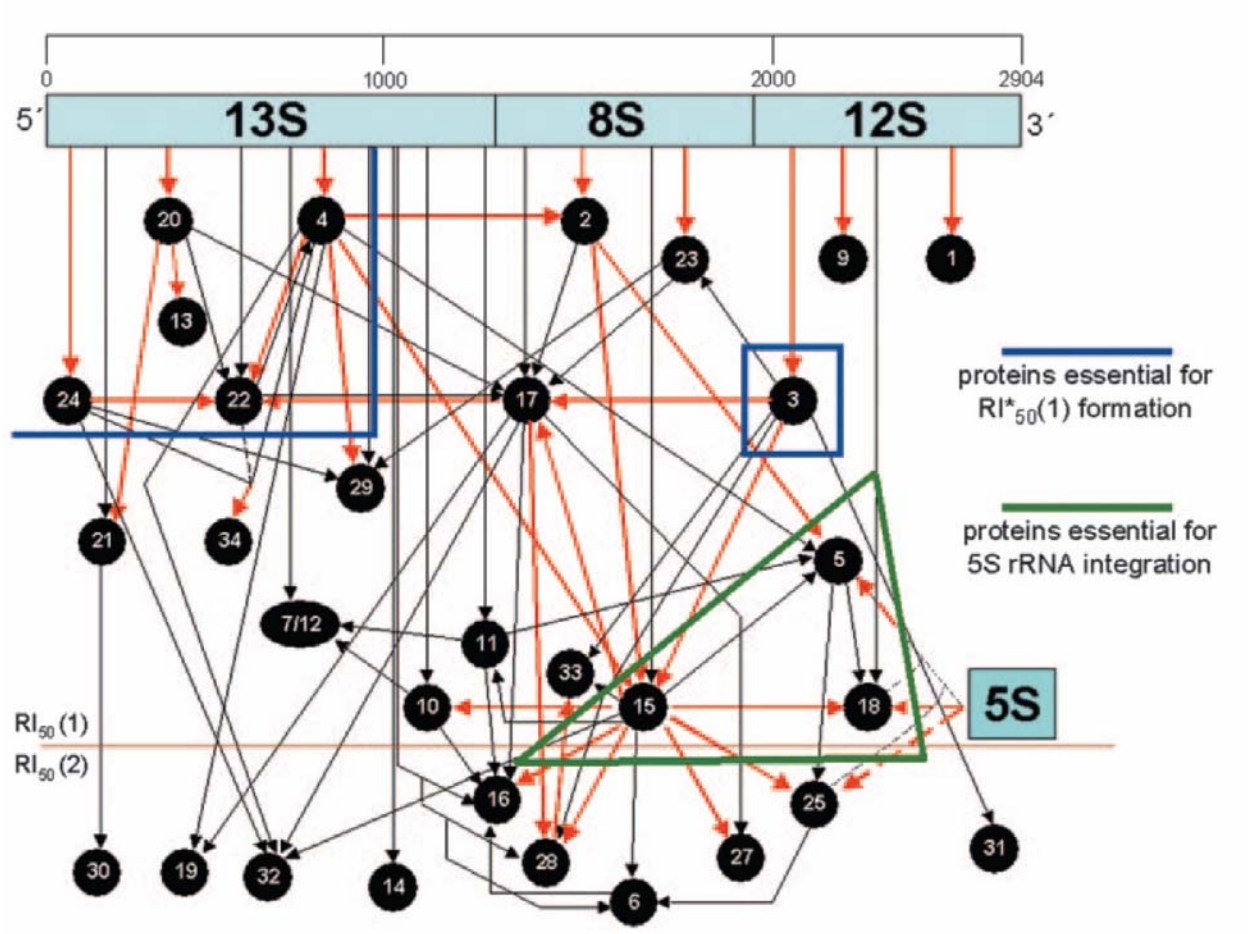

Figure 1.12 50S subunit *in vitro* assembly map

The 50S subunit *in vitro* assembly map depicts the order of assembly of L-proteins. The bar at the top represents the major subfragments of 23S rRNA. Arrows pointing from the rRNA identify the primary binding L-proteins. Arrows in between proteins indicate a strong (orange arrows) or weak (black) dependence on the presence of another L-protein. Assembly map figure is from (Kaczanowska and Rydén-Aulin 2007).

progression of rRNA synthesis and processing defines the evolution of the ribosomal subunits (Spillmann et al. 1977; Sieber and Nierhaus 1978). The assembly gradient is a highly organized process that involves coordination of many events to achieve proper formation of the many rRNA and r-protein interactions in the ribosome. Cells are highly dependent on properly functioning ribosomes especially in bacteria where ribosome biogenesis requires nearly 40% of the cell's energy and ribosomes constitute a large amount of the cellular mass (Nierhaus 1991). Therefore, the assembly of ribosomes must be tightly regulated to be accurate, efficient, and rapid as to not waste energy or space on inactive ribosomes. The assembly gradient, or more modernly defined as the assembly landscape, is marked by a series of rRNA folding and r-protein binding events (Williamson 2005) in addition to modification and processing of the rRNA (Figure 1.13). Similarities between *in vitro* reconstitution intermediates and precursor particles isolated *in vivo* (Figures 1.9 and 1.10) suggest that they proceed down similar pathways and encounter similar kinetic barriers. However, *in vivo* precursor particles are short-lived and difficult to isolate from cells under normal growth conditions whereas *in vitro* reconstitution intermediates occur because of rate-limiting steps encountered on the pathways. These rate-limiting steps in reconstitution are kinetic traps involving misfolded rRNA structures that are formed because the entire rRNA is exposed to all r-proteins at once (Wilson and Nierhaus 2007). *In vitro* misfolded rRNA intermediates are resolved by long incubations at high temperatures and high magnesium concentrations (Culver 2003; Williamson 2003). Precursor particles formed during biogenesis *in vivo* may also be due to similar kinetic traps that are usually overcome by the assembly gradient which couples rRNA transcription with cleavage, covalent modification, folding, and r-protein binding(Sieber and Nierhaus 1978). Covalent modifications at specific sites in the rRNA are made as the rRNA is transcribed and can assist in stabilizing the correct

Figure 1.13 The ribosome assembly gradient

In vivo ribosome assembly involves transcription, processing, modification, and folding of the rRNA and the binding of r-proteins to form the 30S and 50S subunits. 5S rRNA is also cleaved and folded and bound to the nascent 50S subunit but is not shown here. Green squares, S-proteins; purple circles, L-proteins; blue triangles, cleavage sites; pink hexagons, rRNA modifying enzymes. Figure based on (El Hage and Tollervey 2004).

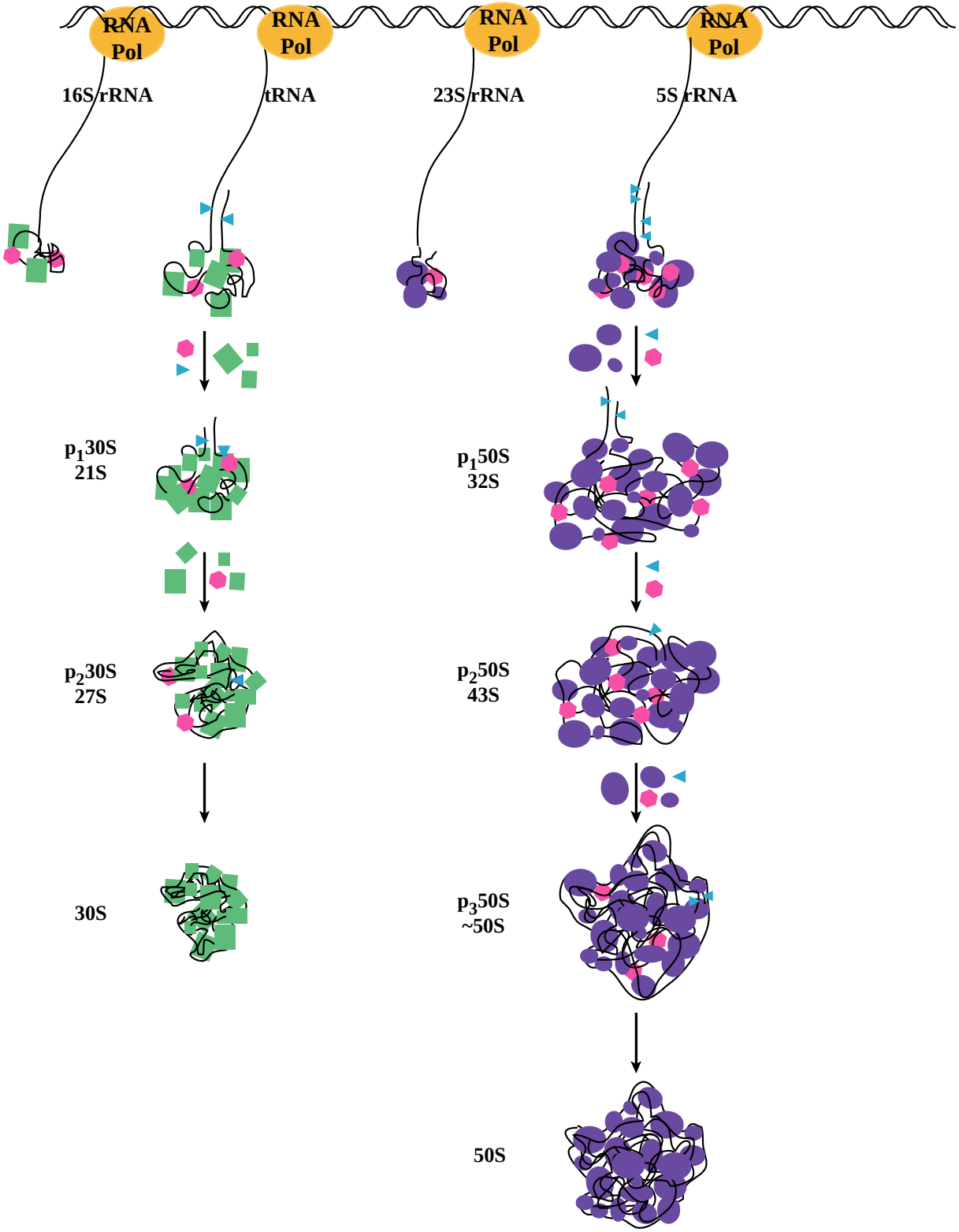
RNA Pol
RNA Pol
RNA Pol
RNA Pol
16S rRNA
tRNA
23S rRNA
5S rRNA
p1 30S 21S
p2 30S 27S
30S
p1 50S 32S
p2 50S 43S
p3 50S ~50S
50S

rRNA structures and preventing incorrect rearrangements as assembly proceeds. Co-transcriptional r-protein binding events also stabilize rRNA structures as well as facilitate rRNA folding, creating binding sites for the next r-protein and decreasing the overall kinetic barriers (Williamson 2005). This simultaneous processing, modifying, folding, and binding allow for assembly to proceed rapidly as well as provide points for regulation and control. *In vitro* reconstitution lacks the benefits of the assembly gradient which is one reason why the process is less efficient.

1.7. Ribosomal assembly factors

Not only do *in vitro* reconstitution experiments lack the benefits of the assembly gradient but they are also missing additional ribosomal assembly factors that may be the key to reconstituting completely active subunits. Recently several proteins have emerged as factors that transiently associate with the nascent ribosome, as part of the assembly gradient (Figure 1.14), and may function by resolving kinetic barriers encountered during assembly. Ribosome assembly factors have been classified into three groups: maturation factors, GTPases, and DEAD-box RNA helicases (Table 1.2). These factors could act as chaperones in ribosome assembly to stabilize intermediate rRNA structures, promote rRNA rearrangements (Herschlag 1995) or assist with r-protein binding events (Lorsch 2002). The exact functional roles and substrate targets for many of these ribosome assembly factors *in vivo* are not yet known. Therefore, identification of such proteins has depended on the observation of ribosome assembly defects in temperature sensitive mutant strains or in deletion strains. However, these defects could be the result of altered rRNA and r-protein production due to slow growth and thus not directly related to the function of the mutated or deleted protein. The challenges of studying

Table 1.2 Ribosome assembly factors

Factor	Role in ribosome assembly
DEAD-box proteins	
CsdA	50S biogenesis
SrmB	50S biogenesis
DbpA	50S biogenesis
RhlE	50S biogenesis
GTPases	
Era	16S rRNA maturation, 30S biogenesis
EngA	50S biogenesis
EngB	50S biogenesis
Obg	16S and 23S maturation, 50S biogenesis
RsgA	30S biogenesis
Maturation factors	
EryC	ribosome biogenesis
DnaK	ribosome biogenesis
GroEL	ribosome biogenesis
RbfA	30S biogenesis
RsgA	30S biogenesis
RimB	ribosome biogenesis
RimC	ribosome biogenesis
RimD	ribosome biogenesis
RimH	ribosome biogenesis
RimM	30S biogenesis
RimN	16S rRNA maturation
YbeB	ribosome biogenesis
Yhby	ribosome biogenesis
YibL	ribosome biogenesis
YjgA	ribosome biogenesis

Data are from (Kaczanowska and Rydén-Aulin 2007; Wilson and Nierhaus 2007), except RhlE, which is from (Jain 2008).

Figure 1.14 Ribosome assembly factors in the assembly gradient

Ribosome assembly factors, red triangles, associate transiently with the nascent ribosome as part of the assembly gradient. Green squares, S-proteins; purple circles, L-proteins; blue triangles, cleavage sites; pink hexagons, rRNA modifying enzymes. Figure based on (El Hage and Tollervey 2004).

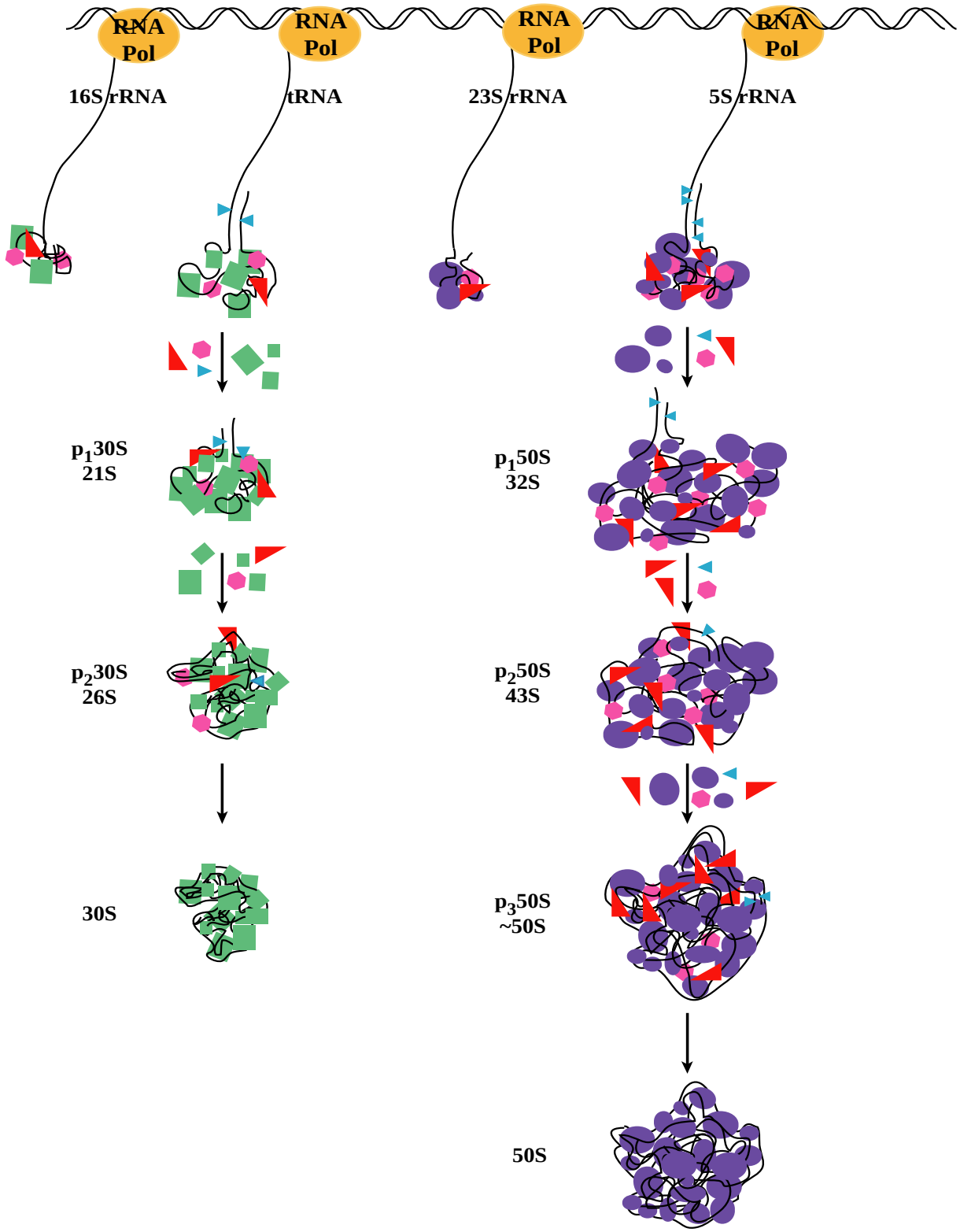
RNA Pol
RNA Pol
RNA Pol
RNA Pol
16S rRNA
tRNA
23S rRNA
5S rRNA
p1 30S 21S
p1 50S 32S
p2 30S 26S
p2 50S 43S
30S
p3 50S ~50S
50S

these factors are to first demonstrate that they actually participate directly in assembly, to identify the precise step on the pathway at which they act, and finally to determine the structure of the partially assembled ribosome that acts as the substrate for the factor.

Maturation factors

Maturation factors are a varied group of proteins that have been implicated in ribosome assembly but their precise roles remain largely unknown. These factors include certain rRNA modifying enzymes, several proteins of unknown function, and a couple of protein chaperones (Table 1.2). All of the enzymes that cleave or modify rRNA, as described in the previous sections, could potentially also have additional roles in ribosome assembly because they bind and release the substrate RNA at a particular point in the pathway (Ofengand and del Campo 2004). It is possible that the binding event itself is equally or more important for ribosome assembly than the covalent modifications. During assembly these enzymes may stabilize a particular rRNA structure in the vicinity of the cleavage or modification event or they could also possibly act as a checkpoint or regulatory step on the assembly pathway. Critical experiments testing for such an alternative function involve determining whether active site mutants that are not able to carry out the covalent modification are still able to promote ribosome assembly. This would demonstrate that enzyme binding and not the subsequent modification, is what was required for assembly. An alternative approach is to change the substrate in a way that blocks the modification without affecting binding. If the resulting mutant strain is unaffected then the modification itself is not essential. For example, the rRNA modifying enzyme $RlmA^{I}$, which methylates G745 of 23S rRNA appears to promote assembly independent of the methylation activity (Gustafsson and Persson 1998). Inactivation of $rlmA^{I}$ resulted in reduced growth rates,

accumulation of ribosomal subunits, and 70S ribosome that are reduced in peptide chain elongation rate (Gustafsson and Persson 1998). However, mutations of G745 that prevent methylation does not affect growth rate suggesting that a second function of $RlmA^{I}$ is essential for cell viability and ribosome assembly (Liu et al. 2004). There is also evidence, although it is less clear, for the methyltransferase RrmJ which makes a 2'-O-methylation at U2552 in hairpin 92 of 23S rRNA (Bügl et al. 2000; Caldas et al. 2000a) to have a secondary role in assembly. An *rrmJ* deletion strain results in severe growth and assembly defects, which disappear upon the addition of a plasmid containing wild type *rrmJ* (Bügl et al. 2000; Caldas et al. 2000b). The addition of two active site mutants of RrmJ that do not methylate U2552 *in vitro* cannot restore wild type growth or ribosome profile defects suggesting that the methylation is the main function of RrmJ (Hager et al. 2002). However, a third RrmJ mutant that could still methylate U2552 *in vitro* also lacked the ability to restore growth defects suggesting that a separate function of RrmJ is important for cell growth. In addition, the overexpression of two other proteins can restore growth defects in the Δ*rrmJ* strain without restoration of the methylation at U2552 (Tan et al. 2002). These two results would suggest that the methylation may not be essential and RrmJ has an alternative function in ribosome assembly. However, the possibility that the methylation itself is important for ribosome assembly has not been ruled out.

The largest group of ribosome assembly maturation factors is proteins of unknown function which are implicated in ribosome assembly because they bind to or associate with ribosomal RNA or proteins or they cause growth and ribosome assembly defects when they are deleted. Four ribosome maturation factors, RimA, RimB, RimC, RimD (ribosome maturation) were initially identified as cold-sensitive mutants that exhibit ribosome assembly defects and have not been studied further (Bryant and Sypherd 1974). Two others, RimM and RimN have

been demonstrated to be important for maturation of 30S subunits (Bylund et al. 1997; Kaczanowska and Ryden-Aulin 2004). Individual deletions or mutations of *rimM* and *rimN* resulted in slow growth, decreased amounts of polysomes, and increased amounts of 17S rRNA (Bylund et al. 1997; Bylund et al. 1998; Lövgren et al. 2004). Suppressor mutants for the RimM mutant were identified in proteins S13 and S19 and in 16S rRNA at various positions in helices 31 and 33 which are all located in the head domain of 30S subunits (Lövgren et al. 2004). Therefore, it is possible that RimM plays a role in the maturation of this particular region of the 30S subunit. On the other hand, the introduction of wild type RimN to Δ*rimN* cell extracts led to a decrease in 17S rRNA which suggests that RimN may stabilize a structure necessary for maturation of 16S rRNA (Kaczanowska and Rydén-Aulin 2005). Another factor, RbfA was initially identified as a multicopy suppressor of a cold sensitive mutation in helix 1 of 16S rRNA, C23U (Dammel and Noller 1995). RbfA deletions result in a cold-sensitive phenotype similar to that of C23U along with an increase in 30S and 50S subunits and a decrease in 70S ribosomes and polysomes (Dammel and Noller 1995). RbfA associates with 30S subunits and it possibly functions late in assembly to stabilize the 5' end of 16S rRNA (Dammel and Noller 1995; Inoue et al. 2003). Several other maturation factors that were identified to associate with ribosomal subunits (Jiang et al. 2006; Jiang et al. 2007) or as mutants resulting in assembly defects (Johnson et al. 1976; Pardo and Rosset 1977) are much less well understood and have not been studied further (Table 1.2).

Two final proposed maturation factors are the well known protein folding chaperones, GroEL and DnaK, which presumably participate in ribosome assembly by assisting with r-protein folding or binding to the nascent ribosome (Alix and Guerin 1993; El Hage et al. 2001). At high growth temperatures (45 °C), strains containing a temperature sensitive GroEL mutant

accumulate 45S particles suggesting GroEL is important for 50S subunit assembly at high temperatures (El Hage et al. 2001). Temperature sensitive mutants of DnaK accumulate 21S, 32S and 45S particles that contain unprocessed rRNA and lack several r-proteins when grown at temperatures above 35 °C (Alix and Guerin 1993; El Hage and Alix 2004). These accumulated particles are true precursors on the assembly pathway as demonstrated by pulse-chase experiments that label precursor particles and monitor their slow conversion to mature subunits even in the absence of added DnaK (El Hage and Alix 2004). Taken together, these results suggest that DnaK may accelerate late steps of ribosome assembly at high temperatures but is not essential at any growth temperature (El Hage and Alix 2004). In contrast and perhaps more controversially, DnaK has been shown to assist *in vitro* assembly of 30S subunits at lower than physiological temperatures (Maki et al. 2002). The addition of the DnaK chaperone system (Dnak, DnaJ, GrpE and ATP) to 30S subunit *in vitro* reconstitution experiments bypasses the requirement for incubation at 42 °C by promoting the assembly of an active 30S particle at 15 °C (Maki et al. 2002; Maki et al. 2003). The DnaK-facilitated reconstituted 30S particle is more active in polyphenylalanine synthesis than the 21S reconstitution intermediate formed at low temperatures, but is less active than reconstituted 30S particles made at high temperatures in the absence of DnaK (Maki et al. 2003). Since the DnaK-reconstituted 30S particles are not fully active, it is likely that other factors also assist with 30S subunit assembly *in vivo* and further experiments need to be addressed in order to determine the exact function (Maki and Culver 2005).

GTPases

The second class of ribosomal assembly factors are members of the GTPase family which

are a well-characterized group of regulatory proteins involved in many cellular processes ranging from signal transduction to translation (Karbstein 2007). Often called molecular switch proteins for the conformational states that occur during their catalytic cycle, GTPases can be classified into many subfamilies based upon a set of conserved sequence motifs (Bourne et al. 1991; Leipe et al. 2002). Some GTPases, particular those implicated in assembly, also contain RNA binding domains that could be important for targeting the GTPase to a particular RNA molecule (Karbstein 2007). One major GTPase subfamily is the translation factors, which include EF-G, EF-Tu, IF2, and the recently characterized LepA that all have different roles in protein synthesis but all participate rRNA rearrangements during the translation cycle (Caldon et al. 2001; Leipe et al. 2002). The GTPases involved in *E. coli* ribosome assembly mostly belong to other subfamilies and are functionally much less well understood. However, unlike with the maturation factors, one can use the structural and biochemical data for other well characterized GTPases to speculate a few different roles for the GTPases in ribosome assembly (Karbstein 2007). For example, GTPases could use energy from GTP hydrolysis to regulate protein binding events or to dissociate rRNA duplexes or rRNA-protein complexes. Additionally GTPases could act as a placeholder, stabilizing an rRNA structural intermediate, or as a nutritional state sensor signaling optimal growth conditions.

Any of these proposed functions could be performed by each of the five known *E. coli* GTPases that participate in ribosome assembly, EngA, Obg, Era, EngB, and RsgA (Table 1.2). Several of these were initially implicated in ribosome assembly because they were identified as suppressors of other ribosome assembly mutants. For example, both EngA and Obg can restore wild type growth and ribosome assembly in the Δ*rrmJ* strain, which lacks a methylation at U2552 in 23S rRNA (Tan et al. 2002). Neither of these proteins restores the methylation,

therefore their role in assembly is possibly to stabilize an rRNA structure that would otherwise be stabilized by the modification or RrmJ itself. Another GTPase, Era, was identified as a suppressor of defects in the deletion strain of the maturation factor RbfA (Inoue et al. 2003). However, Era does not suppress the slow growth phenotypes of Δ*rimM* or C23U strains, which are both suppressed by RbfA overexpression suggesting that Era and RbfA have overlapping functions but distinct binding sites (Inoue et al. 2003; Inoue et al. 2006). The final two *E. coli* GTPases, RsgA and EngB, were initially studied because they were found to be essential for cell viability (Arigoni et al. 1998), however RsgA was later demonstrated to be nonessential as deletion strains were still viable at various temperatures (Himeno et al. 2004).

Much of the information known about the function of these GTPases are for the most part based on their interactions with other ribosomal assembly factors. However, there has also been individual deletion or mutational studies for some GTPases, which further demonstrates their roles in ribosome assembly. For example, depletion of both EngA and Obg result in slow growth and the accumulation of ribosomal subunits (Sato et al. 2005; Hwang and Inouye 2006; Jiang et al. 2006). Additionally, when ribosomes from Obg or EngA depleted cells are run on sucrose gradients containing low Mg^{2+} (1 mM), pre-50S particles (40S and 45S) accumulate (Hwang and Inouye 2006; Jiang et al. 2006). The precursor particles from either strain contain pre-23S rRNA along with reduced amounts of L-proteins. The 40S particle from Obg depleted cells contains reduced amounts of L33, L34, and to a lesser extent L16, which are all late assembly proteins suggesting that Obg is involved in a late step of ribosome assembly (Jiang et al. 2006). Depletion of the EngA homolog in *B. subtilis* results in a 45S particle that contains reduced levels of L16, L27, and L36, (Schaefer et al. 2006) which is very different from the particle found in EngA depleted *E. coli* cells, containing reduced levels of L9, L18, L2 and L6 (Hwang

and Inouye 2006). Despite this discrepancy, EngA is presumed to participate late in assembly because it has been shown to cofractionate with 50S subunits in sucrose gradients (Bharat et al. 2006; Hwang and Inouye 2006). More studies are needed to further understand the role of EngA in ribosome assembly and whether or not the different particles are actually from different stages in assembly or due to the method of collection and purification or the fact that they are from different types of bacteria. The essential GTPase, EngB has only been studied in *B. subtilis*, in which EngB depletion results in a 44.5S particle that contains reduced amounts of L16, L27, and L36 (Schaefer et al. 2006). Therefore, like EngA and Obg, EngB is presumed to be important in late stage assembly. Similar experiments and results have been shown for the other *E. coli* GTPases and have been extensively reviewed elsewhere (Karbstein 2007; Wilson and Nierhaus 2007). Although as with the maturation factors, the precise roles and substrates for GTPases in ribosome assembly are still largely unknown. It will be interesting to see how future studies with these proteins define the roles they play in ribosome assembly.

DEAD-box proteins

The final class of ribosomal factors is the DEAD-box proteins, which are part of the large superfamily 2 RNA helicases and are known to function in most aspects of RNA metabolism (Rocak and Linder 2004). DEAD-box proteins, like the GTPases, are defined by nine conserved amino acid sequence motifs including the characteristic and defining D-E-A-D sequence (Figure 1.15) (Linder et al. 1989; Gorbalenya and Koonin 1993; Cordin et al. 2004). Crystal structures of several DEAD-box proteins (Story and Steitz 1992; Benz et al. 1999; Caruthers et al. 2000; Story et al. 2001; Carmel and Matthews 2004; Shi et al. 2004; Cheng et al. 2005; Sengoku et al. 2006) revealed that the conserved motifs lie at the interface of two domains, which each fold

similar to the classic RecA ATPase (Figure 1.16). A pocket formed between the two domains is the binding site for ATP and the RNA binds perpendicularly, both making contacts with several conserved residues throughout both domains (Sengoku et al. 2006). As the protein cycles between ATP bound, ADP bound, and unbound states, the two domains cycle between open and closed conformations, which in turn change the nature of the contacts made to the bound RNA substrate (Sengoku et al. 2006). In the structure of *Drosophila* Vasa DEAD-box protein bound to an ATP analog and polyU RNA, the RNA is bent which could cause disruption of base pairs at the 3' or 5' ends or at internal sites within the duplex, eventually resulting in destabilization and strand separation (Sengoku et al. 2006; Yang et al. 2007). In addition to the conserved core motifs, many DEAD-box proteins have N- or C-terminal extensions of varying length and sequence that are likely involved in substrate recognition and specificity. One of the most well-studied DEAD-box proteins is the translation factor, eIF4A, which has been shown through *in vivo* depletion studies (Daga and Jimenez 1999), mutational studies (Pause and Sonenberg 1992; Pause et al. 1994), structural studies (Benz et al. 1999; Caruthers et al. 2000) and *in vitro* assays (Svitkin et al. 2005) to utilize energy from ATP hydrolysis to help unwind secondary structures in the 5'-utranslated region of mRNA allowing it to proceed through the small subunit of the ribosome during translation.

Although many DEAD-box proteins have been shown to have RNA-dependent ATPase activity and can either unwind RNA duplexes or RNA-protein complexes *in vitro* (Cordin et al. 2006) their roles *in vivo* are much less well understood, especially in the case of those implicated in ribosome assembly (Iost and Dreyfus 2006). In *E. coli* there are five DEAD-box proteins, SrmB, CsdA, RhlE, DbpA, and RhlB, and the first four are proposed to be involved in ribosome assembly (Iost and Dreyfus 2006) (Figure 1.17). CsdA and SrmB were initially identified as

Figure 1.15 DEAD-box proteins conserved motifs

DEAD-box proteins are grouped according to nine conserved amino acid sequence motifs; Q, I, Ia, Ib, II, III, IV, V, and VI, which are located in two RecA-like domains. Some DEAD-box proteins have N-terminal or C-terminal extensions of varying length that define their specific function. Symbols used are; x: any amino acid; o: S or T; and l: I, L, or V.

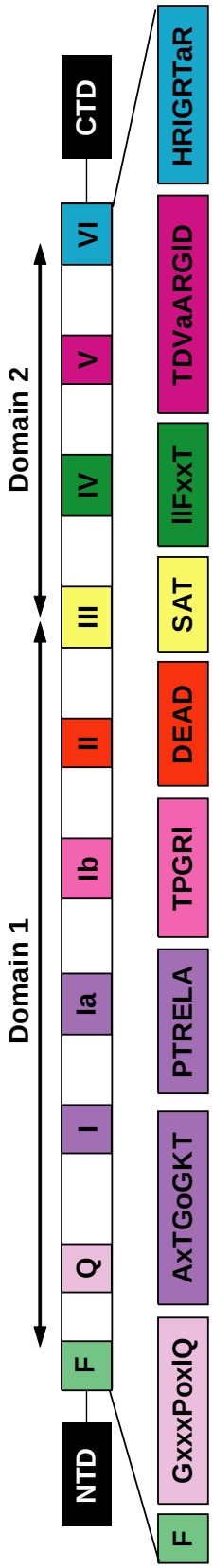
NTD
F
Q
I
Ia
Ib
II
III
IV
V
VI
CTD
Domain 1
Domain 2
F
GxxxPoxlQ
AxTGoGKT
PTRELA
TPGRI
DEAD
SAT
IIFxxT
TDVaARGID
HRIGRTaR

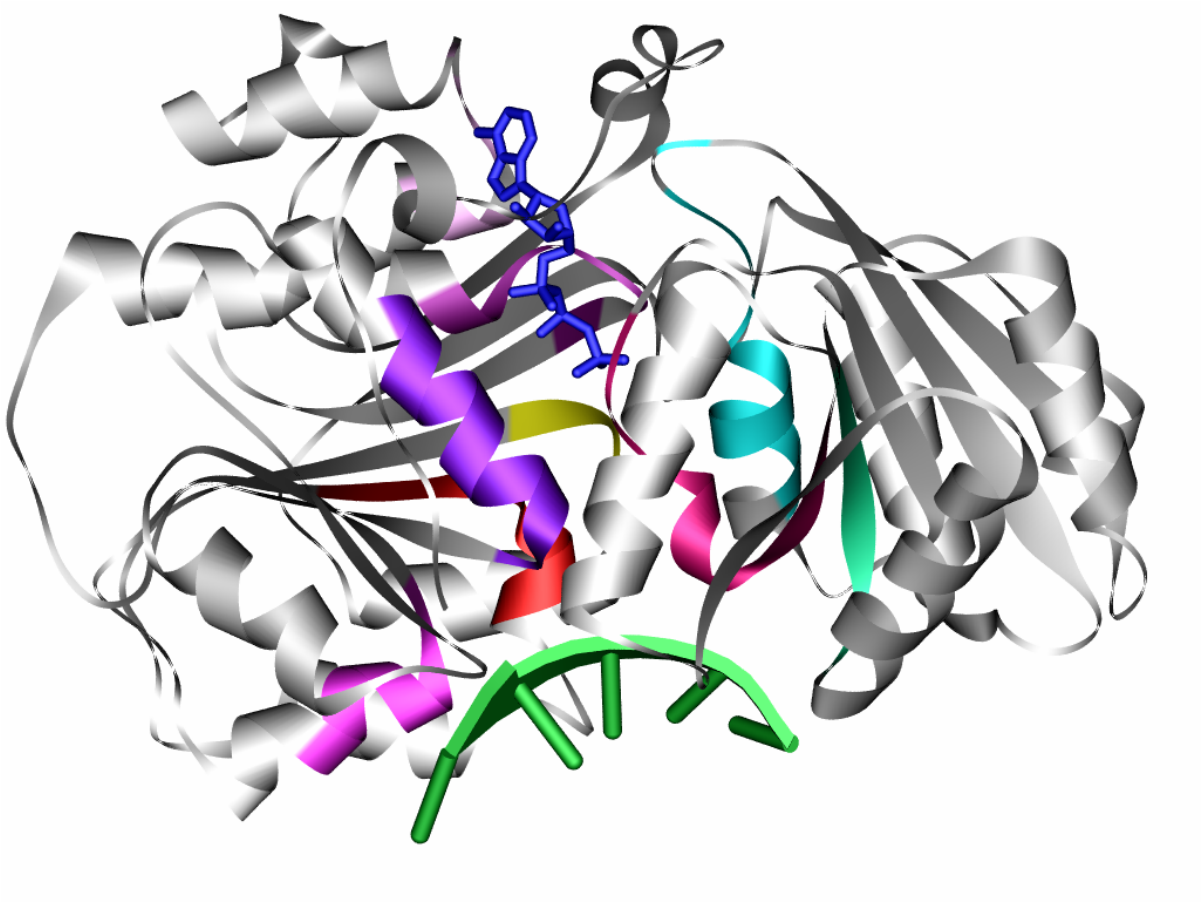

Figure 1.16 Crystal structure of a DEAD-box protein

The crystal structure of DEAD-box protein, *Drosophila* Vasa with bound ATP non-hydrolyzable analog, blue, and polyU RNA, green (PDB: 2db3). Conserved motifs lie at the interface of two domains and are color-coded as in Figure 1.15.

multicopy suppressors of mutations in r-protein genes (Nishi et al. 1988; Toone et al. 1991). Individual deletion mutants of SrmB and CsdA each result in a cold sensitive, slow-growth phenotype and accumulation of 40S particles that contain precursor 23S rRNA and are missing different sets of r-proteins and are thus 50S subunit precursors (Charollais et al. 2003; Charollais et al. 2004). Ribosomal proteins missing from Δ*csdA* 40S particles are primarily those that bind late in assembly, while Δ*srmB* 40S particles are also missing at least one protein that is associated with early assembly suggesting that it acts prior to CsdA in 50S subunit assembly (Charollais et al. 2003; Charollais et al. 2004). Aside from being implicated in ribosome assembly, CsdA and SrmB are involved in mRNA decay. Additionally, CsdA is proposed to participate in other cellular processes, including 30S subunit biogenesis, translation initiation, and gene regulation (Iost and Dreyfus 2006). The *in vitro* ATPase activity of both CsdA and SrmB is stimulated by various RNA substrates to similar extents with little to no sequence-specific requirements (Bizebard et al. 2004). ATP-stimulated helicase activity of CsdA and SrmB similarly does not require specific sequences however the RNA duplexes must be short and have either a 3' or 5' single strand extension of at least 12 or 25-35 nucleotides long, respectively (Bizebard et al 2004). The lack of substrate specificity is consistent with SrmB and CsdA participating in multiple processes, including rRNA conformational rearrangement during ribosome assembly.

A third DEAD-box protein, RhlE, was shown to interact genetically with SrmB and CsdA (Iost and Dreyfus 2006; Jain 2008) and can replace RhlB in *in vitro* assays (Khemici et al. 2004; Prud'homme-Genereux et al. 2004). RhlE was shown to have non-specific RNA-stimulated ATPase activity although more robust than the activity measured for SrmB and CsdA (Bizebard et al. 2004). Additionally, RhlE can unwind short RNA duplexes, with or without

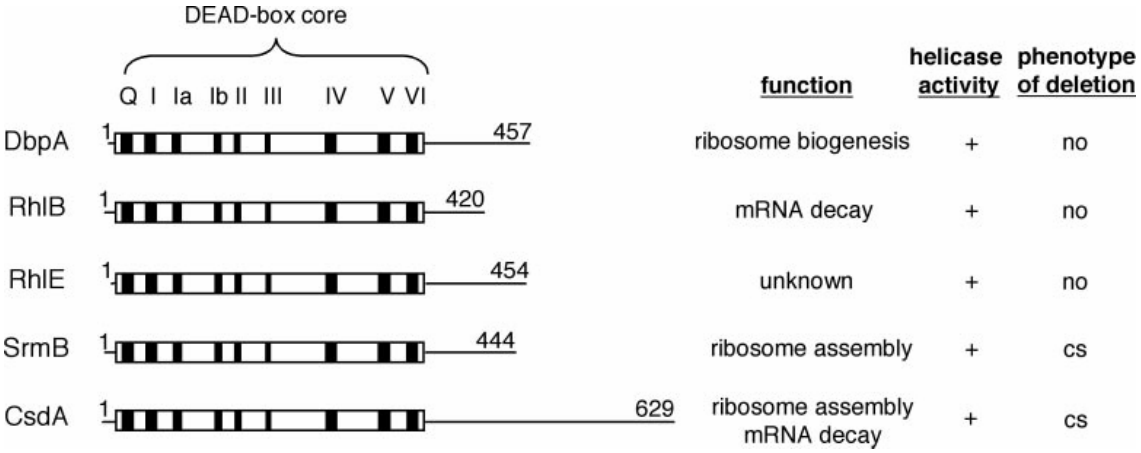

Figure 1.17 DEAD-box proteins in *E. coli*

Sequence alignment and summary of properties of the five DEAD-box proteins in *E. coli*, DbpA, RhlB, RhlE, SrmB, and CsdA. The conserved motifs are represented by black strips within the conserved core, wherease the N- and C-terminal extensions (drawn to scale) are shown as thin lines. Also shown are the proposed functions of each, helicase activity (+ means that the protein is able to dissociate an RNA duplex in an ATP-dependent manner), and the phenotype associated with gene deletion (no, no growth defect; cs, cold-sensitive growth). Figure is from (Iost and Dreyfus 2006). Recently RhlE was also proposed to participate in ribosome biogenesis (Jain 2008), but more data is needed to demonstrate this function.

single-strand extensions, in the presence of ATP (Bizebard et al. 2004). Deletion of *rhlE* alone does not reveal any growth defects and ribosome profiles are similar to wild type (Jain 2008). However, overexpression of RhlE in Δ*csdA* strains rescues the cold-sensitive growth defects (Iost and Dreyfus 2006; Awano et al. 2007; Jain 2008) while overexpression of RhlE in Δ*srmB* exacerbated the growth defects (Jain 2008). These genetic interactions between RhlE and the known ribosome assembly factors SrmB and CsdA lead to the assumption it is also participating in ribosome assembly in a similar role. Interestingly, double mutations of RhlE and either SrmB or CsdA performed in two separate labs revealed conflicting results. Iost *et al*., found that double mutants did not exhibit any growth differences on rich medium at low temperatures (Iost and Dreyfus 2006). However, Jain *et al*., found the same double mutants resulted in decreased (Δ*csdA*Δ*rhlE*) or increased (Δ*srmB*Δ*rhlE*) growth rates compared to the CsdA or SrmB deletions alone (Jain 2008). Even though RhlE co-sediments with 70S ribosomes, 50S subunits and 40S particles when introduced on a plasmid to the Δ*csdA* and Δ*csdA*Δ*rhlE* strains, it is not clear that this interaction is specific to the function or due to non-specific binding that results from the overexpression of RhlE. Therefore, discrepancies between these results warrant a need for more evidence in order to confirm that RhlE is a ribosome assembly factor.

The final *E. coli* DEAD-box protein that is implicated in ribosome assembly is the RNA-stimulated ATPase and helicase, DbpA. DbpA is unique among the five known *E. coli* RNA helicases because it binds tightly and specifically to its substrate, 23S rRNA (Fuller-Pace et al. 1993; Nicol and Fuller-Pace 1995; Tsu and Uhlenbeck 1998; Pugh et al. 1999). Fragments of 23S rRNA that activate DbpA's robust ATPase activity, contain hairpin 92 which is located in the PTC (Nicol and Fuller-Pace 1995; Tsu and Uhlenbeck 1998; Tsu et al. 2001) (Figure 1.18). RNA substrates containing hairpin 92, stimulate ATP-dependent unwinding of short duplexes

Figure 1.18 Domain V of 23S rRNA is the DbpA binding site

DbpA binds to a 153 nucleotide region of 23S rRNA in domain V (left). DbpA footprinting covers hairpin 92 (in red) and is extended to two other regions, including helix 93, in the presence of AMPPNP (right) (Karginov and Uhlenbeck 2004).

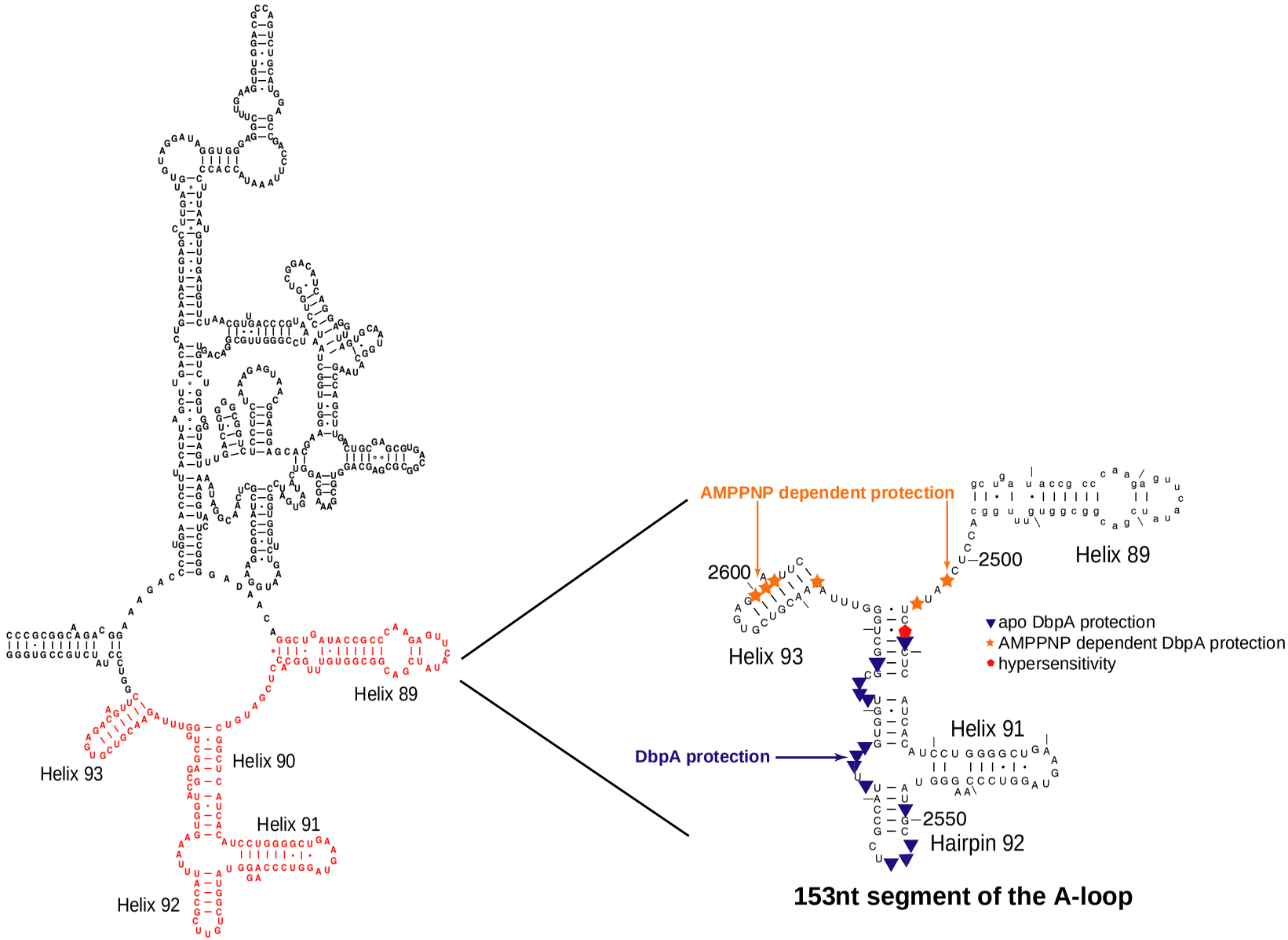
Helix 89
Helix 90
Helix 93
Helix 91
Helix 92
AMPPNP dependent protection
2600
2500
Helix 89
Helix 93
apo DbpA protection
AMPPNP dependent DbpA protection
hypersensitivity
Helix 91
DbpA protection
2550
Hairpin 92
153nt segment of the A-loop

extending 5' or 3' from the hairpin demonstrating that DbpA is a 3' to 5' non-processive RNA helicase (Diges 2001; Diges and Uhlenbeck 2005). Biochemical data (Kossen and Uhlenbeck 1999; Kossen et al. 2002) and crystal structures (Wang et al. 2006) demonstrated that the CTD of DbpA is responsible for recognizing and binding to hairpin 92. The CTD alone can bind to hairpin 92-containing substrates tightly and specifically, while the N-terminal ATPase domains bind weakly and nonspecifically demonstrating the functional modularity of DbpA and suggesting that the CTD targets the catalytic domains to spatially nearby regions of the rRNA (Karginov et al. 2005). Footprinting studies in the presence of the nonhydrolyzable ATP analog, AMPPNP, revealed that DbpA contacts two additional regions in the PTC (orange stars in Figure 1.18) suggesting that these residues include the region of rRNA that the catalytic domains of DbpA bind to and act upon (Karginov and Uhlenbeck 2004). These additional RNA-protein interactions were also demonstrated by an increased binding affinity for rRNA substrates containing helix 89 in the presence of AMPPNP (Polach and Uhlenbeck 2002). In a different set of experiments, cooperativity or thermodynamic coupling was shown by a greater than 10-fold higher affinity for RNA when DbpA is bound to ADP-P_i compared to DbpA without nucleotide (Henn et al. 2008). This suggests a significant conformational change occurs when both RNA and ADP-P_i are bound (Henn et al. 2008), which is possibly similar to the closed conformation observed by fluorescence spectroscopy (Henn et al. 2002; Talavera et al. 2006; Theissen et al. 2008) and as depicted by the crystal structure of Vasa DEAD-box protein bound to RNA and AMPPNP (Sengoku et al. 2006). These studies together suggest a mechanism in which RNA duplex destabilization coincides with the closed conformation and strong DbpA binding in the presence of ATP (Henn et al. 2008).

As summarized in the above discussion, DbpA has been biochemically well-

characterized although the function *in vivo* is much less well understood. Unlike with CsdA and SrmB, deletions of DbpA result in wild type growth and normal ribosome assembly (Baba et al. 2006; Iost and Dreyfus 2006). DbpA's affinity for 23S rRNA, specifically at the PTC, which is a major functional center of the 50S subunit, initially suggested that it either functions in ribosome assembly or translation (Nicol and Fuller-Pace 1995). However, 50S subunits and 70S ribosomes fail to stimulate DbpA's ATP hydrolysis activity, which seemed to rule out a role for DbpA in translation (Tsu and Uhlenbeck 1998). Therefore, DbpA is presumed to function as an rRNA chaperone in 50S subunit assembly.

Statement of Thesis

The goal of this thesis began as a mechanistic study of the ATPase and helicase activity of *E. coli* DbpA. However, these experiments (Chapter 2) revealed a dominant-negative mutation, which led to further studies indicating the molecular function of DbpA in ribosome assembly (Chapter 3).

A series of eleven point mutations in the conserved ATPase motifs were made and compared to the biochemical activities of wild type DbpA. As expected, all of the mutants bound to substrate RNA efficiently because the majority of DbpA's substrate affinity is determined by the CTD, which was not mutated. However, mutations in residues that directly contact ATP caused drastic reductions in ATPase and helicase activities. One of the mutants (arginine 331 to alanine, R331A) displays a dominant negative, cold sensitive, slow growth phenotype when overexpressed *in vivo*.

The slow growth phenotype of cells overexpressing R331A mutant is attributed to a decrease in mature 70S ribosomes due to the accumulation of a 45S particle that cannot bind 30S

subunits. The 45S particle is most likely a precursor to 50S subunits because it contains pre-23S rRNA and reduced levels of five late assembly L-proteins. The fact that the L-proteins reduced in the 45S particle bind near the DbpA-ATP binding site, harpin 92 and helix 89, along with experiments showing that 45S particles stimulate DbpA's ATPase activity, is consistent with DbpA acting to promote a conformational rearrangement that is necessary for the maturation of the 50S subunit. However, DbpA is not essential because, strains containg a deletion of the *dbpA* gene grow and produce ribosomes normally. Therefore, it is the inactivity of the overproduced mutant that must block the conformational rearrangement, resulting in the accumulation of the 45S particle.

CHAPTER 2

Mutation of the arginine finger in the active site of *E. coli* DbpA abolishes ATPase and helicase activity and confers a dominant slow growth phenotype

2.1. Introduction

DbpA is an *E. coli* DEAD-box protein that binds tightly and specifically to 23S rRNA and stimulates rapid ATP hydrolysis (Fuller-Pace et al. 1993; Nicol and Fuller-Pace 1995). Extensive truncation (Nicol and Fuller-Pace 1995; Tsu and Uhlenbeck 1998; Tsu et al. 2001) and footprinting (Karginov and Uhlenbeck 2004) experiments have shown that DbpA binds to a 153 nucleotide region (153mer) of 23S rRNA consisting of helices 89 through 93, which are all part of the PTC of the ribosome. Shorter fragments that contain only hairpin 92 bind to DbpA with similar affinity as the 153mer, demonstrating this hairpin as the primary binding site (Tsu et al. 2001). In the presence of RNA duplexes containing hairpin 92, DbpA demonstrates weakly processive 3' to 5' RNA helicase activity (Diges 2001). However, mature ribosomes are poor substrates for DpbA because hairpin 92 is buried within the PTC (Tsu and Uhlenbeck 1998).

The N-terminal 381 amino acids of DbpA contains the ATPase core, 9 conserved motifs spanning two domains that define DExD/H proteins and are responsible for the ATP binding and hydrolysis activities. The C-terminal 76 amino acids form a basic domain that forms an RRM and is involved in RNA binding specificity (Wang et al. 2006). The isolated C-terminal domain of YxiN, the *Bacillus subtilis* ortholog of DbpA, can bind hairpin 92 tightly and specifically (Karginov et al. 2005). However, the isolated N-terminal domain of YxiN binds RNA weakly and nonspecifically but does show ATPase activity, thus demonstrating the functional modularity

of this DExD/H protein (Karginov et al. 2005).

Despite this extensive biochemical characterization, relatively little is known about the function of DbpA in *E. coli*. DbpA mRNA levels are found in low amounts in logarithmic cells, but they increase upon acid shock, addition of ciprofloxacin, and at stationary phase (Blattner et al. 1997). Several groups have deleted the *dbpA* gene using different methods, however no growth defects were observed in different culture media and growth conditions (Baba et al. 2006; Iost and Dreyfus 2006)(Tsu, C. and Uhlenbeck, O. C. unpublished data). Because DbpA is activated by 23S rRNA *in vitro*, it was hypothesized that DbpA is either involved in the ribosome assembly pathway or in some specialized aspect of translation (Nicol and Fuller-Pace 1995). Under many growth conditions, DbpA is not essential and therefore, either one of the other *E. coli* DExD/H proteins can substitute for its function or it is only required under certain growth conditions.

The goal of this study is to identify a dominant negative mutant of DbpA that can be used to better understand its cellular function. DbpA is a good candidate for creating a dominant negative mutant because its binding affinity and specificity lies almost completely in the CTD, while its ATPase and helicase activity are determined by the conserved ATPase core (Karginov et al. 2005). These modular characteristics make it possible to inactivate DbpA by mutating catalytic residues without affecting the ability of the CTD to bind substrate RNA. Unlike a knockout mutation of DbpA, a site-directed mutation would produce a protein that could compete with wild type DbpA for the rRNA binding site and subsequently block action at the normal site of function. Therefore, several point mutations were made in the conserved sequence motifs of DbpA that were identical to those showing dominant negative properties in other DExD/H proteins, including eIF-4A, Prp16, Prp22, Prp28, Prp43, Rok1p, Sub2p, Ded1p, Dbp8p

(Schmid and Linder 1991; Chang et al. 1997; Hotz and Schwer 1998; Iost et al. 1999; Oh and Kim 1999; Schwer and Meszaros 2000; Daugeron and Linder 2001; Zhang and Green 2001; Martin et al. 2002).

2.2. Materials and methods

Site-directed mutagenesis and purification of His-tagged DbpA mutations.

The gene coding for DbpA with an N-terminal Met-His_6 sequence was cloned into the pET-3a vector between the NdeI and BamHI sites (Karginov and Uhlenbeck 2004). Site-directed mutagenesis was performed on this plasmid using QuikChange® XL Site-Directed mutagenesis kit (Stratagene). DbpA-containing plasmids were transformed into BL21(DE3) pLysS cells (Stratagene) and purified as previously described (Karginov and Uhlenbeck 2004) with the following changes. Cell lysate was purified by FPLC over a nickel column or by batch purification over Ni-NTA beads (Qiagen) in buffer A (500 mM NaCl, 20 mM MOPS pH 7, 1 mM β-mercaptoethanol, 10% glycerol) and 10 mM imidazole. His_6-DbpA was eluted in buffer A with 300 mM imidazole and further purified using a Pharmacia Superdex75 sizing column in buffer A.

Preparation of RNA.

Native *E. coli* rRNA (16S and 23S) was from Roche Diagnostics or purified from *E. coli* MRE600 cells by the following method. The cell pellet was thawed on ice and resuspended in ribosome lysis buffer (50 mM Tris pH 7.5, 10 mM $MgCl_2$, 100 mM NH_4Cl, 0.5 mM EDTA pH 8, 6 mM DTT) and RQ1 DNase (Promega). Cells were lysed by a Thermo IEC french press and cell debris removed by centrifugation for 20 min at 11,000 rpm in an Eppendorf table top

centrifuge. Ribosomes were collected by centrifugation for 1 h at 40,000 rpm in a Ti45 rotor in a Beckman Optima LE-80K ultracentrifuge. The pellet was cleared by rinsing with TE buffer and then resuspended in SDS-Urea extraction buffer (6 M Urea, 0.1% SDS, 10 mM Tris pH 7.8, 10 mM EDTA pH 8, and 350 mM NaCl). Ribosomal RNA was purified by phenol-chloroform extraction, ethanol precipitation, LiCl precipitation, a second ethanol precipitation and elution over NAP-25 columns (Amersham Biosciences).

9mer and 32mer RNA were purchased from Dharmacon. A 153mer segment of domain V of 23S rRNA was prepared by *in vitro* transcription. The 153mer DNA template was PCR amplified from p2454-2606 (Tsu and Uhlenbeck 1998) and purified with the QIAquick Gel Extraction kit (QIAGEN). Transcription of 153mer RNA was carried out in transcription buffer (80 mM Tris pH 7.5, 20 mM DTT, 4 mM Spermidine, 0.1% TritonX, 12 mM $MgCl_2$, 0.004 U/mL pyrophosphatase) with 4 mM NTPs, 15 ng/μL template DNA and 0.1 mg/mL T7 RNA polymerase at 37 °C for 3 hours, concentrated by ethanol precipitation and then purified by 10% PAGE. RNA was extracted from the gel by passive elution (0.5 M NaOAc and 1 mM EDTA pH 8) overnight at 4 °C and then concentrated by ethanol precipitation. The concentration of the final product was calculated using ε_{260} = 1.3 x 10^6 L/mol cm. RNA substrates were 5'-^{32}P labeled with polynucleotide kinase and γ-^{32}P ATP and purified by 10% denaturing PAGE. Labeled RNA was extracted from the gel by passive elution overnight at 4 °C and then precipitated with ethanol.

DbpA Assays.

The rate of ATP hydrolysis of DbpA in the presence of 23S + 16S rRNA was measured

using the previously described high-throughput coupled spectroscopic assay (Karginov et al. 2005). All reported values are the average of at least three data sets and are all within 2-fold error.

The binding of DbpA to a 153mer portion of 23S rRNA was determined based on the previously described gel shift assay (Polach and Uhlenbeck 2002). Binding reactions were carried out in binding buffer (50 mM Hepes pH 7.5, 5 mM $MgCl_2$, 100 mM KCl, 100 μM DTT, 100 μg/mL BSA and 5 % (v/v) glycerol) with 200 pM 5'-^{32}P RNA, 70 μM polyA, and increasing amounts of DbpA protein. Samples (20 μL) were equilibrated at 24 °C for 30 min then an 18 μL aliquot was loaded on a 5% native acrylamide gel (29:1 acrylamide:bis) running at 200 V in 1/3x TBE buffer. Gels were run for 2 hours, dried and exposed to a phosphor screen. The fraction of bound protein was determined from the ratio of counts in the bound RNA band relative to the total counts of the free and bound RNA. The fraction of bound RNA vs. DbpA concentration was plotted and fit to simple binding equilibria to determine the dissociation constant (K_d) (Polach and Uhlenbeck 2002). The binding affinity was also evaluated in the presence of a non-hydrolyzable ATP analog, AMPPNP. Reactions were carried out as above with 50 pM 5'-^{32}P RNA and the addition of 4 mM AMPPNP. All reported values are the average of at least three data sets and are corrected for percent activity as measured by a stoichiometric binding assay (described below). The errors are less than 2.5-fold for all measurements.

The stoichiometry of RNA binding for each wild type and mutant protein was measured using the gel shift binding assay in the presence of 500 nM 5'-^{32}P 153mer and varying protein concentrations (Polach and Uhlenbeck 2002). The fraction of bound RNA vs. protein concentration was plotted and fit linearly (data not shown). The linear slope is the percent active protein, which is then multiplied by the average value of K_d to obtain final values corrected for

percent protein activity.

Helicase activity was measured using a 5'-^{32}P labeled 9mer (*9mer) annealed 5' to 32mer RNA `containing hairpin 92 (Figure 2.4A) using the assay described previously. (Diges and Uhlenbeck 2005) with the following modifications. 1.2 μM 32mer and 0.6 μM *9mer were annealed by mixing in 50 mM Hepes pH 7.5 and 50 mM KCl and then heating to 95 °C for 1 min, 80 °C for 1 min, 75 °C for 2 min, 70 °C for 3 min. At 70 °C, 5 mM $MgCl_2$ was added and the reaction was cooled to 24 °C for 15 min and then to 4 °C and used immediately. Helicase assays in the presence of excess protein were based on the previously described method (Diges and Uhlenbeck 2005) and carried out at 24 °C in binding buffer (as above). 75 μL aliquots of the RNA mixture (5 nM annealed substrate with 70 μM polyA) and protein mix (0.6 μM DbpA, 2 mM ATP, 2 mM $MgCl_2$) were combined to initiate unwinding. At various times, 9 μL of the reaction mixture was removed and mixed with 3 μL of quench dye (2.5 mM EDTA pH 8, 0.025% SDS (w/v), 1.25% glycerol (v/v), pinch xylene cyanol). Then 9 μL of the quenched reaction was immediately loaded onto a 10% native acrylamide gel (29:1 acrylamide:bis) running at 150 V in 1/3x TBE buffer at 24 °C. Gels were run at 200 V for 2 hours, dried and exposed to a phosphor screen. The fraction of bi-substrate (*9mer + 32mer) was determined from the ratio of counts in the displaced RNA band (*9mer alone) relative to the total counts of the annealed and displaced RNA bands. The fraction of duplex RNA was plotted versus time and fit to a single exponential curve. All reported rates of unwinding represent the average of at least three measurements and the error is within 2-fold.

Western blots.

XL10-Gold® (Stratagene) or Tuner™ (DE3)pLacI (Novagen) modified to be RecA$^-$ (a gift from M.E. Saks) cells were transformed with wild type or mutant plasmids. Overnight cultures were diluted in LB, grown to OD_{600} ~ 0.3-0.4, then the cells were harvested, quick-cooled by pouring over an equal volume of ice and centrifuged. Cells were lysed as described by J. Charollais et. al. (Charollais et al. 2003) except the lysis buffer contained 20 mM Hepes pH 7.5, 30 mM NH_4Cl, 10 mM $MgCl_2$, and 4 mM β-Mercaptoethanol. Clarified lysates were diluted in lysis buffer plus 5x SDS load dye (85 mM Tris Hal pH 6.8, 4% SDS, 40% glycerol, 10% β-Mercaptoethanol, bromophenol blue) and then 10-25 μL were loaded on a 15% Tris-HCl Ready gel (Bio-Rad). Gels were transferred to PVDF (Bio-Rad) membrane in transfer buffer, 25 mM Tris HCl pH 8.3, 192 mM glycine, 20% methanol and 0.1% SDS, at 100 V for 1 hour at 4 °C. PVDF membranes were treated according to the Li-Cor Odyssey® manual, probed with a 1:10,000 dilution of rabbit anti-DbpA (provided by F. Fuller-Pace) and a 1:5000 dilution of secondary antibody Alexa Fluor® 680 goat anti-rabbit IgG (H+L) (Invitrogen) and then scanned on the Odyssey® Infrared Imaging System, which can report relative intensities of each band on the blot. The number of moles of each protein was estimated using a standard curve based on the band intensities for a serial dilution of purified DbpA protein. Molecules per cell were estimated using the number of moles divided by the approximate amount of cells (according to the volume collected and lysed) and loaded on the blot. Due to the small amount of endogenous DbpA, 40 times more of wild type Tuner™ (DE3)pLacI RecA$^-$ cells were loaded compared to those containing DbpA and mutant plasmids.

2.3. Results

DbpA mutant design.

Mutations were focused in regions of the protein expected to be involved in ATP binding and hydrolysis in order to disrupt the activity of DbpA without affecting its substrate binding. Although the complete structure of DbpA is not available, the structures of the C-terminal half of the ATPase core and the CTD of the *B. Subtilis* ortholog, YxiN, are known (Caruthers et al. 2000; Wang et al. 2006). The C-terminal half of the ATPase core forms a parallel αβ-fold as in other RNA helicase structures (Story and Steitz 1992; Yao et al. 1997; Zhao et al. 2004; Sengoku et al. 2006) and RecA (Story and Steitz 1992; Caruthers et al. 2000; Caruthers and McKay 2002), while the CTD structure as mentioned above forms a RRM-fold and is responsible for RNA binding and specificity (Wang et al. 2006). The structure of a closely related DEAD-box family member, *Drosophila* Vasa, in complex with single-stranded RNA and a non-hydrolyzable ATP analog, helps to identify the likely critical catalytic residues of DbpA (Figure 2.1). In addition, extensive biochemical characterization of ATPase core mutations in human eIF-4A and yeast Prp16, Prp22 and Prp43 have been reported (Pause and Sonenberg 1992; Schneider et al. 2002). Finally, several mutations in the ATPase active sites of yeast eIF-4A, Prp16, Prp22, Prp28, Prp43, Rok1p, Sub2p, Ded1p, Dbp8p were previously found to have dominant negative phenotypes (Schmid and Linder 1991; Hotz and Schwer 1998; Iost et al. 1999; Oh and Kim 1999; Schwer and Meszaros 2000; Daugeron and Linder 2001; Martin et al. 2002; Zhao et al. 2004; Cheng et al. 2005). Therefore, mutational analysis of DbpA was designed according to the structures, focusing on residues that contact ATP, and based on the other RNA helicase mutations that caused dramatic biochemical differences or dominant negative phenotypes.

Eleven DbpA residues that span four conserved motifs (I, II, III, and VI) were mutated to

Figure 2.1 Conserved ATPase motifs of DbpA

(A) Conserved ATPase core motifs with the conserved DbpA amino acid sequence below the corresponding motif. Residues mutated in this study are shown in bold. (B) *Drosophila* Vasa RNA helicase ATP binding pocket crystal structure (PDB: 2db3) showing only the residues that were mutated in DbpA (*E. coli* DbpA numbering). Colors coordinate to the motifs shown in A; purple, motif I; red, motif II; yellow, motif III; cyan, motif VI; and the AMPPNP is green. The white sphere is the Mg^{2+} that is coordinated to the AMPPNP. Important contacts to the AMPPNP, as defined for Vasa, are indicated with a dashed line.

A

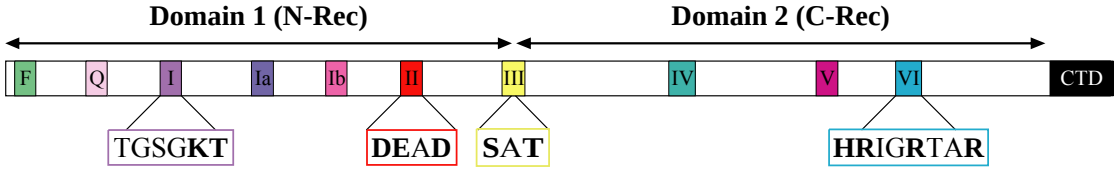
Domain 1 (N-Rec)
Domain 2 (C-Rec)
F
Q
I
Ia
Ib
II
III
IV
V
VI
CTD
TGSGKT
DEAD
SAT
HRIGRTAR

B

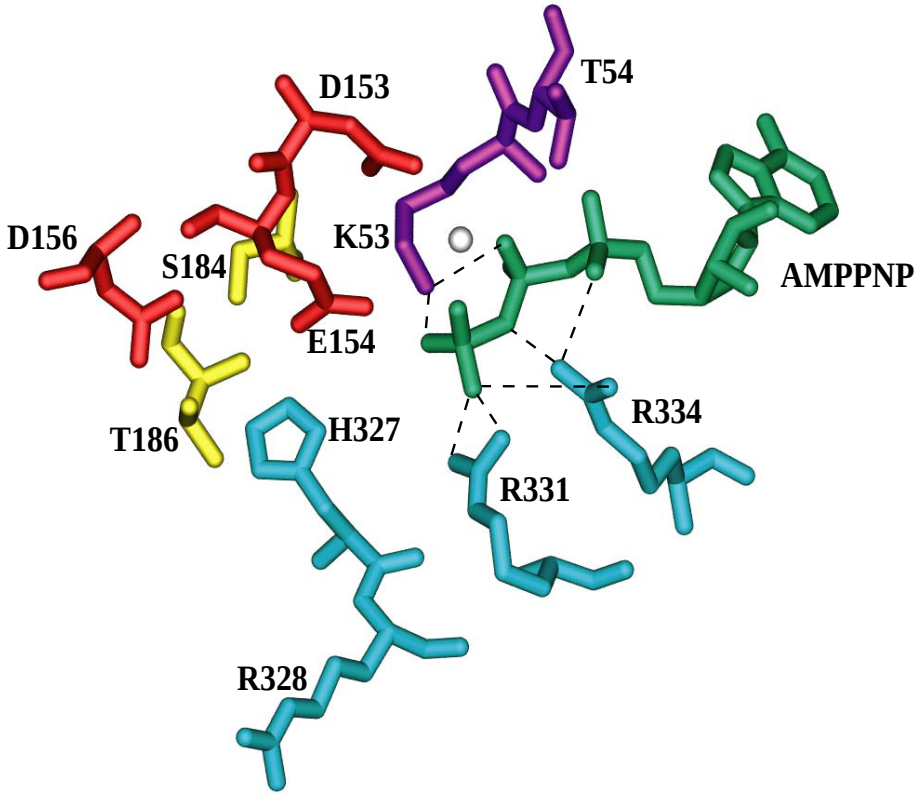
D153
T54
D156
K53
S184
AMPPNP
E154
R334
T186
H327
R331
R328

alanine. Motifs I, II, and III are in the N-terminal RecA-like domain of the catalytic core, (N-Rec) and motif VI lies in the C-terminal RecA-like domain of the core (C-Rec) (Figure 2.1). In the GSGKT sequence of motif I, also known as the Walker A motif, the conserved lysine (K53) hydrogen bonds with the β and γ phosphates of ATP, whereas the threonine (T54) coordinates a Mg^{2+} ion that also interacts with the β and γ phosphates (Caruthers and McKay 2002; Sengoku et al. 2006). In the DEAD sequence of motif II, the Walker B motif, the highly conserved aspartate (D153) and glutamate (E154) residues also coordinate the Mg^{2+} ion that interacts with the β and γ phosphates of ATP (Caruthers and McKay 2002; Sengoku et al. 2006) and are responsible for hydrolysis (Cordin et al. 2006). The last aspartate (D156) makes interdomain contacts with motif III (Caruthers and McKay 2002; Sengoku et al. 2006). The serine (S184), alanine (A185) and threonine (T186) residues that form motif III do not interact directly with ATP, but are thought to coordinate ATP binding and helicase activities (Pause and Sonenberg 1992). In the HRIGRTAR sequence, motif VI, the second arginine (R331) interacts with the γ phosphate of ATP, while the third arginine (R334) interacts with the α, β and γ phosphates (Caruthers and McKay 2002; Cordin et al. 2006; Sengoku et al. 2006). One of the arginines that contacts the γ phosphate is proposed to be an "arginine finger" that is involved in transition state stabilization during hydrolysis and may be critical for coupling the ATPase cycle with helicase activity (Caruthers and McKay 2002; Dittrich et al. 2004; Cordin et al. 2006; Sengoku et al. 2006).

RNA binding.

The majority of DbpA's RNA binding affinity is derived from the interactions of the CTD (Karginov et al. 2005) therefore, mutants in the ATPase motifs are not expected to

significantly affect binding. A native gel electrophoretic mobility shift assay was used to evaluate the binding affinity (K_d) of wild type DbpA and the eleven mutants for the 153-nucleotide fragment of 23S rRNA (Polach and Uhlenbeck 2002). In agreement with other experiments (Polach and Uhlenbeck 2002), the binding affinity for wild type DbpA is 1.7 nM and, as expected, most of the mutant proteins bind to substrate RNA with similar affinities (Figure 2.2 and Table 2.1). Surprisingly, the K_d for two of the mutants, D153A and R328A is approximately 10-fold weaker than wild type (Table 2.1). As with all the mutants, the CTD is likely to remain unchanged, so these two mutations must affect the overall structure of DbpA thereby, causing the decrease in binding affinity.

In the presence of saturating amounts of non-hydrolyzable ATP (AMPPNP), DbpA's binding affinity for 153mer RNA is 8.5-fold tighter (Figure 2.2) (Polach and Uhlenbeck 2002). This additional RNA binding affinity is thought to be due to interactions with the catalytic domains that only form when their structure is pre-organized by the binding of ATP (Polach and Uhlenbeck 2002). The RNA binding affinity of each mutant was measured in the presence of 153mer and AMPPNP to determine whether they have this additional affinity (Table 2.1). Most of the mutants displayed little or no increase in affinity when AMPPNP was present (Table 2.1) indicating that their ATP binding site is either partially or fully disrupted thus preventing the additional contacts with the RNA. Only two of the mutants, K53A and D156A, show a greater than 5-fold increase in RNA binding affinity in the presence of AMPPNP, suggesting that their ATP binding site remains nearly fully intact (Table 2.1).

RNA-dependent ATPase activity.

The ATPase activity of each mutant protein was initially assayed in the presence of 250

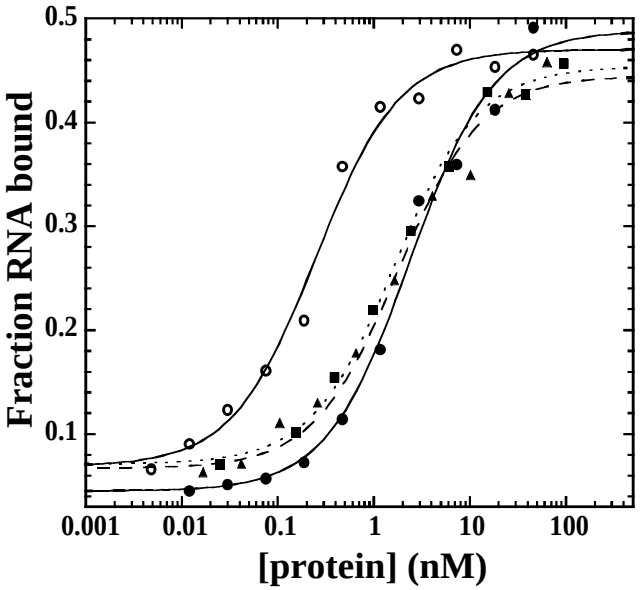

Figure 2.2 RNA binding curves for DbpA, H327A, and R334A

RNA binding curves for wild type DbpA (circles and solid line), H327A (triangles and dashed line), R334A (squares and dotted line) and wild type DbpA with 4 mM AMPPNP (open circles and solid line) derived from gel mobility shift assays. All experiments are performed with 200 pM 5'-^{32}P labeled 153mer RNA in binding buffer (50 mM Hepes pH 7.5, 5 mM $MgCl_2$, 100 mM KCl, 100 μM DTT, 100 μg/mL BSA, 5% (v/v) glycerol) and 70 μM polyA at 24 ºC.

Table 2.1 RNA binding affinity

Motif	Protein	K_d RNA (nM)	K_d RNA + AMPPNP (nM)
	wild type	1.7	0.2
I	K53A	2.4	0.4
	T54A	2.8	4.0
II	D153A	14	14
	E154A	5.0	3.4
	D156A	1.9	0.1
III	S184A	2.8	1.5
	T156A	1.8	0.9
VI	H327A	1.5	0.7
	R328A	18	18
	R331A	2.3	0.8
	R334A	1.1	0.4

Binding affinities for wild type and the eleven DbpA mutants to 153mer RNA in the absence and presence of 4 mM AMPPNP. Dissociation constants (*Kd*) were determined from data such as those presented in Figure 2.2. *Kd* RNA values are corrected for percent active protein and are averages of at least 3 determinations which vary by less than 2.5-fold.

nM 23S rRNA and 5 mM ATP which are saturating for wild type DbpA. For each mutation, the measured hydrolysis rate was plotted versus concentration of protein to determine the specific activity, k_{obs}. For all of the mutants, k_{obs} values were significantly reduced compared to wild type, with the activities ranging from less than 5% to approximately 70% active (Table 2.2). The mutants with high specific activity (D156A, S184A, T186A, and H327A) make interdomain contacts but do not contact the ATP directly (Figure 2.1B), suggesting that they are not directly involved in hydrolysis (Caruthers and McKay 2002). The two mutants with the lowest specific activity, R331A and K53A, both contact the phosphates of the ATP directly (Sengoku et al. 2006). This lysine is invariant in all ATPases, and when mutated usually abolishes hydrolysis and unwinding (Figure 2.1B) (Cordin et al. 2006). As expected, the K53A mutant of DbpA shows very weak ATPase activity (k_{obs} = 0.7 min^{-1}). Interestingly, K53A still demonstrates increased RNA binding affinity in the presence AMPPNP suggesting that the mutation affects catalysis without affecting ATP binding (Tables 2.1 and 2.2). It has been proposed that one of the arginines in motif VI acts as an "arginine finger" that stabilizes the transition state of the hydrolysis reaction and connects domain two to the ATP bound in domain one (Caruthers and McKay 2002). In DbpA, R331 is the likely "arginine finger" due to the very low ATPase activity (k_{obs} = 0.4 min^{-1}) of the mutant. Alanine substitutions of the other two arginines in motif VI of DbpA, (R328 and R334), have more ATPase activity than R331A and thus are less likely to serve as the arginine finger. In addition, R328 does not seem to bind the ATP in the crystal structure of Vasa (Figure 2.1B) (Sengoku et al. 2006).

Four mutants, D156A, S184A, T186A, and H327A, have sufficient ATPase activity to allow the determination of the apparent RNA binding constant, $K_{app, RNA}$, the maximum catalytic rate, k_{max}, and the Michaelis-Menten constants, $K_{M, ATP}$ and k_{cat}. $K_{app, RNA}$ and k_{max} were measured

Table 2.2 ATPase activity

Motif	Protein	k_{obs} (min^{-1})	k_{max} (min^{-1})	$K_{app, RNA}$ (nM)	k_{cat} (min^{-1})	$K_{M, ATP}$ (μM)
	wild type	120	140	33	160	400
I	K53A	0.7	--	--	--	--
	T54A	6.0	--	--	--	--
II	D153A	1.7	--	--	--	--
	E154A	2.0	--	--	--	--
	D156A	28	31	98	19	64
III	S184A	53	68	44	59	410
	T156A	79	97	64	87	1020
VI	H327A	50	82	210	58	2600
	R328A	1.1	--	--	--	--
	R331A	0.4	--	--	--	--
	R334A	14	--	--	--	--

ATPase activities of wild type and the eleven DbpA mutants in the presence of 23S rRNA substrate and ATP. The k_{obs} is the slope of a plot of the rate of ATP hydrolysis versus protein concentration at constant ATP (5 mM) and RNA (250-500 nM) at 24 ºC. The $K_{app, RNA}$, k_{max}, $K_{M, ATP}$ and k_{cat} for D156A, S184A, T186A and H327A were determined from data such as presented in Figure 2.3. Values are averages of at least 3 data sets and are within 2-fold error.

with 5 mM ATP and RNA concentration between 0 and 500 nM (Figure 2.3A), whereas the Michaelis-Menten values are measured at 250-500 nM RNA with ATP concentration between 0 and 4 mM ATP (Figure 2.3B). As had been determined previously, wild type DbpA has a very tight $K_{app,\ RNA}$ of 33 nM (Table 2.2) (Tsu and Uhlenbeck 1998). The mutants D156A, S184A, and T186A all have apparent binding constants within 2.5-fold of wild type (Table 2.1 and Figure 2.2), indicating that they bind substrate RNA equally well. This conclusion is consistent with the gel mobility shift data for these mutants, except for H327A, which has a 6-fold higher $K_{app,\ RNA}$ even though the K_d is similar to wild type (Tables 2.1 and 2.2). This discrepancy could be due to the weaker ATP binding of this mutant or just an artifact of the indirect measurement of RNA binding using the ATPase assay.

The Michaelis-Menten constant for wild type DbpA ($K_{M,\ ATP}$ = 400 μM) is consistent with a previous measurement (Table 2.2 and Figure 2.3B) (Tsu and Uhlenbeck 1998). $K_{M,\ ATP}$ values for T186A and H327A are moderately weaker than wild type DbpA, while mutant D156A shows a slightly tighter $K_{M,\ ATP}$ than wild type, suggesting that it may bind ATP better (Figure 2.3B, Tables 2.1 and 2.2). These data are all consistent with gel mobility shift data in the presence of AMPPNP described earlier. The two mutants that fail to bind ATP in this assay do not increase in affinity for RNA when AMPPNP is present in the gel shift assay. The D156A mutant has a tighter $K_{M,\ ATP}$ which is also reflected by the 20-fold increase in binding affinity when AMPPNP is present compared with the 10-fold increase for wild type DbpA (Table 2.1). The only inconsistency between the two assays is in the case of S184A, which binds ATP equally well as wild type ($K_{M,\ ATP}$ = 410 μM) but does not show an expected increase in affinity for RNA in the presence of AMPPNP in gel shift assays (Tables 2.1 and 2.2).

Figure 2.3 ATPase activity of DbpA and four mutants

ATPase activities for wild type DbpA (circles), D156A (diamonds), S184A (upside down triangles), T186A (squares), and H327A (triangles) at (A) saturating ATP (5 mM) and RNA concentration between 0 and 500 nM and (B) saturating RNA (250-500 nM) and ATP concentration between 0 and 4 mM. All experiments were carried out in 50 mM Hepes pH 7.5, 10 mM $MgCl_2$, 50 mM KCl, 100 μM DTT, 200 μM NADH, 1 mM phospho(enol)pyruvate, 10 mM phosphate kinase/lactate dehydrogenase buffer at 24 ºC. Lines are the best fit of the data using the Michaelis-Menton equation.

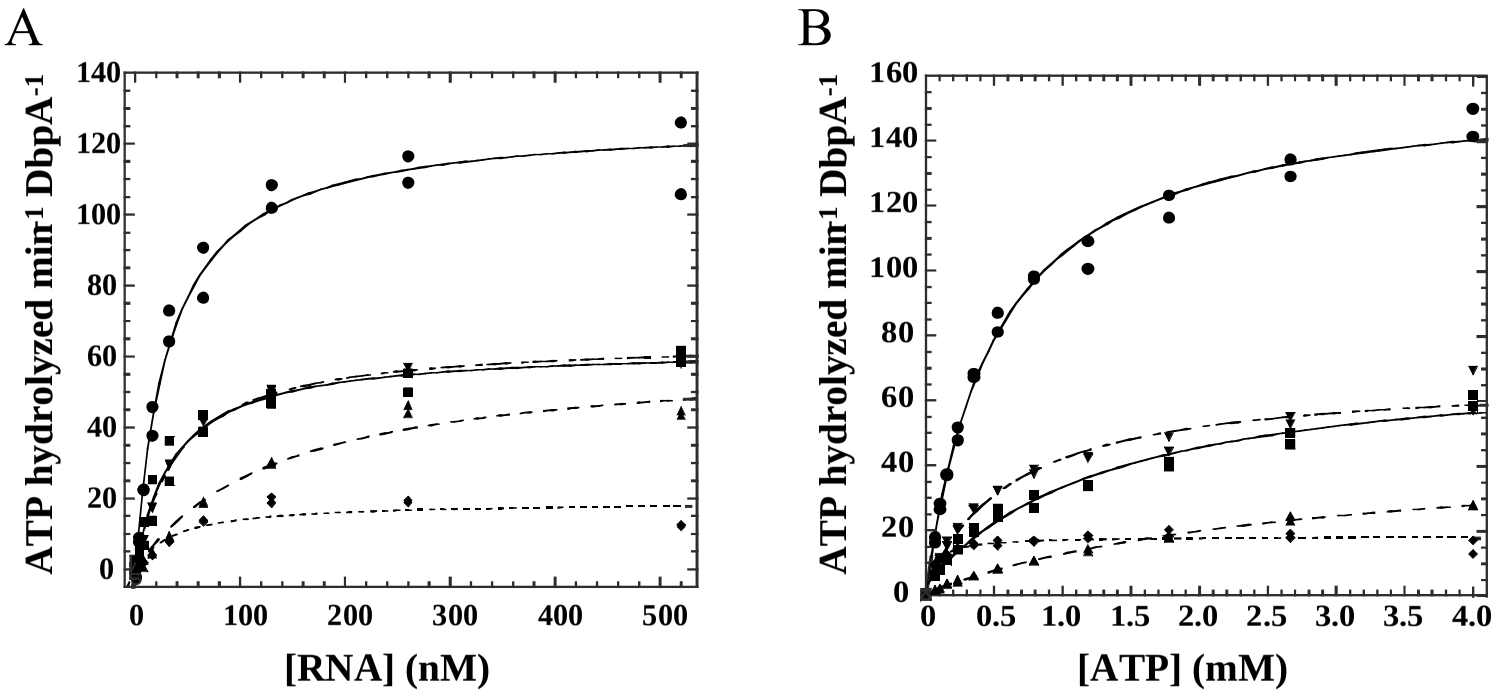
A
ATP hydrolyzed min-1 DbpA-1
140
120
100
80
60
40
20
0
0
100
200
300
400
500
[RNA] (nM)
B
ATP hydrolyzed min-1 DbpA-1
160
140
120
100
80
60
40
20
0
0
0.5
1.0
1.5
2.0
2.5
3.0
3.5
4.0
[ATP] (mM)

RNA helicase assay.

The RNA substrate used in the helicase assay contains a 32 nucleotide oligomer containing hairpin 92 annealed to a 5'-^{32}P labeled 9mer (Figure 2.4A) (Diges and Uhlenbeck 2005). In the presence of saturating (2 mM) ATP, wild type DbpA unwinds the substrate at a rate of 2.2 min^{-1} (Figure 2.4B). As expected, the majority of the mutants that hydrolyze ATP poorly; K53A, D153A, E154A, R328A, and R331A are unable to unwind the duplex RNA substrate (Table 2.3). However, T54A, D156A, S184A, T186A, and H327A, which have k_{obs} greater than ~6 min^{-1}, can unwind the RNA duplex at varying rates. Interestingly, R334A has a higher k_{obs} of 14 min^{-1} (~12% active), but cannot unwind the duplex (Figure 2.4B, Tables 2.1 and 2.3). In the structure of *Drosophila* Vasa, the equivalent Arginine (R582) seems to contact all phosphates of the AMPPNP (Sengoku et al. 2006). It is possible that this residue is more involved in release of ATP and coordination of the hydrolysis to helicase action, which would result in this uncoupling of activities.

Growth phenotype.

The wild type *dbpA* gene was cloned into the pET-3a system (Novagen) where the target genes are under the control of the T7 RNA polymerase promoter (Karginov and Uhlenbeck 2004). Eleven point mutations were made using this *dbpA*-containing plasmid and Stratagene's QuikChange® XL Site-Directed mutagenesis kit. Plasmids were initially transformed into the T7-lacking *E. coli* XL10-Gold strain (Stratagene). When mutant DbpA plasmids were transformed into XL10-Gold, all eleven strains behaved the same as wild type DbpA and wild type XL10-Gold controls. In order to produce protein for biochemical studies, the same eleven plasmids were transformed into *E. coli* BL21(DE3) pLysS (Stratagene), which harbors a T7

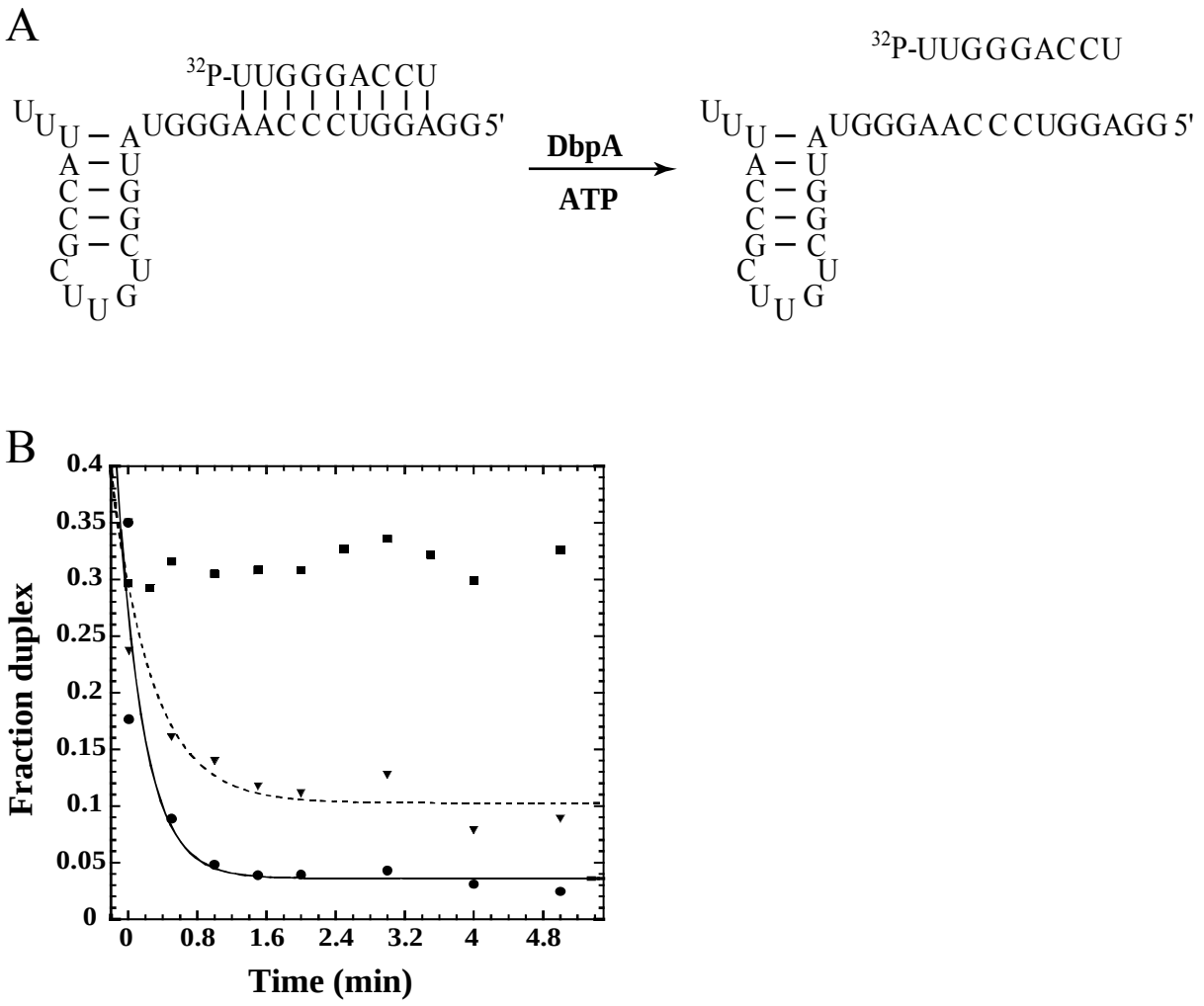

Figure 2.4 ATP-dependent unwinding activity

(A) An annealed duplex consisting of 32mer containing hairpin 92 and 5'-^{32}P labeled 9mer, is unwound upon addition of DbpA and saturating ATP (2 mM). (B) Helicase assays for wild type DbpA (circles), S184A (triangles), and R334A (squares) performed in binding buffer in the presence of 600 nM protein, 5 nM duplex RNA and 2 mM ATP at 24 ºC. Lines are the best fit of the data and an end point using a single exponential equation.

Table 2.3 Helicase activity

Motif	Protein	unwinding rate (min^{-1})
	wild type	2.2
I	K53A	<0.1
	T54A	0.1
II	D153A	<0.1
	E154A	<0.1
	D156A	0.4
III	S184A	0.8
	T156A	0.2
VI	H327A	0.3
	R328A	<0.1
	R331A	<0.1
	R334A	<0.1

Unwinding rates were determined from data such as those presented in Figure 2.4 and are the average of at least 3 separate determinations that vary by less than 2-fold.

RNA polymerase gene under control of the lac repressor. During the course of this experiment we noticed that strains containing the R331A mutant plasmid consistently produced a small colony phenotype while the other ten strains showed colony sizes similar to controls (BL21(DE3) pLysS with wild type DbpA plasmid and BL21(DE3) pLysS expressing endogenous levels of DbpA). This small colony phenotype for R331A is only seen in cells containing the T7 RNA polymerase gene and is likely the result of "leaky" expression of the mutant from the plasmid (Studier and Moffatt 1986). Presumably, the nonfunctional R331A protein from the multicopy plasmid competes with the endogenous DbpA to produce the small colony phenotype. It is striking that none of the other DbpA mutations show the small colony phenotype, even when cells are plated at 24 °C instead of 37 °C because mutations in DExD/H proteins are often cold sensitive (Noble and Guthrie 1996; Charollais et al. 2003; Charollais et al. 2004). This may reflect the fact that of the eleven mutations tested, R331A shows the lowest amount of ATPase activity (Table 2.2). To confirm that the small colony phenotype was a consequence of the R331A point mutation, the mutation was made a second time with identical results.

Two additional growth experiments support the idea that the small colony phenotype results from competition between the R331A protein and the endogenous wild type DbpA. First, when the R331A plasmid is transformed into *E. coli* BL21(DE3) cells, even smaller colonies are observed, consistent with an even greater amount of "leaky" plasmid expression in the absence of the pLysS gene encoding the T7 lysozyme, which inhibits T7 RNA polymerase (Studier 1991). Second, when the R331A plasmid is transformed into an *E. coli* BL21(DE3) strain with a deletion of the DbpA gene (provided by I. Iost), even smaller colonies were observed, which is expected when the competing wild type protein is unavailable. Finally, if T7 RNA polymerase is

induced by the addition of 1 mM IPTG to any of the strains discussed above, there is no significant change in the results. Presumably, the relatively large amount of "leaky" expression from the plasmid encoded gene is more than sufficient to compete with the wild type protein.

Further analysis of the R331A mutant in BL21(DE3) pLysS cells was complicated by the fact that when cells were grown in liquid culture for many hours, and then plated, the colony size was no longer homogenously small. Instead, a significant fraction of larger colonies was observed. This phenotypic instability is probably the result of recombination between the mutant plasmid gene and the genomic copy of the DbpA gene. Thus, the R331A plasmid and several other mutations were transformed into a Tuner™ (DE3) pLacI RecA$^-$ strain. In this case the small colony phenotype of R331A still occurs (Figure 2.5A) and is much more stable at both 22 °C and 37 °C. When the R331A mutation in Tuner™ (DE3) pLacI RecA$^-$ was grown in liquid culture at both temperatures, it had a modestly slower growth rate (1.6 fold at 37 °C, 2.2-fold at 22 °C) than either the wild type DbpA or the empty vector control (Figure 2.5B). In addition, at both temperatures, cells harboring the R331A mutation took significantly longer to exit stationary phase and enter log phase (Figure 2.5B).

To compare the expression of uninduced R331A mutant with that of endogenous DbpA, a semi-quantitative western blot experiments using a polyclonal antibody against DbpA (provided by F. Fuller-Pace) were performed on the R331A mutant and wild type DbpA expressed in Tuner™ (DE3) pLacI RecA$^-$ along with K53A in Tuner™ (DE3) pLacI RecA$^-$ and wild type Tuner™ (DE3) pLacI RecA$^-$ controls (Figure 2.6). The amount of endogenous DbpA present in wild type cells cannot be detected even when large amounts of lysate are analyzed. Based upon the detection limit of the DbpA antibody, we estimate that there are less than 1,000 molecules of DbpA per cell. However, when plasmids containing wild type DbpA, R331A or K53A are

Figure 2.5 Growth phenotype of R331A

(A) Wild type DbpA and mutants K53A and R331A in Tuner™ (DE3) pLacI RecA$^-$ cells at 37 ºC. (B) Growth rates and doubling times at 22 ºC for DbpA (circles, 113 min), K53A (squares, 134 min), and R331A (triangles, 251 min) in Tuner™ (DE3) pLacI RecA$^-$ cells (M.E. Saks). Doubling times are an average of 3-4 growth experiments.

A

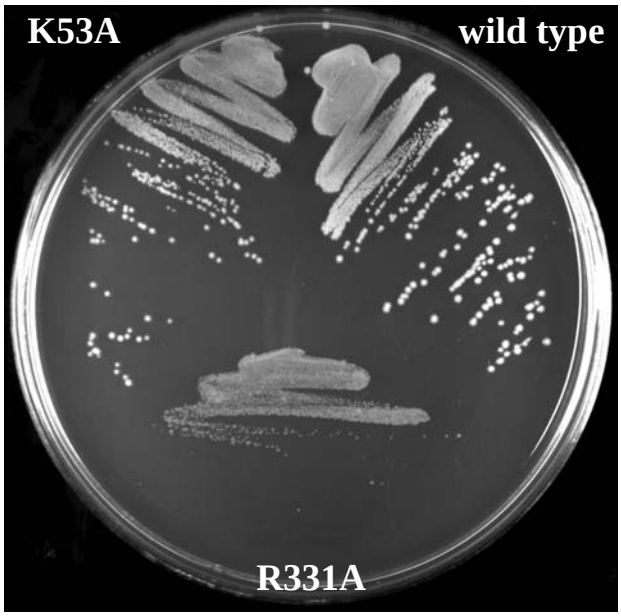

B

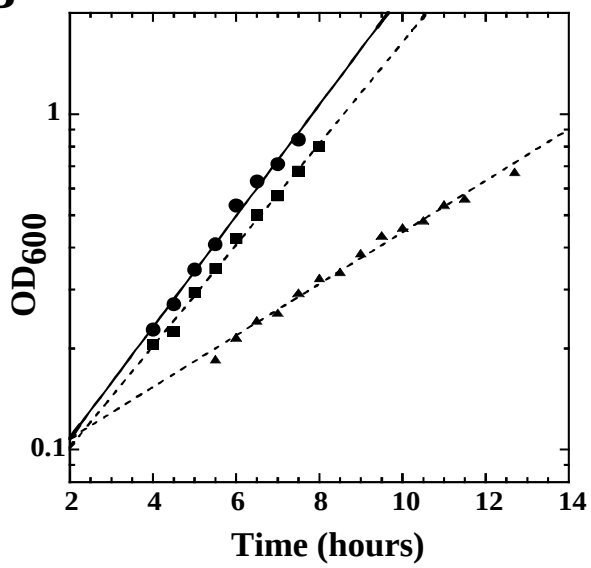

present, much larger amounts of protein were observed. Based on three separate experiments ~75,000 copies per cell could be estimated for all three proteins. This high level of expression is observed as the result of "leaky" expression from T7 RNA polymerase (Studier and Moffatt 1986) compounded by the multiple copies of the plasmid. Because the amount of R331A protein is not significantly different from the others, its small colony phenotype is not due the presence of a larger or smaller amount protein. Furthermore, the 75-fold excess of R331A mutant protein over endogenous DbpA protein means that it can effectively compete for the available 23S rRNA hairpin 92 binding site, despite the fact that in the presence of ATP it binds less well than wild type DbpA.

2.4. Discussion

The mutations in the active site of DbpA possess similar biochemical properties as those observed in several other DExD/H proteins including, human eIF-4A, yeast Prp16, Prp22, Prp43 (Pause and Sonenberg 1992; Martin et al. 2002; Schneider et al. 2002). The classic ATPase motifs I and II, also known as the Walker A and B motifs, are highly conserved and important in the ATP hydrolysis cycle (Caruthers and McKay 2002; Cordin et al. 2006). In DbpA, alanine substitution of the strictly conserved residues of these motifs (K53, T54, D153, and E154), causes drastic reductions in ATP hydrolysis rates and helicase activities as expected. Residue K53 of motif I is expected to make contacts with the β and γ-phosphates of ATP and, when mutated in DbpA, k_{obs} is low (0.7 min^{-1}) and helicase activity is abolished. According to crystal structures and other mutagenesis data, motif II residue E154 coordinates a Mg^{2+} ion while the D153 residue binds to the ATP through that Mg^{2+} and is proposed to catalyze hydrolysis of the β–γ phosphate bond (Caruthers and McKay 2002; Cordin et al. 2006). Similar mutation of all

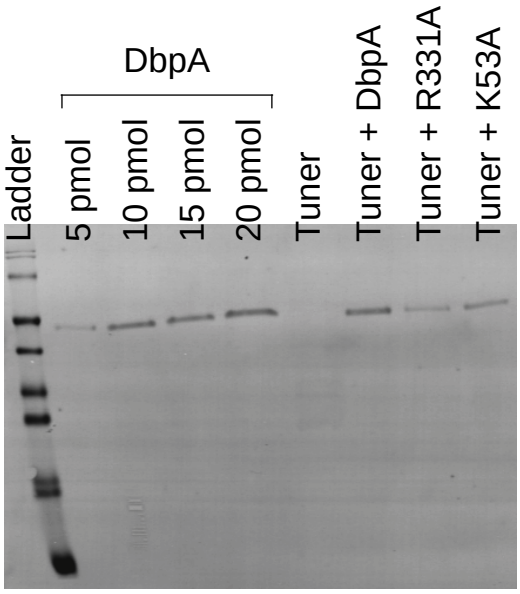

Figure 2.6 Western blot of cell lysates

A serial dilution of purified DbpA was used to calibrate the sensitivity of the blot and allow an estimate of the amount of DbpA present in a given cell, lanes 2-5. Aliquots of 10-25 μL of clarified lysates from Tuner™ (DE3)pLacI with no plasmid or with wild type *dbpA*, K53A, or R331A plasmids were run on a 15% SDS gel and probed with anti-DbpA antibody (provided by F. Fuller-Pace).

these residues to alanine in yeast Prp22, Prp16 and Prp43, as well as more conservative mutation to other residues in human eIF-4A, also show little to no ATPase and no RNA helicase activity (Pause and Sonenberg 1992; Martin et al. 2002; Schneider et al. 2002). In contrast with the Walker A and B residues, crystal structures of Vasa show that the last residue of motif II, D156, does not contact the ATP but instead makes interdomain contacts with the H327 of motif VI (Sengoku et al. 2006). In DbpA, D156A is the only mutant from these two motifs that has significant ATPase activity and moderate helicase activity as also shown with similar mutations of this last residue (D/H) in HCV NS3, human eIF-4A, and yeast Prp16 and Prp43 (Pause and Sonenberg 1992; Kim et al. 1997; Martin et al. 2002; Schneider et al. 2002).

Motif III does not contact ATP directly but makes important interdomain contacts, i.e. S184 and T186 contact D156 in motif II and T186 contacts H327 in motif VI, which most likely assists in domain closure (Sengoku et al. 2006). Individual mutations of S184 and T186 to alanine in DbpA only moderately decrease helicase and ATPase activity similar to Prp16 and Prp43 (Martin et al. 2002; Schneider et al. 2002). However, simultaneous mutations of the serine and threonine in motif III of human eIF-4A causes a small decrease in ATP hydrolysis while almost completely abolishing unwinding, suggesting this motif is coupling the ATPase and helicase activities (Pause and Sonenberg 1992).

Motif VI, unlike motifs I, II and III, is found in domain 2, along the ATP binding pocket at the interface of the two domains (Figure 2.1B). As mentioned above, H327 makes contacts to domain 1 and to motif III (Sengoku et al. 2006) and its mutation to alanine in DbpA, like the other interdomain contacting mutants, (D156A, S184A, and T186A) only moderately affects the ATPase and helicase activities. However, individual mutations of each of the three arginines all have severe effects on ATPase and helicase activity as seen with yeast Prp16, Prp 22, and human

eIF-4A (Polach and Uhlenbeck 2002; Schneider et al. 2002). Two of these arginines in the Vasa structure, R331 and R334, make contacts with the ATP (Figure 2.1B) (Sengoku et al. 2006) and when mutated to alanine in DbpA, k_{obs} decreases to less than 12% of wild type for R334A and less than 0.5% of wild type for R331A (Table 2.2). The first arginine of motif VI, R328, does not contact the ATP but also has severely decreased ATPase activity when mutated in DbpA (Figure 2.1B and Table 2.2). The reduced binding affinity of the R338A mutant might explain the low k_{obs} (Table 2.1 and 2.2) but it is unclear why the binding is affected. One of the arginines in motif VI is thought to act as an "arginine finger", important in transition state stabilization of the ATP hydrolysis cycle (Caruthers and McKay 2002; Dittrich et al. 2004; Cordin et al. 2006). Out of the three arginine mutations in DbpA, the R331A mutant has the most dramatic effect, with no helicase activity, and the lowest k_{obs} of 0.4 min^{-1} (Tables 2.2 and 2.3). Therefore, we propose that R331 is most likely to act as the "arginine finger" in DbpA.

The DbpA R331A mutant is also the only one of the eleven ATPase mutants that displays a dominant negative phenotype (Figure 2.5). It is interesting to compare its biochemical properties to the K53A mutation, which does not display a phenotype. In other DExD/H helicases, yeast Prp16, Prp22, Prp43 and human and yeast eIF-4A, mutations in either of the amino acids corresponding to K53 or R331 result in lethal or dominant negative phenotypes and greatly reduced ATPase and helicase activities (Schmid and Linder 1991; Pause and Sonenberg 1992; Hotz and Schwer 1998; Martin et al. 2002; Schneider et al. 2002). In DbpA, the severely decreased ATPase activity for R331A and K53A are nearly the same (0.4 and 0.7 min^{-1} respectively) and both show no helicase activity (Tables 2.2 and 2.3). They both can bind substrate well (Table 2.1) and therefore both should block the binding and activity of the wild type protein *in vivo*. Why then does only the R331A mutation show a phenotype? The only

major biochemical difference between the two mutant proteins is, that K53A binds RNA substrate 6-fold tighter in the presence of AMPPNP, similar to wild type DbpA, where the R331A binding affinity for RNA is only 3-fold tighter when AMPPNP is present (Table 2.1). This would suggest that the K53A mutation would be more effective than the R331A mutation in competing with wild type protein *in vivo* where ATP is present. Thus a more likely explanation of this caveat lies in the specific activities of the two mutant proteins. It could be that the slightly higher residual ATPase activity of the K53A mutation is sufficient to permit the catalytic cycle and substrate rearrangement to occur and thus avoid the phenotype. In contrast, the R331A mutation eliminates the "arginine finger" which thereby removes the ATP-dependent interdomain motion that is critical for helicase function (Dittrich et al. 2004).

Until now, there has not been an available DbpA phenotype. This dominant slow growth mutation will be extremely useful to further investigate the molecular function of DbpA (Nicol and Fuller-Pace 1995). From what is known thus far, DbpA is expected to be important in some role of ribosome biogenesis or translation because it interacts with the 23S rRNA at the peptidyl transferase center. Initially, it will be interesting to study the ribosome populations in the mutant strains to hopefully begin to understand the actual function of DbpA *in vivo*.

CHAPTER 3

A dominant negative mutant of the *E. coli* RNA helicase DbpA blocks assembly of the 50S ribosomal subunit

3.1 Introduction

Biogenesis of the two subunits of the *E. coli* 70S ribosome involves coordinated transcription, processing and folding of three ribosomal RNA (rRNA) molecules along with the sequential binding of the 54 ribosomal proteins (r-proteins) in a process called the assembly gradient (Spillmann et al. 1977; Sieber and Nierhaus 1978). *In vivo* ribosome assembly progresses via two small subunit (30S) precursors (Mangiarotti et al. 1968; Nierhaus et al. 1973) and three large subunit (50S) precursors (Mangiarotti et al. 1968; Osawa et al. 1969; Hayes and Hayes 1971; Nierhaus et al. 1973), which are short-lived at normal growth conditions (Lindahl 1975). Reconstitution of the individual subunits from natural rRNA and total r-proteins (TP30 and TP50) is characterized by intermediate particles (Traub and Nomura 1969; Nierhaus and Dohme 1974; Dohme and Nierhaus 1976) which are similar in sedimentation value and r-protein content to the precursors observed *in vivo* (Homann and Nierhaus 1971; Spillmann et al. 1977). Therefore, assembly maps (Held et al. 1974; Herold and Nierhaus 1987) that define the sequence of r-protein binding events and concurrent rRNA folding during *in vitro* reconstitution are good models for the biogenesis of ribosomes *in vivo*. Although it is likely that ribosome assembly *in vivo* and *in vitro* progress via similar pathways, successful reconstitution requires non-physiological conditions such as long incubation times and elevated temperatures to overcome kinetic barriers due to misfolding of the rRNA (Williamson 2003). Recent genetic and

biochemical experiments have identified several proteins that act transiently with the maturing ribosome that may serve to overcome similar kinetic barriers *in vivo* (Kaczanowska and Rydén-Aulin 2007; Wilson and Nierhaus 2007). These ribosomal assembly factors have been implicated in the assembly of both subunits, although more are involved in 50S subunit assembly possibly because of its larger size and much more complex tertiary structure (Ban et al. 2000; Yusupov et al. 2001). The more than 20 *E. coli* ribosomal assembly factors identified to date have been categorized into three groups; maturation factors, GTPases, and DEAD-box proteins (Kaczanowska and Rydén-Aulin 2007), although their exact roles in assembly are yet to be defined.

One putative large subunit assembly factor is the biochemically well characterized *E. coli* DEAD-box ATPase, DbpA which hydrolyzes ATP only in the presence of fragments of 23S rRNA containing hairpin 92, which is found in the PTC (Nicol and Fuller-Pace 1995; Tsu and Uhlenbeck 1998). DbpA contains a CTD that folds into an RRM that binds tightly and specifically to hairpin 92, targeting DbpA to the PTC (Kossen et al. 2002; Karginov et al. 2005; Wang et al. 2006). The ATPase active site of DbpA is formed between two RecA-like domains that bind to regions of rRNA near hairpin 92 as shown by the extended footprint (Karginov and Uhlenbeck 2004) and increased binding affinity in the presence of AMPPNP (Polach and Uhlenbeck 2002). Although the biological function of DbpA is yet to be established, the fact that 50S subunits and mature 70S ribosomes fail to stimulate ATPase activity led to the hypothesis that it acts in ribosome assembly rather than translation (Tsu and Uhlenbeck 1998). Additionally, under different growth temperatures DbpA deletion mutants grow normally (Baba et al. 2006; Iost and Dreyfus 2006) although, in the presence of low levels of chloramphenicol Δ*dbpA* strains display small colonies on solid media (unpublished data Sharpe Elles, L. and

Uhlenbeck, O. C.). This is interesting since chloramphenicol binds in the PTC (Schlünzen et al. 2001; Hansen et al. 2003) near the DbpA binding site and addition of low, non-toxic, levels of this antibiotic to *E. coli* cultures also slows ribosome assembly sufficiently to yield precursor particles (Osawa et al. 1969). Since effects from the slow growth of the Δ*dbpA* deletion strain in the presence of chloramphenicol were difficult to separate from the effects of chloramphenicol alone, DbpA mutants containing individual alanine substitutions of highly conserved residues in the ATPase motifs were tested for dominant negative effects *in vivo*. As described in a previous paper (Sharpe Elles and Uhlenbeck 2008), one of eleven active site mutants resulted in a dominant negative, slow growth phenotype when overexpressed in a wild type background. This R331A mutant is still able to bind substrate rRNA but is almost completely inactive in ATPase and helicase activities. Here we examine the effects of overproducing the R331A mutant protein on the assembly of the 50S subunit *in vivo*.

3.2. Materials and Methods

Protein, RNA and DNA preparation

Site-directed mutagenesis of *dbpA* and purification of DbpA, R331A, K53A, and E154A proteins were performed as described previously (Karginov and Uhlenbeck 2004; Sharpe Elles and Uhlenbeck 2008).

BL21(DE3) Δ*dbpA* was a generous gift from I. Iost. The deletion was originally constructed in the strain WJW45 by replacing the *dbpA* ORF with a kanamycine resistance gene (Zhang et al. 1998). A tetracycline marker, Tn10, near the *dbpA* region (using strain CAG 12081, zda-3061::tn10) was added for transduction selection into BL21(DE3) cells. The resulting strain is kanamycine and tetracycline resistant.

Native *E. coli* ribosomal RNA (23S + 16S rRNA), RNA from ribosomal subunits collected from sucrose gradients (described below), and 23S rRNA transcript was transcribed from pCW1 (Tsu and Uhlenbeck 1998) were prepared as described in Sharpe Elles 2008. The 32 nucleotide minimal substrate for DbpA (Diges 2001; Tsu et al. 2001) and 2'-O-methyl U2552 derivative were purchased from IDT DNA.

DNA primers (listed below) were purchased from IDT DNA and 5'-^{32}P labeled with polynucleotide kinase and γ-^{32}P ATP. Labeled DNA was purified by 20% denaturing PAGE, extracted from the gel by passive elution overnight at 4 °C and then precipitated with ethanol.

DNA Primer Sequences:

1. Primer 1 (complementary to residues 35-55 of 23S rRNA): 5'-CCT TCA TCG CCT CTG ACT GCC-3' (Charollais et al. 2003).
2. Primer 2 (complementary to residues 2567-2592 of 23S rRNA): 5'-CGT TCT AAA CCC AGC TCG CGT ACC AC-3'
3. Primer 3 (complementary to residues 2519-2545 of 23S rRNA): 5'-CCC TTG GGA CCT ACT TCA GCC CCA GGA-3'

Ribosome profiles

Plasmids containing wild type *dbpA* or mutants, K53A, E154A or R331A were transformed into *E. coli* Tuner™ (DE3) pLacI (Novagen) modified to be RecA$^-$ (a gift from M.E. Saks), grown to OD_{600} ~0.3-0.4, quick-cooled by pouring over ice and harvested by centrifugation in a Sorvall SLC6000 rotor spun at 6000 RPM for 12 min. Cells were lysed as described previously (Charollais et al. 2003) except the lysis buffer contained 20 mM Hepes pH 7.5, 30 mM NH_4Cl, 10 mM $MgCl_2$, and 4 mM β-Mercaptoethanol. Clarified lysate was layered

over 40% sucrose in buffer A (10 mM $MgCl_2$, 20 mM Hepes KOH pH 7.5, 150 mM NH_4Cl, 4 mM β-mercaptoethanol) and centrifuged in a Type 70.1 Ti rotor in a Beckman Optima LE-80K ultracentrifuge at 42,000 RPM and 4 ºC for 15 hours twice to purify the ribosomes. Pelleted ribosomes were resuspended in buffer B (10 mM $MgCl_2$, 50 mM Hepes KOH pH 7.5, 50 mM KCl), aliquoted and used immediately or flash frozen and stored at -80 ºC. To separate polysomes, 70S ribosomes and the individual subunits, clarified lysate or purified ribosomes were loaded onto linear gradients containing 10-50% sucrose in buffer A and centrifuged in a Beckman SW-41 rotor at 24,000 RPM and 4 ºC for 13.37 hours. To completely dissociate all polysomes and 70S ribosomes into the individual subunits, clarified lysate or purified ribosomes were loaded onto linear gradients containing 20-40% sucrose in buffer C (1 mM $MgCl_2$, 20 mM Hepes KOH pH 7.5, 150 mM NH_4Cl, 4 mM β-mercaptoethanol) and centrifuged in a Beckman SW-41 rotor at 31,500 RPM and 4 ºC for 14 hours. Gradients were analyzed and fractionated using a Teledyne Isco density gradient system with a UA-6 detector and Foxy Jr. fraction collector. Fractions were collected in a 96-well flat bottom UV-Vis plate and analyzed with a Molecular Devices plate reader at 254 nm. Fractions corresponding to 70S ribosomes, 50S or 30S subunits, or 45S particles were pooled and pelleted by centrifuging in a Beckman Type 70.1 Ti rotor at 40,000 RPM and 4 ºC for 15 hours. Pelleted ribosomes and subunits were resuspended in buffer B and loaded on subsequent gradients at the same conditions to further purify the subunits. Pelleted subunits were resuspended in buffer B and flash frozen and stored at -80 ºC. Analytical ribosome profiles were analyzed by pumping the gradient through a flow cell cuvette and measuring the Absorbance at 254 nm every 2 seconds over a total of 18 min with a SpectraMax Plus 384 spectrophotometer (Molecular Devices).

Recombination of 70S ribosomes from subunits was performed by incubating 50S

subunits or 45S particles with 30S subunits from MRE600 cells in buffer B at 37 °C for 30 minutes. This was then loaded onto sucrose gradients containing 10 mM Mg^{2+} and analyzed with a flow cell cuvette as explained above. Additional recombination experiments were performed in the presence of 1.8 μM DbpA and 2 mM ATP or 10 pmol $tRNA^{fmet}$ and 10 pmol mRNA, a 27 nucleotide oligomer derived from the initiation region of the T4 gp32 mRNA that has been used for X-ray crystallographic studies of mRNA bound to the ribosome (Fahlman et al. 2004), and analyzed similarly.

Partial reconstitution of 50S subunits was performed by adding 1 μM DbpA and 15 mM ATP to fresh R331A lysates, incubating at 24 °C for 60 min and analyzed by running on 20-40% sucrose gradients containing 1 mM Mg^{2+} followed by measuring the absorbance of the gradient in a flow cell cuvette as described above.

Primer Extension

Detection of single nucleotide modifications was performed by primer extension in the presence of a low concentration of dNTPs based on experiments described previously (Lowe and Eddy 1999). 5'-^{32}P end labeled 23S DNA Primer 2 or 3 (300 nM) were annealed to 23S + 16S rRNA or rRNA purified from 50S subunits or 45S particles (150 nM) in annealing buffer (500 mM Tris HCl pH 7.5, 500 mM KCl and 100 mM DTT) by heating at 95 ºC for 2 minutes then 50 ºC for 5 minutes and cooling on ice for 5 minutes. Reverse transcription was performed in the presence of high (1 mM) or low (4 μM) dNTPs and 1 unit AMV RT enzyme and 1X reaction buffer (Promega) at 37 ºC for 1 hour. To each reaction tube, 1 μg of RNaseA was added and then incubated for 1 hour at 37 ºC. Formamide load dye was added and the entire reaction

loaded on a 20% acrylamide sequencing gel and run at 100 W for ~8 hours. Gels were exposed to phosphor screens overnight.

Primer extension to determine the length of the 5' end of 23S rRNA from purified 50S subunits and 45S particles was performed using 5'-^{32}P end labeled DNA Primer 1 annealed to rRNA purified from 50S subunits or 45S particles as above. Reverse transcription was performed as above with 1 unit of AMV RT in the presence of 1 mM dNTPs.

LiCl washed 50S subunits (LiCl cores)

MRE600 cells grown to midlog at 37 °C were lysed and run on 20-40% sucrose gradients containing 1 mM Mg^{2+} as explained above. Fractions containing 50S subunits were collected and purified on 40% sucrose cushions as explained above. Purified 50S subunits were washed with 0.4 M, 0.6 M, or 0.8 M LiCl in wash buffer (1 M TrisHCl pH 7.5, 1 M MgOAc) for 5 hours on ice and pelleted as described previously (Homann and Nierhaus 1971; Nierhaus and Montejo 1973). Particles were resuspended in buffer B flash frozen and stored at -80 °C.

Mass spectrometry protein analysis

Ribosomal subunits and particles collected from sucrose gradients were analyzed for ribosomal protein content using electrospray ionization time-of-flight mass spectrometry (ESI-TOF MS). Total proteins from wild type DbpA and R331A 50S subunits and 45S particles were purified by TCA precipitation. A 50-100 pmol aliquot of these purified proteins were mixed with an equal volume of a standard mixture of fully ^{15}N-labeled L-proteins and subjected to an overnight digestion by trypsin. The resulting mixture of labeled and unlabeled peptides was analyzed by ESI-TOF MS, with pairs of peaks matched to unlabeled and ^{15}N-labeled versions of

a single peptide based on the mass/charge ratio of the peaks and the charge of the ions. Typically, on average data on multiple peptides are collected for each protein; however there are several individual proteins from which only 1-2 peptides were observed in multiple experiments.

The unlabeled fraction for each peptide was determined from the amplitude of the unlabeled and ^{15}N-labeled isotope distributions as described in (new Williamson paper), giving a relative amount of peptide (and thus a relative amount of protein) compared to the ^{15}N-labeled standard mixture. The unlabeled fraction was then normalized according to the value obtained for protein L2, which is a primary binding protein and thus anticipated to be present at maximum in all samples. In addition, L2 is a large protein, which consistently provides a higher than average number of peptides for the data analysis. After normalization, proteins that are present at the same level in both the sample and standard have a value of 1.

This normalized value provides the level of protein in the sample of interest compared to the standard mixture, but does not account for differences between the standard mixture and the wild type 50S particles. In order to eliminate these differences, the values for the normalized unlabeled fraction obtained for the proteins in a sample of interest are then divided on a per-protein basis by the same values obtained from the wild type 50S subunit. The resulting number gives the relative abundance of a protein in the sample of interest compared to the wild type 50S subunits.

ATPase assay

The rate of ATP hydrolysis by DbpA in the presence of 32mer RNA with and without the 2'-O-methyl at U2552 was measured using the previously described high-throughput coupled spectroscopic assay (Karginov et al. 2005).

Endpoint or kinetic rates of ATP hydrolysis by DbpA in the presence of ribosomal subunits or particles was measured using a TLC plate assay as described previously (Fuller-Pace et al. 1993) with the following modifications. In a total volume of 25 μL, 100 nM of RNA (transcribed 23S rRNA, purified ribosome subunits or particles, or LiCl cores) was incubated with 40 nM DbpA and 20 μM ATP plus 0.1 μCi α-^{32}P ATP in buffer (50 mM Hepes pH 7.5, 20 mM KCl, 5 mM $MgCl_2$, 1 mM DTT, 0.1% Tween 20) for 30 minutes at 24 ºC. At various time points 2 μL aliquots (or the entire reaction) were quenched with 500 mM EDTA pH 8 and 2 μL aliquots were spotted on a PEI cellulose TLC plate, run in a LiCl:Formic acid buffer (750 mM:1 M), dried and exposed to a phosphor screen. The fraction of ATP hydrolyzed was quantitated and converted to the concentration of ATP hydrolyzed per DbpA. This value was plotted versus time and the resulting linear slopes were determined as the rates of ATP hydrolysis.

3.3. Results

DbpA mutant strains accumulate incomplete large subunits

Sucrose gradient profiles of ribosomes derived from *E. coli* Tuner™ (DE3) pLacI RecA$^-$ cells containing a multicopy plasmid with either wild type DbpA or the dominant negative R331A mutant were compared. Previous western blot experiments have shown that while expression of endogenous DbpA was very low, high levels of wild type DbpA or the R331A mutant were expressed from either plasmid even without IPTG induction (Sharpe Elles and Uhlenbeck 2008). On 10-50% sucrose gradients containing 10 mM Mg^{2+}, ribosomes from cells overexpressing the R331A mutant that had been grown to midlog at 37 °C, exhibit fewer polysomes and 70S ribosomes, in addition to enhanced levels of subunits, compared with cells overexpressing wild type DbpA (Figure 3.1A). Similar to rapidly growing wild type *E. coli*, a

majority (~75%) of the ribosomes from cells overexpressing wild type DbpA are found as polysomes and 70S ribosomes with smaller amounts of the 50S (14%) and 30S (11%) subunits. However, with cells containing the R331A plasmid the fraction of 70S ribosomes and polysomes is reduced to 42% and the fraction of large subunits is increased to 36% (Figure 3.1A). When the experiment is repeated with cells grown at 22 ºC where the growth phenotype is more severe (Sharpe Elles and Uhlenbeck 2008), the proportion of polysomes and 70S ribosomes remains close to 70% in the cells with the wild type DbpA plasmid, but is reduced to 21% in the strain containing R331A plasmid (Figure 3.1B). Under these conditions the fraction of large subunits in ribosomes from R331A is again higher with 31% compared to 17% found in wild type DbpA ribosomes (Figure 3.1B). These experiments suggest that the slow growth caused by the overexpression of R331A mutant can be explained by a reduced level of protein synthesis that results from fewer actively translating 70S ribosomes.

Further assessment of this increased fraction of large subunits in R331A comes from analysis of ribosome profiles on 20-40% sucrose gradients containing 1 mM Mg^{2+} which causes the ribosomes to dissociate into individual subunits. Ribosomes from cells containing wild type DbpA plasmid grown at 37 ºC to midlog and run on this type of gradient are completely dissociated into the large and small subunits as expected (Figure 3.1C). On these gradients only a minor fraction, 5%, of ribosomes migrated between the two subunit peaks where precursors of large subunit assembly are known to appear (Charollais et al. 2003). However, under similar conditions ribosomes from cells containing the R331A mutant dissociate into three distinct peaks with 14% migrating in between the subunits at approximately 45S (Figure 3.1C). When the growth temperature is reduced to 22 ºC, ribosomes from cells with wild type DbpA plasmid continue to show a small fraction, 6%, running in between the two peaks while ribosomes from

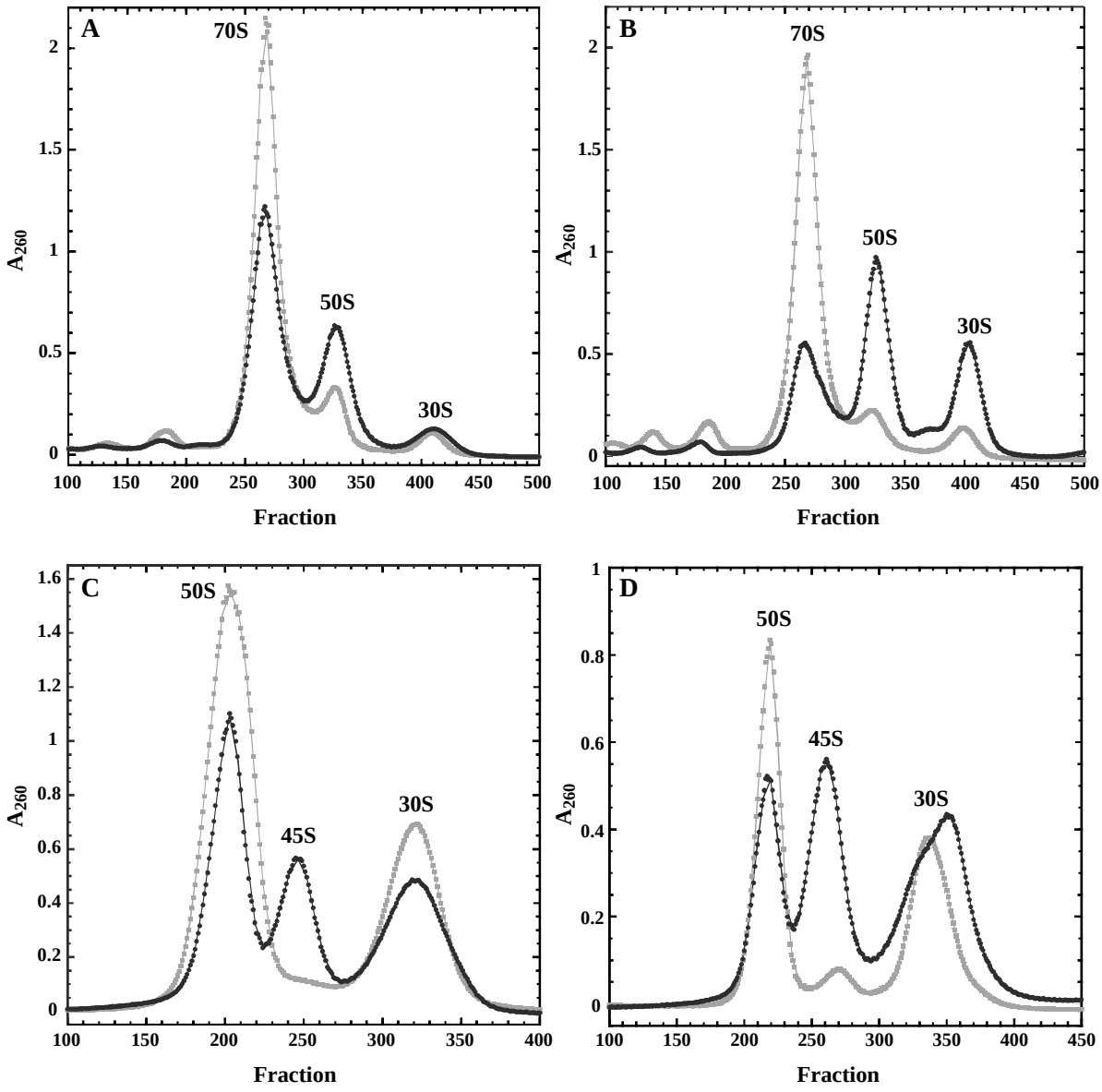

Figure 3.1 Ribosomes from cells overexpressing wild type DbpA or the R331A mutant

Ribosomes from cells overexpressing wild type DbpA (grey squares) or the R331A mutant (black circles) grown at 37 ºC (A and C) or 22 ºC (B and D) and analyzed on sucrose gradients containing 10 mM Mg^{2+} (A and B) or 1 mM Mg^{2+} (C and D).

cells with R331A plasmid now contain 24% 45S particles (Figure 3.1D). In summary, at both growth temperatures the larger proportion of free subunits observed in ribosome profiles from cells overexpressing R331A analyzed in sucrose gradients containing 10 mM Mg^{2+}, is correlated with the appearance of the 45S particle peak observed when the ribosomes are analyzed on sucrose gradients containing 1 mM Mg^{2+}.

The experiments shown in Figure 3.1 suggest that overexpression of the R331A mutant but not wild type DbpA leads to accumulation of a large ribosomal particle that is in some way incomplete and not able to form 70S ribosomes. To test this hypothesis, two experiments were performed. In the first experiment, 70S ribosomes and 50S subunits from cells containing the R331A plasmid and grown at 22 ºC were collected from a gradient run in 10 mM Mg^{2+} and then rerun on gradients containing 1 mM Mg^{2+} (Figure 3.2A). The R331A 70S ribosomes dissociate into 50S and 30S subunits with no clear peak between the two suggesting they are complete and functional. However, the R331A 50S subunits collected from sucrose gradients containing 10 mM Mg^{2+} fractionate into 50S, 45S, and 30S particles when rerun on sucrose gradients containing 1 mM Mg^{2+}. It is likely that the smaller amounts of 50S and 30S subunits are derived from 70S ribosomes that contaminate the 50S subunit fraction in the initial 10 mM Mg^{2+} gradient. Therefore, in agreement with the hypothesis, the increased accumulation of 50S particles in sucrose gradients containing 10 mM Mg^{2+} is due to an increase in 45S particles that are only resolved from 50S subunits when run in sucrose gradients containing 1 mM Mg^{2+}. This could be due to a number of reasons; the resolution of peaks is lower in sucrose gradients containing 10 mM Mg^{2+} where the gradient is steeper (10-50% versus 20-40%), the tight packing of the rRNA and r-proteins in the particle may relax in 1 mM Mg^{2+} causing it to sediment slower, or several L-proteins may wash off also causing a slower sedimentation rate due to the

Figure 3.2 R331A ribosome profiles and recombination of 70S ribosomes

A) R331A 50S subunits (black circles) and 70S ribosomes (grey squares) collected from gradients containing 10 mM Mg^{2+} analyzed on a second gradient containing 1 mM Mg^{2+}. B) R331A 50S subunits (grey circles) and R331A 45S particles (black circles) incubated with native 30S subunits and analyzed on gradients containing 10 mM Mg^{2+}.

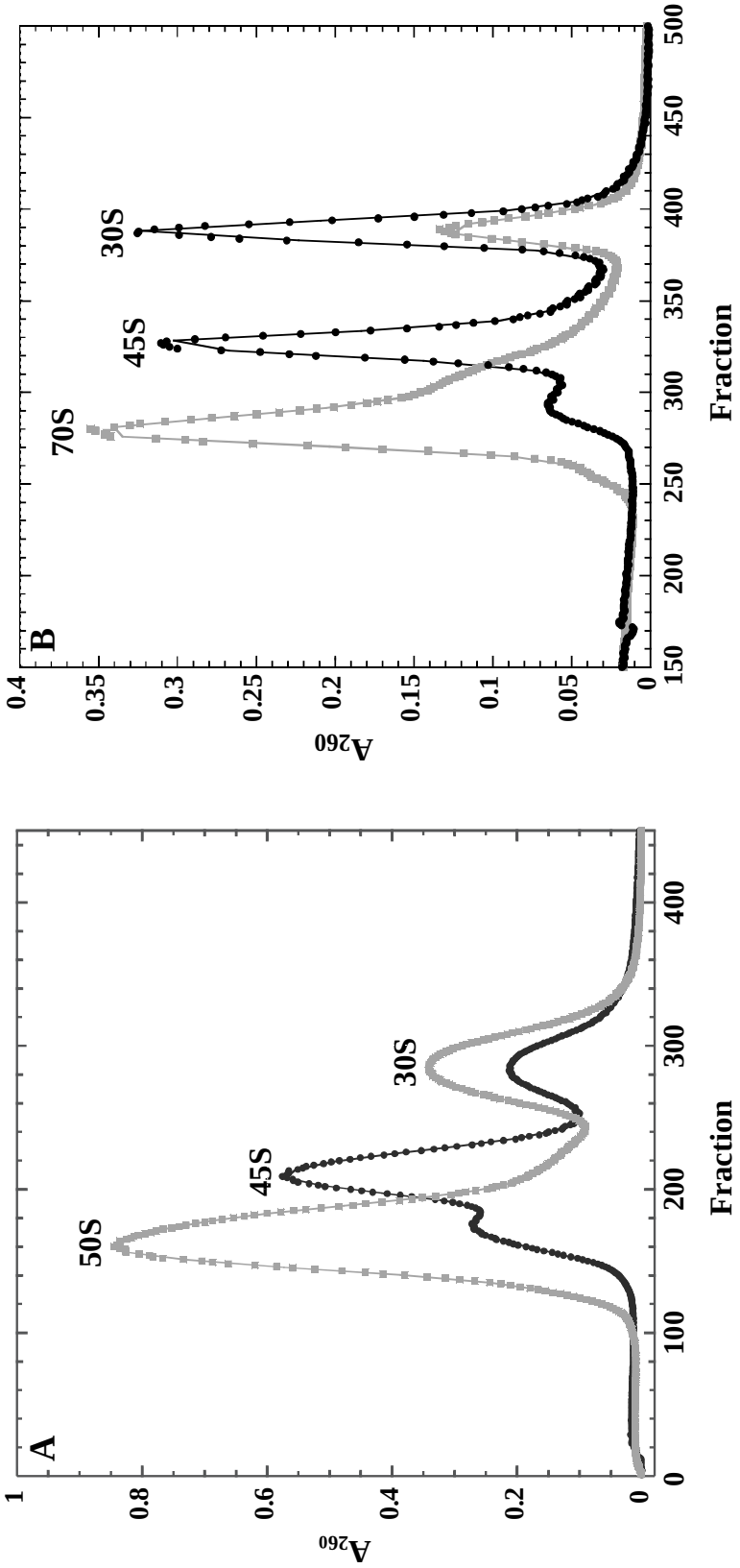
A
50S
45S
30S
A260
Fraction
0
0.2
0.4
0.6
0.8
1
0
100
200
300
400
B
70S
45S
30S
A260
Fraction
0
0.05
0.1
0.15
0.2
0.25
0.3
0.35
0.4
150
200
250
300
350
400
450
500

decrease in molecular weight.

In a second experiment, 45S particles and 50S subunits from the cells overexpressing R331A were collected from gradients run in 1 mM Mg^{2+} and incubated with wild type MRE600 30S subunits in buffer B and analyzed for presence of recombined 70S ribosomes on subsequent sucrose gradients containing 10 mM Mg^{2+} (Figure 3.2B). While the R331A 50S subunits could reassemble into 70S ribosomes, the R331A 45S particles could not. Incubation of the R331A 45S particle with DbpA and ATP or DbpA, ATP, mRNA, and $tRNA^{fmet}$ prior to the addition of 30S subunits could not promote 70S ribosome formation resulting in ribosome profiles similar to those in Figure 3.2B. This indicates that the large subunits from the cells containing R331A plasmid are a mixture of active 50S subunits that can assemble into 70S ribosomes and inactive 45S particles that cannot. In summary, overexpression of R331A in cells causes accumulation of a 45S particle that is not able to form 70S ribosomes suggesting that this particle is incompletely assembled.

E. coli cells containing other DbpA mutations were analyzed to determine whether the different growth phenotypes correlate with the presence of the 45S particles. Ribosomes from BL21 (DE3) with a deletion of the chromosomal copy of *dbpA* (Δ*dbpA*, a gift of I. Iost) grown at 22 °C to midlog dissociate primarily into 50S and 30S subunits in 1 mM Mg^{2+} gradients, similar to wild type BL21 (DE3) cells (Figure 3.3A). The minor peak that sediments between the two subunits in the BL21 (DE3) Δ*dbpA* strain is no greater than that seen in the wild type control. Therefore, the deletion of *dbpA* does not result in any ribosome defects confirming the results we and others have observed with different *dbpA* deletion strains (Baba et al. 2006; Iost and Dreyfus 2006). Ribosomes from *E. coli* Tuner™ (DE3) pLacI $RecA^-$ cells overexpressing DbpA with either a K53A or E154A mutation were also analyzed. These mutants were chosen because

Figure 3.3 Δ*dbpA*, K53, and E154A ribosome profiles

A) BL21(DE3) (grey squares) and BL21(DE3) Δ*dbpA* (black circles) were grown to midlog at 22 °C and analyzed on sucrose gradients containing 1 mM Mg^{2+}. B) Ribosomes from cells overexpressing DbpA mutants, R331A (black circles), K53A (dark grey diamonds) or E154A (grey squares) were analyzed on sucrose gradients containing 1 mM Mg^{2+}.

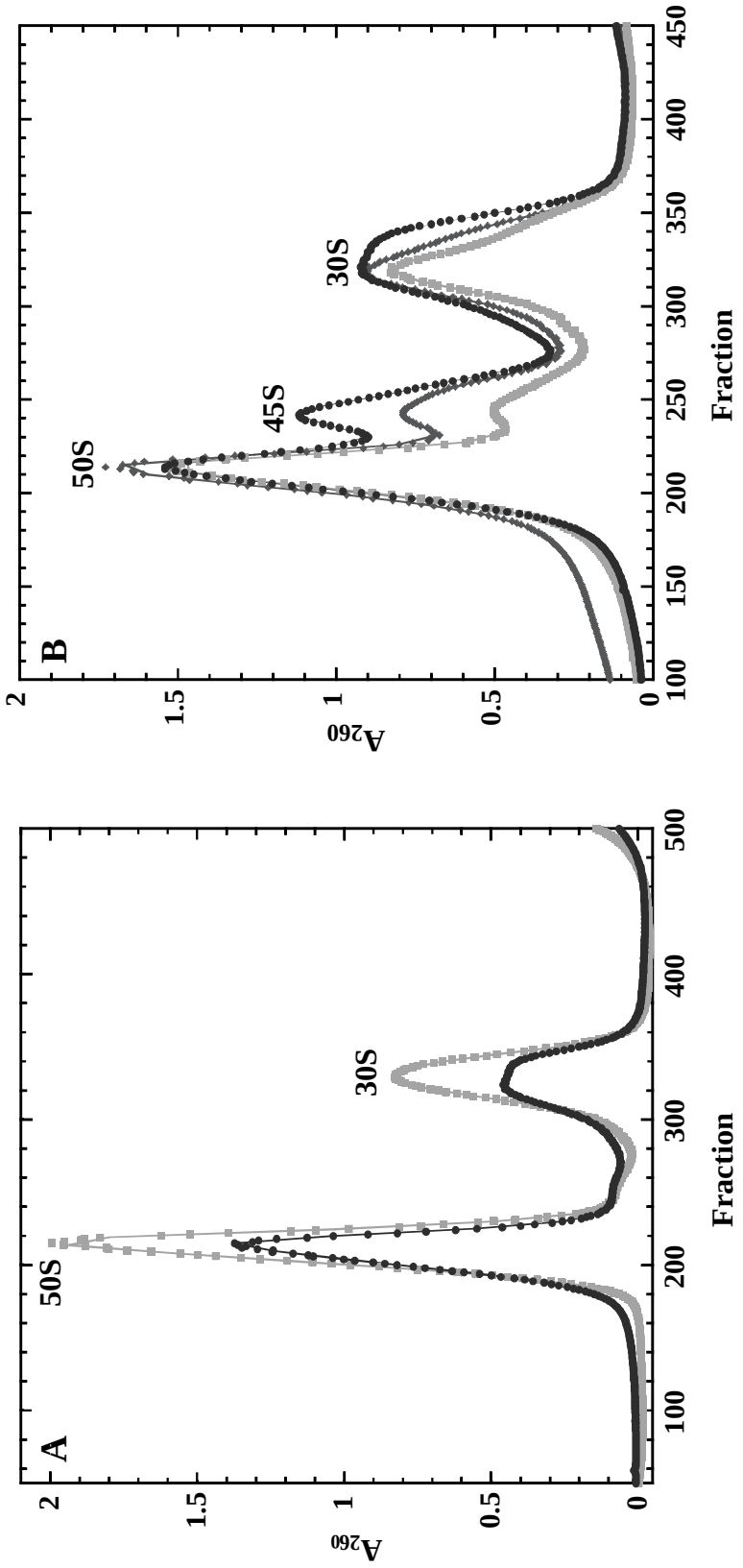
A
B
50S
30S
45S
A_{260}
Fraction
0
0.5
1
1.5
2
100
200
300
400
500
150
250
350
450

unlike the other DbpA mutations they have low RNA-dependent ATPase activity that is only slightly higher than R331A's ATPase activity (Sharpe Elles and Uhlenbeck 2008). Cells containing either K53A or E154A grow at 22 °C with doubling times of ~130 min which is slightly slower than wild type DbpA (110 min) but faster than cells containing R331A plasmid (~250 min) when grown at similar conditions (Sharpe Elles and Uhlenbeck 2008). As seen in ribosome profiles shown in Figure 3.3B, cells overexpressing K53A or E154A and grown at 22 °C accumulate lower amounts of 45S particles than observed in cells overexpressing the R331A mutant. Unlike with cells containing R331A, cells containing K53A or E154A plasmids only show reduced growth rates and accumulate 45S particles when the cells are grown at low temperatures. At 37 ºC the cells containing K53A or E154A plasmids grow at rates similar to wild type cells and their ribosome profiles also resemble wild type profiles (data not shown).

In summary, the dominant slow growth phenotype associated with overexpression of the R331A DbpA mutant is caused by the accumulation of an inactive 45S particle along with a corresponding decrease in mature 70S ribosomes. Cells expressing other DbpA mutants which show less severe growth defects and slightly higher RNA-dependent ATPase activities accumulate fewer 45S particles. Deletion of endogenous *dbpA* does not confer any slow growth or ribosome profile differences consistent with the fact that DbpA is non-essential *in vivo* (Baba et al. 2006; Iost and Dreyfus 2006). The presence of large amounts of inactive DbpA causes ribosome assembly defects. However, assembly is not completely blocked because these cells are viable and some mature 50S subunits and 70S ribosomes are formed.

Characterization of the 45S particles

To further explore the ribosomal particles observed in cells overexpressing the R331A

mutant, rRNA was analyzed for incomplete processing and missing covalent nucleotide modifications. 50S subunits and 45S particles from cells overexpressing R331A or wild type DbpA were collected from sucrose gradients run in 1 mM Mg^{2+} and the rRNA was purified from each. A 5'-end labeled primer complementary to nucleotides 35 to 55 near the 5' end of 23S rRNA (Primer 1) was used in a primer extension experiment to define the 5'end of the particle rRNA. The 50S subunits from cells overexpressing wild type DbpA or R331A primarily contain the mature 5' end of 23S rRNA as well as small amounts of a band that corresponds to the incompletely processed +3 nucleotide extension (Figure 3.4), consistent with results observed by others (Srivastava and Schlessinger 1988; Charollais et al. 2003; Charollais et al. 2004). However, primer extension analysis of the rRNA from R331A 45S particles reveals reduced amounts of the mature 23S rRNA band and substantial amounts of bands corresponding to the +3 and +7 nucleotide extension products (Figure 3.4). These results have been observed in other ribosomal particles isolated from deletion strains of different ribosome assembly factors (Charollais et al. 2003; Charollais et al. 2004; Hwang and Inouye 2006; Jiang et al. 2006) and are consistent with observations that the final steps of 23S rRNA processing does not occur until after a 70S ribosome translation initiation complex is formed (Sirdeshmukh and Schlessinger 1985b; Srivastava and Schlessinger 1988). Primer extension experiments with 30S subunits from cells overexpressing R331A using the 23S DNA primer revealed a small amount of pre-23S rRNA was present (data not shown) suggesting a possible second incomplete 50S-like particle that co migrates with 30S subunits and explains the interesting shape of the 30S subunit peak in Figure 3.1D. This result was not further explored due to the inability to separate the two peaks on the sucrose gradients used.

Similar primer extension experiments were performed with primers complementary to the

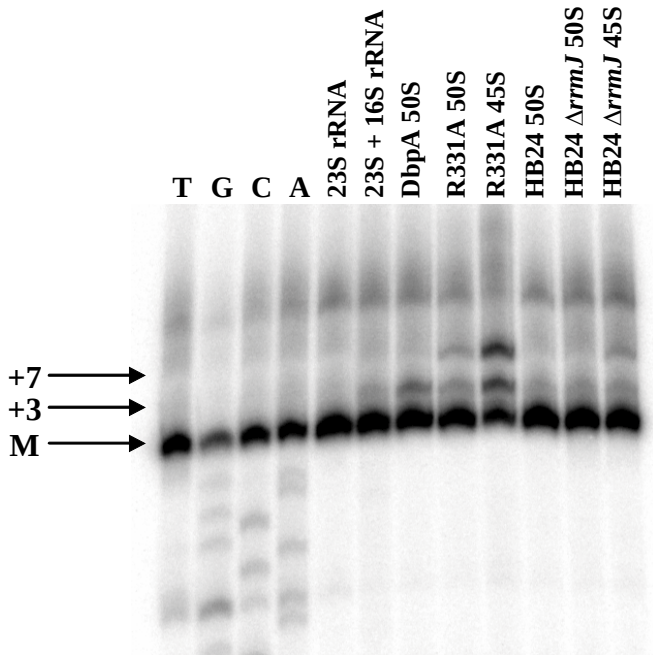

Figure 3.4 Primer extension of 23S rRNA from subunits and particles

RNA from wild type DbpA 50S subunits, R331A 50S subunits, R331A 45S particles, RrmJ 50S subunits, Δ*rrmJ* 50S subunits and Δ*rrmJ* 40S particles was analyzed by primer extension using 5'-end labeled Primer 1. The first four lanes show a sequencing ladder obtained using the same primer and 23S rRNA transcript. Control experiments were performed with 23S rRNA transcript and 23S + 16S rRNA purified from MRE600 cells. The positions of the mature 5' end (M) and the longer products (+3 and +7) are indicated.

5' ends of 16S or 5S rRNA that was isolated from 30S and 50S subunits and 45S particles (data not shown). These experiments revealed mature 5S rRNA in both 50S subunits from cells containing wild type DbpA or R331A plasmid and in 45S particles from cells containing R331A plasmid. While the 16S rRNA from 30S subunits from cells overexpressing wild type DbpA is fully processed as expected, the 16S rRNA from cells overexpressing R331A mutant contained a small amount of an approximately +115 nucleotide product. This product is most likely the 17S precursor of 16S rRNA that is matured late in assembly, possibly after subunit association and the formation of a 70S ribosome (Srivastava and Schlessinger 1990). The presence of this 17S precursor in cells overexpressing R331A is probably an indirect result of the defect in 50S subunit assembly which leads to an accumulation of 30S subunits that do not form 70S ribosomes and therefore the rRNA processing cannot be completed. A similar indirect effect on 30S subunit biogenesis was observed in deletion strains of other *E. coli* ribosomal large subunit assembly factors (Charollais et al. 2003; Charollais et al. 2004; Hwang and Inouye 2006; Jiang et al. 2006).

Different covalent modifications of rRNA occur at specific times during ribosome maturation (Ofengand and del Campo 2004). Therefore, it was of interest to examine whether cells overexpressing the R331A mutant showed an altered rRNA modification pattern in the region where DbpA footprints in the presence of AMPPNP (Karginov and Uhlenbeck 2004). The three methylations in the DbpA binding site, Um2552, m^2A2503 and Cm2498, can be detected as primer extension stops in the presence of low dNTP concentrations (Bakin and Ofengand 1993; Lowe and Eddy 1999). As shown in Figure 3.5, 23S rRNA isolated from 50S subunits from *E. coli* HB24 cells (Bügl et al. 2000) or cells overexpressing wild type DbpA showed clear primer extension stops at all three positions, indicating that the methyl groups were

Figure 3.5 Detection of rRNA modifications in the PTC of subunits and particles

A) Primer 2 is complementary to nucleotides 3' of hairpin 92 and permits detection of 2'-O-methyl at U2552 by reverse transcription in the presence of low dNTP concentration. B) Primer 3 is complementary to nucleotides 5' of hairpin 92 and permits detection of Cm2498 and m^2A2503 by reverse transcription in the presence of low dNTP concentration. On both gels the first four lanes show a sequencing ladder obtained using the same primers and 23S rRNA transcript. H and L indicate high (1 mM) and low (4 μM) dNTP concentrations. Primer extension stops at modification sites are seen as bands in the low dNTP lanes.

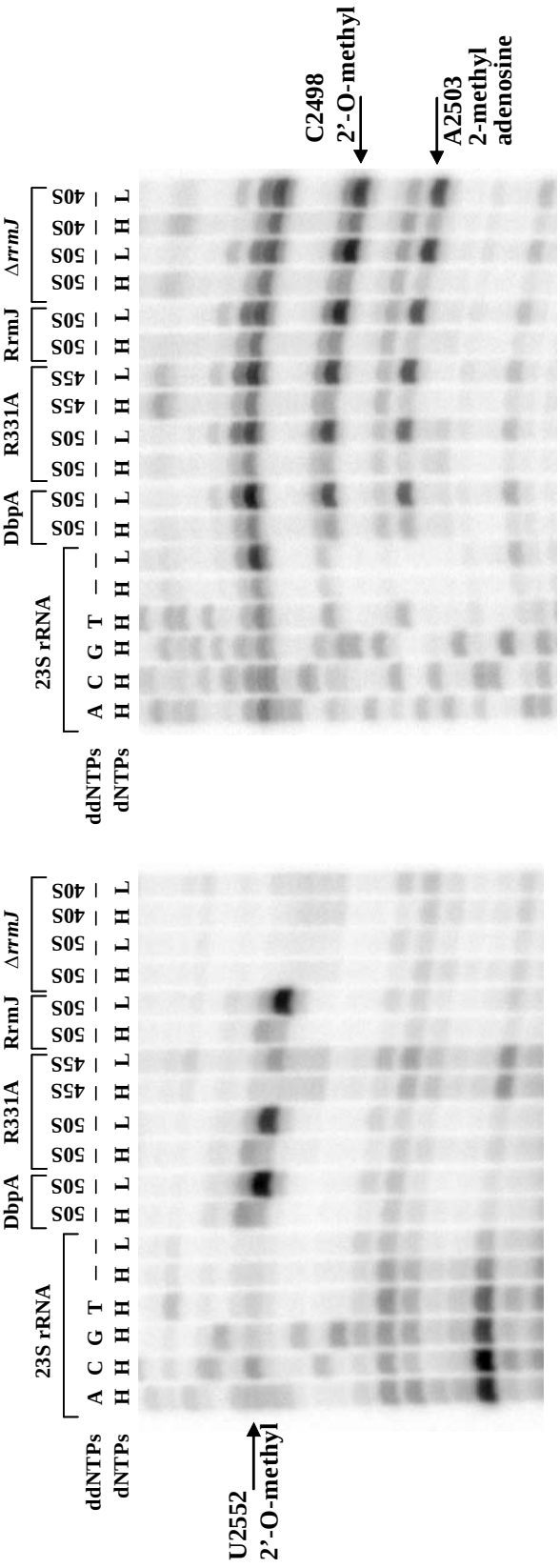
C2498
2'-O-methyl
A2503
2-methyl
adenosine
U2552
2'-O-methyl
DbpA
R331A
RrmJ
ΔrrmJ
23S rRNA
ddNTPs
dNTPs
A C G T
H H H H
L H L H
– – – –
50S
45S
40S

present. In the case of cells overexpressing the R331A mutant, the rRNA from 50S subunits contained all three methylations (Figure 3.5). However, rRNA from the 45S particles showed normal primer extension stops at A2503 and C2498 but only a very weak primer extension stop corresponding to the 2'-O-methylation at U2552 (Figure 3.5), suggesting that the U2552 methyl group is severely reduced or missing in the 45S particles. This result is particularly interesting because U2552 is part of hairpin 92, the primary binding site of DbpA. To confirm that a missing 2'-O-methylation at U2552 can be detected by this method, 23S rRNA was prepared from 50S subunits and 40S particles isolated from *E. coli* HB24 strains with a deletion of RrmJ, the methyltransferase that modifies U2552 (Bügl et al. 2000). As seen in Figure 3.5A, there is no primer extension stop at U2552, thus the 23S rRNA from Δ*rrmJ* strains is completely missing the 2'-O-methyl group. Therefore, the 45S particles from cells overexpressing the R331A mutant are in fact missing the 2'-O-methylation at U2552.

The absence of the 2'-O-methyl at U2552 raised the possibility of a functional relationship between DbpA and RrmJ methyltransferase. It was therefore important to establish whether the methyl group had any effect on the binding or activity of DbpA. Earlier experiments comparing DbpA activity in the presence of modified and unmodified 23S rRNA suggested that there was no preference. However, it was important to confirm this result with structurally better defined substrates of DbpA. Chemically synthesized 32 nucleotide minimal substrates of DbpA (Diges 2001; Tsu et al. 2001) with and without the 2'-O-methyl at U2552 were assayed with purified DbpA. As shown in Table 3.1, the k_{max} and $K_{app,\ RNA}$ values for these two substrates are identical, confirming that the 2'-O-methyl group has no effect on DbpA function *in vitro*.

Although slower sedimenting subunits present during assembly (Nierhaus et al. 1973) or accumulating in mutant strains (Charollais et al. 2003) often have reduced amounts of certain r-

Table 3.1 ATPase activity of DbpA with and without the 2'-O-methylation at U2552

	k_{max} (min^{-1})	$K_{app, RNA}$ (nM)
32mer	45 ± 3.6	220 ± 32
2'-O-methyl 32mer	43 ± 2.6	230 ± 31

The $K_{app, RNA}$ and k_{max} values were measured in the presence of saturating (5 mM) ATP, 60 nM DbpA and 0 to 2 mM RNA.

proteins, it cannot be assumed that this is always the case. For example, the final large subunit precursors detected in biogenesis ($p_3$50S) and in *in vitro* reconstitution experiments (RI_{50}(2)) contain a full complement of L-proteins and thus their different sedimentation values are primarily due to their conformational differences and not to a lower molecular weight (Dohme and Nierhaus 1976). In order to determine whether the 45S particles and 50S subunits from cells overexpressing the R331A mutant are lacking any L-proteins, they were purified from two successive sucrose gradients run in 1 mM Mg^{2+}. The L-protein composition and relative abundance in these two particles as compared to the wild type 50S subunit was determined by ESI-TOF MS. Figure 3.6A shows a control experiment in which the standard mixture of ^{15}N labeled L-proteins is mixed with an equivalent standard mixture of ^{14}N labeled L-proteins, and normalized such that the amount of L2 is 1. This control shows the amount of error inherent in the method, which is about 3% (average unlabeled fraction of 0.990 +/- 0.027). The relative protein levels for the 45S particle, ^{14}N, were compared to the wild type 50S subunit, ^{15}N, to observe any differences in L-protein composition (Figure 3.6B). Five proteins (L16, L25, L28, L33, and L35) were reduced in the R331A 45S particles and five others (L20, L27, L29, L30, and L34) have very slightly reduced ratios, which may be significant. However, with the exception of L35, which is almost completely missing, none of the proteins are reduced by more than 40%. This means that the 45S particles are heterogeneous and on average missing only 1-2 proteins, so the major reason for their slower sedimentation is not because of a large difference in molecular weight but because they are in a more open conformation. All five of the major missing proteins are among those that assemble late in assembly experiments *in vitro* (Roth and Nierhaus 1980; Rohl and Nierhaus 1982; Herold and Nierhaus 1987).

In order to test for the presence of DbpA in ribosomal particles, western blots were

Figure 3.6 L-protein analysis of R331A 45S particles

ESI-TOF MS analysis of the L-protein content of wild type 50S subunits and R331A 45S particles. (Top) Normalized fraction of ^{14}N peptides from wild type TP50 compared with ^{15}N wild type TP50. The amount of error inherent in the method is approximately 3% (average fraction of ^{14}N TP50 is 0.990 +/- 0.027) (Bottom) Normalized fraction of ^{14}N peptides from R331A 45S particles compared with ^{15}N labeled peptides from wild type 50S subunits. Proteins reduced in R331A 45S particles are colored red, L16, L25, L28, L33, and L35. Error bars indicate the fraction of each different peptide observed from a given L-protein within one experiment.

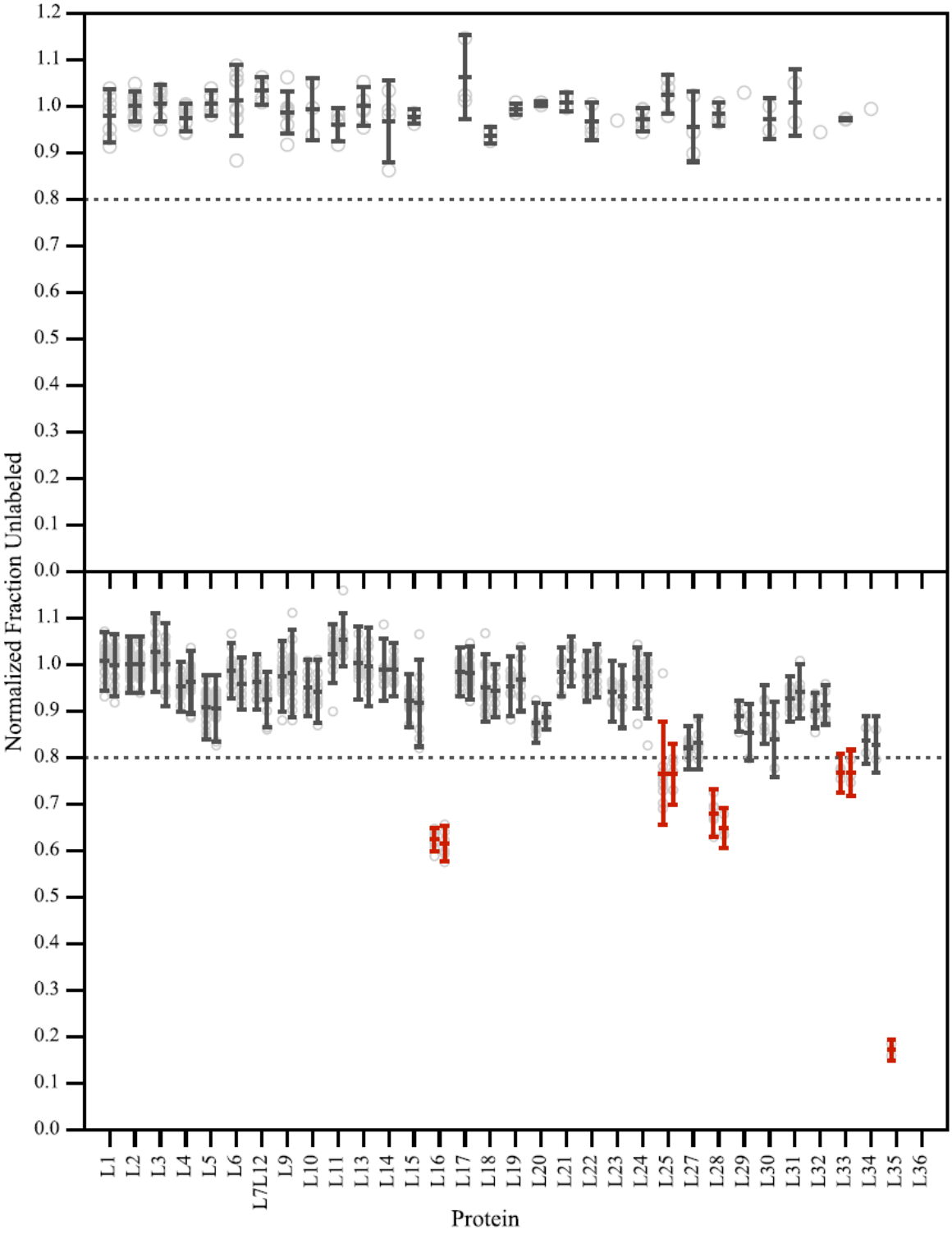
Normalized Fraction Unlabeled
1.2
1.1
1.0
0.9
0.8
0.7
0.6
0.5
0.4
0.3
0.2
0.1
0.0
L1
L2
L3
L4
L5
L6
L7L12
L9
L10
L11
L13
L14
L15
L16
L17
L18
L19
L20
L21
L22
L23
L24
L25
L27
L28
L29
L30
L31
L32
L33
L34
L35
L36
Protein

performed on particles isolated from sucrose gradients using a polyclonal antibody against DbpA as described earlier (Sharpe Elles and Uhlenbeck 2008). While no DbpA could be detected in 50S and 30S subunits from wild type *E. coli* cells, significant signals were detected in cells that overproduced either wild type or the R331A mutant from the expression plasmid (data not shown). Approximately similar amounts of DbpA was detected in 30S and 50S subunits from cells overexpressing wild type DbpA and 30S and 50S subunits and 45S particles from cells overexpressing the R331A mutant. When ribosome particles were purified on two sucrose gradients, roughly equivalent, but much lower levels of DbpA was observed in all the particles. Taken together, these data suggest that the overproduced wild type DbpA and R331A mutant proteins associate weakly and non-specifically to ribosomal particles. This is in contrast to results demonstrating that two other *E. coli* DEAD-box proteins, SrmB and CsdA both selectively associate with 40S precursor particles on sucrose gradients when added to cell lysates from Δ*srmB* and Δ*csdA* mutant strains (Charollais et al. 2003; Charollais et al. 2004).

R331A 45S particles closely resemble other precursor particles

Accumulation of slower sedimenting large subunits has previously been observed in cells containing mutations of other proteins proposed to participate in ribosome assembly. Deletions of two other *E. coli* DEAD-box proteins, SrmB and CsdA, result in slow growth and accumulation of 40S precursor particles which contain incompletely processed 23S rRNA (Charollais et al. 2003; Charollais et al. 2004). However, these particles are somewhat smaller, containing reduced amounts of at least 14 different L-proteins and thus presumably from earlier stages in ribosome assembly. Deletion or mutation of two different *E. coli* GTPases, $CgtA_E$ and EngA, also results in the accumulation of 50S and 30S subunits and a precursor particle that

contains incompletely processed 23S rRNA (Sato et al. 2005; Bharat et al. 2006; Hwang and Inouye 2006; Jiang et al. 2006). A strain containing a mutant form of $CgtA_E$ (G80E D85N) clearly resembles cells overexpressing R331A because it accumulates a 40S particle that is only observed on sucrose gradients run in low magnesium and contains reduced levels of L33, L34 and to a lesser extent L16 (Jiang et al. 2006). However, the large subunit precursor particle that most closely resembles the R331A 45S particle is the one that accumulates when RrmJ, the methyltransferase that 2'-O-methylates U2552 in hairpin 92 of 23S rRNA, is deleted (Bügl et al. 2000; Caldas et al. 2000b). Since RrmJ targets the same hairpin as DbpA binds to, ribosomes from a Δ*rrmJ* strain were directly compared with ribosomes from cells overexpressing R331A. As shown in Figure 3.7, in agreement with previous reports (Bügl et al. 2000), a precursor particle is observed when Δ*rrmJ* ribosomes are analyzed on sucrose gradients containing 1 mM magnesium. Although the Δ*rrmJ* precursor particle was termed 40S in previous experiments (Bügl et al. 2000), it runs at a similar position on sucrose gradients as the R331A 45S particle. The Δ*rrmJ* 40S particle also contains equivalently reduced amounts of the same L-proteins that are reduced in the R331A 45S particle, L25, L27, L28, L29, L30, L33, L34, and much lower levels of L16 (Hager et al. 2002) (Sykes, M. and Williamson, J. R. data not shown). Primer extension analysis of the rRNA from the Δ*rrmJ* 40S particle revealed lesser amounts of the +3 and +7 extensions than observed for the rRNA from R331A 45S particles (Figure 3.4). Finally, as shown above, rRNA from the Δ*rrmJ* 40S particle is also missing the 2'-O-methyl at U2552, as expected, but the other nearby methylations at C2498 and A2503 are present similar to the rRNA from R331A 45S particles (Figure 3.5A and 3.5B). In summary, 40S particles from Δ*rrmJ* are nearly identical to the 45S particles from cells overexpressing R331A.

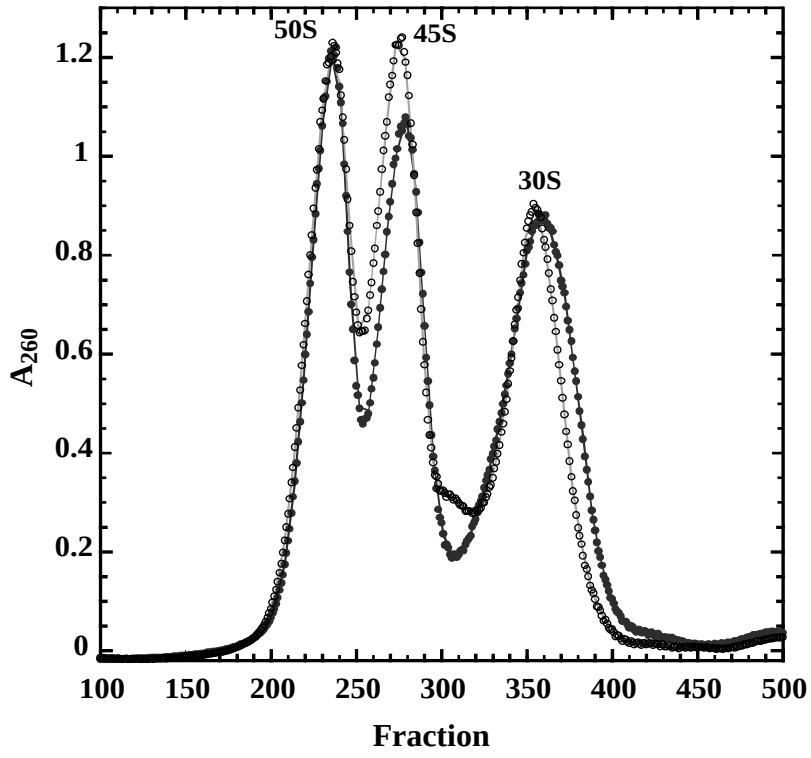

Figure 3.7 Ribosome profiles from R331A and HB24 Δ*rrmJ*

Ribosomes from cells overexpressing the R331A mutant (closed circles) or HB24 with a deletion of RrmJ, which methylates U2552 (open squares) (Bügl et al. 2000), were grown at 22 ºC and analyzed on sucrose gradients containing 1 mM Mg^{2+}.

Since the R331A 45S particle is primarily missing proteins that bind late in assembly, similar precursor particles can be prepared by washing 50S subunits with an appropriate concentration of LiCl, which removes late assembly L-proteins (Homann and Nierhaus 1971; Herold and Nierhaus 1987). Therefore, 50S subunits were washed with three different concentrations of LiCl and the L-protein content of the core particles was determined using mass spectrometry as explained above. Core particles resulting from washing 50S subunits with 0.4 M LiCl showed only very slightly reduced levels of a few proteins (Sykes, M. and Williamson, J. R. data not shown). The 0.6 M LiCl core particles contained reduced amounts of L28, while the 0.8 M LiCl core particles contained clearly reduced amounts of L16 and L28 and slightly reduced amounts of L7/L12 and L10 (data not shown). Washing 50S subunits with 1.0 M LiCl results in core particles that contain severely reduced levels of L16 and L28 and slightly reduced levels of L25 along with several other proteins, L9, L10, L11, L7/L12, that are not reduced in the R331A 45S particle. Therefore, the 0.8 M LiCl particle most closely resembles resemble the R331A 45S particles. This is supported by the fact that 0.8 M LiCl core particles also sediment at approximately 45S and are unable to reassemble into 70S ribosomes when incubated with wild type 30S subunits (Figure 3.8).

Pre-50S particles are substrates for DbpA

The binding site of DbpA is buried within the 50S subunit and correspondingly wild type 50S subunits and 70S ribosomes do not stimulate the ATPase activity of DbpA (Tsu and Uhlenbeck 1998). It was therefore of interest to test whether 45S particles from R331A, 40S particles from Δ*rrmJ* and the three different LiCl core particles were able to stimulate the ATPase activity of DbpA. Thin layer chromatography assays described previously (Fuller-Pace

et al. 1993) were used to determine the rate of ATP hydrolysis by DbpA over time in the presence of subsaturating ATP and saturating rRNA or ribosomal particles. Both the R331A 45S and Δ*rrmJ* 40S particles, which are similar in size and composition can stimulate ATP hydrolysis by DbpA at a rate of ~10 min^{-1}, which is higher than the rate stimulated by 50S subunits (0.4 min^{-1}) but lower than the rate with 23S rRNA (25 min^{-1}) (Figure 3.9A and Table 3.2). This suggests that the DbpA binding site, hairpin 92, is not completely buried within these particles as it is in mature 50S subunits. However, since the rate of ATP hydrolysis by DbpA is still not as high as that observed with 23S rRNA, hairpin 92 may still be slightly occluded by L-proteins or other rRNA helices. Interestingly, 0.4 M LiCl core particles can stimulate ATP hydrolysis by DbpA at a rate of 4.5 min^{-1}, approximately 10-fold higher than mature 50S subunits even though they only contain slightly reduced amounts of a few L-proteins (Figure 3.9A and Table 3.2). Wild type 50S subunits washed with 0.6 M LiCl, which reduces L28 levels, or with 0.8 M LiCl, which reduces L16 and L28 levels, both result in greater stimulation of ATP hydrolysis by DbpA with rates of 15.3 min^{-1} and 19 min^{-1} respectively (Figure 3.9A and Table 3.2). Particles that stimulate the ATP hydrolysis rate at or above 10 min^{-1} (Table 3.2) must have a more open conformation of the rRNA allowing DbpA greater accessibility to hairpin 92 than in mature 50S subunits.

The inactive R331A mutant of DbpA binds to full 23S rRNA and 23S rRNA fragments equally as well as wild type DbpA (Sharpe Elles and Uhlenbeck 2008) and therefore the accumulation of the 45S particle results from the large amounts of R331A protein binding and blocking access to hairpin 92 by active DbpA during ribosome assembly. To confirm R331A can effectively compete with wild type DbpA for substrates, competition assays were performed where the activity of the DbpA stimulated by saturating amounts of 23S rRNA or 45S particles

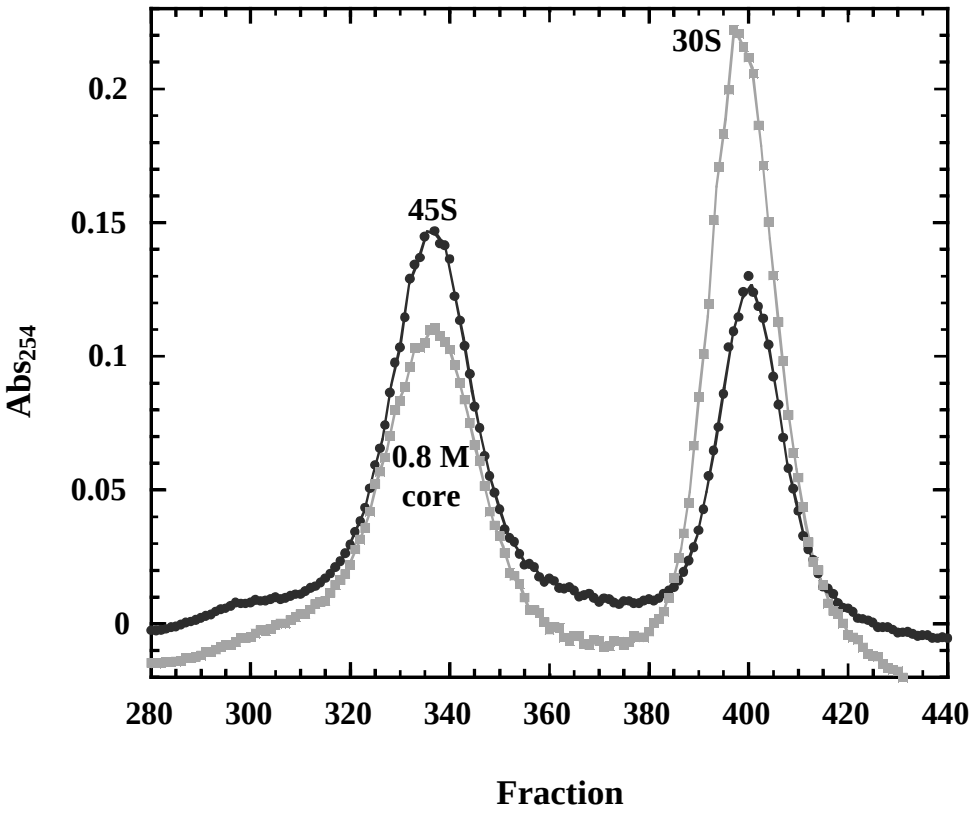

Figure 3.8 Recombination of R331A 45S particles or 0.8 M LiCl with 30S subunits

0.8 M LiCl core particles (grey squares) or R331A 45S particles (black circles) were incubated with native 30S subunits in buffer B at 37 °C for 30 minutes and analyzed on sucrose gradients containing 10 mM Mg^{2+}.

Figure 3.9 DbpA's ribosome particle-stimulated ATPase activity and inhibition by R331A

A) The rate of ATP hydrolysis by 40 nM DbpA was measured in the presence of 100 nM 23S rRNA (squares), 0.4 M LiCl cores (black diamonds), 0.6 M LiCl cores (grey diamonds), 0.8 M LiCl cores (open diamonds), or R331A 45S particles (circles). B) The rate of ATP hydrolysis by 40 nM DbpA was measured in the presence of 100 nM 23S rRNA either alone (squares) or with the addition of 40 nM (black diamonds), 100 nM (grey diamonds), or 200 nM (light grey diamonds) of the mutant R331A protein.

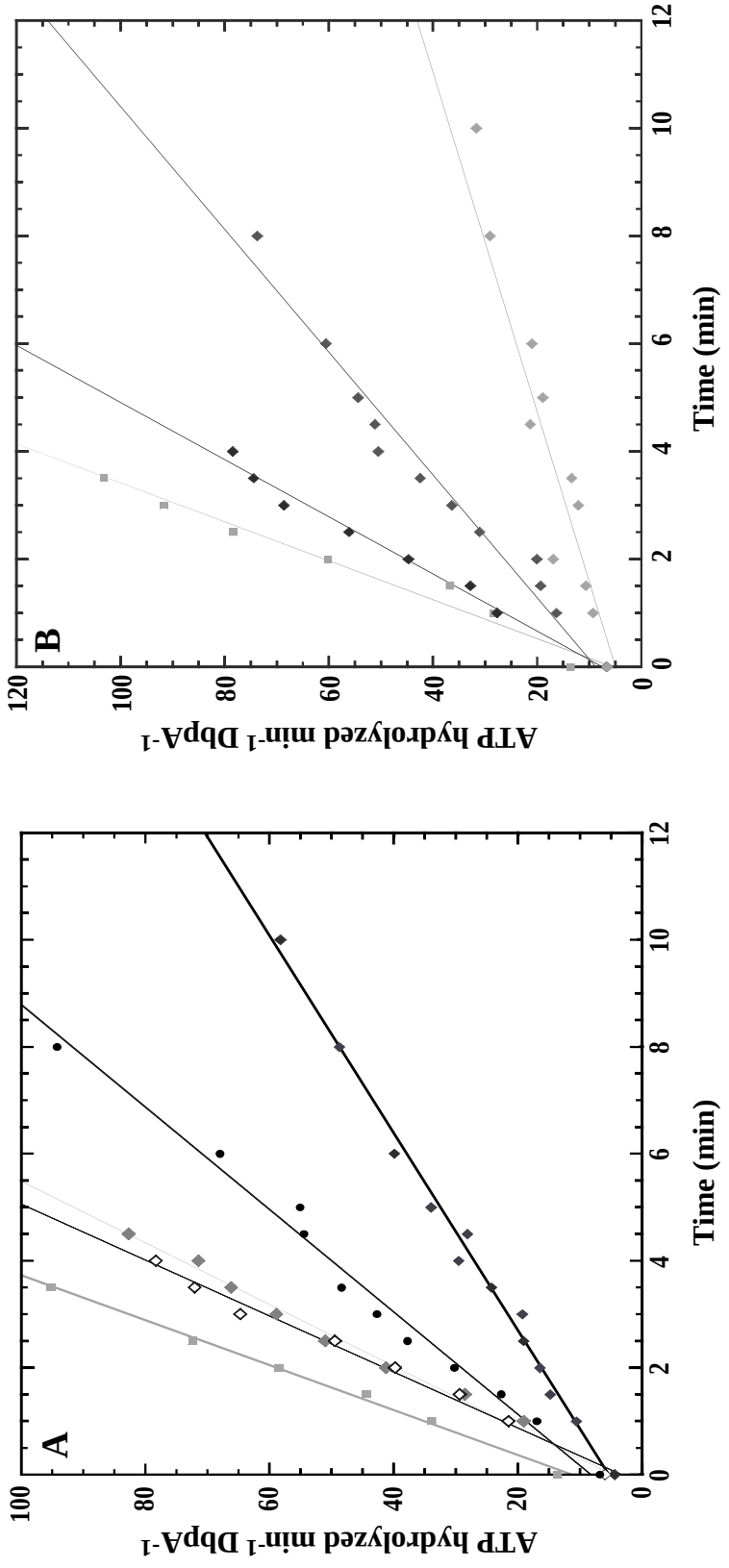
A
B
ATP hydrolyzed min-1 DbpA-1
Time (min)
0
20
40
60
80
100
120
0
2
4
6
8
10
12

Table 3.2 DbpA ATPase activity in the presence of ribosome subunits or particles

Strain	Substrate	ATP hydrolyzed per DbpA (min^{-1})
	ATP only	0.05 ± 0.01
	23S rRNA	25.1 ± 0.9
Tuner + *dbpA*	50S	0.4 ± 0.1
Tuner + *R331A*	45S	10.6 ± 1.5
	50S	2.1 ± 0.2
RrmJ	50S	0.5 ± 0.2
ΔRrmJ	40S	10.3 ± 1.4
	50S	5.1 ± 1.5
LiCl cores	0.4M	4.5 ± 0.6
	0.6M	15.3 ± 2.0
	0.8M	19.3 ± 1.4

The fraction of ATP hydrolyzed at various time points was measured in the presence of 40 nM DbpA and 100 nM 23S rRNA or ribosome particles. The rate of ATP hydrolysis was determined from plots as seen in Figure 3.9A.

was measured in the presence of the R331A mutant protein. As seen in Figure 3.9B, the addition of increasing concentrations of the mutant R331A protein significantly reduces the rate of ATP hydrolysis in the presence of 23S rRNA from 25 min^{-1} to 4.6 min^{-1}. Similarly, the rate of ATP hydrolysis in the presence of 45S particles is reduced from 10.6 min^{-1} in the absence of R331A protein to 4.0 min^{-1} when R331A protein is added (data not shown). This inhibition confirms that the inactive R331A mutant can compete with active DbpA and therefore can block its function *in vivo*.

Since the R331A 45S particles are substrates for DbpA *in vitro*, it is possible that in the presence of wild type DbpA a structural rearrangement could occur, which would allow the particle to continue on the assembly pathway and form 50S subunits *in vitro*. As mentioned above, this type of rearrangement of 45S particles does not occur in the absence of other components such as L-proteins, because the addition of DbpA and ATP alone to 45S particles did not permit the formation of 70S ribosomes (Figure 3.2B). Thus, R331A lysates were supplemented with high concentrations of DbpA and ATP, enough to compete with the endogenous R331A protein and relieve the block in assembly, in an environment where L-proteins are available. Fresh clarified lysates of R331A cells were incubated with up to 1 μM DbpA protein and 1.5 mM ATP for 60 minutes at 24 °C and then run on sucrose gradients containing low magnesium. The resulting ribosome profiles showed no difference and were similar to the profiles of extracts not treated with DbpA (Figures 1C and 1D).

3.4. Discussion

We have characterized R331A, an inactive DbpA mutant that when overexpressed confers a dominant slow growth phenotype that becomes more severe at low growth

temperatures. Data is presented that demonstrates the slow growth is due to the reduced amounts of 70S ribosomes resulting from the accumulation of a 45S particle that cannot bind to 30S subunits. The amount of this 45S particle increases when cells are grown at 22 °C, thus correlating well with the severity of the growth defect. However, even under these conditions about 20% of the 50S subunits are able to assemble properly and form a sufficient amount of 70S ribosomes to permit slow growth. The slow growth rate and accumulation of 45S particles also correlates with the biochemical activity of the overproduced mutant DbpA. Other DbpA mutants that have slightly greater ATPase activity than the R331A mutant show faster growth rates and fewer 45S particles. In addition, fully active wild type DbpA shows no phenotype at all when overproduced. Because *E. coli* in which the DbpA gene has been deleted grows normally and does not accumulate 45S particles, it is clear that the phenotype is not a consequence of the absence of DbpA activity in *E. coli*, but rather is the result of overproduction of inactive DbpA protein.

Analysis of the R331A 45S particles revealed that they contain 23S rRNA that had not undergone the final cleavage events that occur after the large subunit is fully assembled (Srivastava and Schlessinger 1990). The particles were also missing the 2'-O-methylation at U2552, which has been proposed to occur when 50S subunit assembly is nearly complete (Bügl et al. 2000). Finally, the 45S particle contained reduced amounts of five L-proteins that bind late in assembly (Herold and Nierhaus 1987). 50S subunits from the same strain appear to assemble completely normally and contain mature and fully modified 23S rRNA and all 33 L-proteins. All of these data support, but do not prove, that the 45S particle is a late stage precursor in the assembly of the large subunit. This is consistent with the view that DbpA, like CsdA and SrmB (Charollais et al. 2003; Charollais et al. 2004), transiently associates with the nascent subunit and

acts to promote its assembly.

DEAD-box proteins have been shown to catalyze structural rearrangements in RNA-protein complexes (Silverman et al. 2003; Cordin et al. 2006; Yang et al. 2007) and thus it is reasonable to propose that DbpA carries out a similar role in the large subunit assembly pathway. Cells lacking DbpA show no defect in ribosome assembly under the growth conditions tested and thus, the conformational rearrangement that DbpA is proposed to stimulate must occur spontaneously at a sufficiently fast rate not to limit assembly. Alternatively, ribosome assembly in the absence of DbpA may proceed through a slightly different pathway, possibly involving other DEAD-box proteins. If DbpA is not essential for 50S subunit maturation, why then do 45S particles accumulate when inactive DbpA is overproduced? Biochemical experiments have shown that the inactive R331A mutant can bind rRNA substrates at affinities similar to wild type DbpA but cannot hydrolyze ATP (Sharpe Elles and Uhlenbeck 2008). This suggests that the R331A mutant is able to bind to 23S rRNA at the stage of assembly that DbpA normally acts, but cannot promote the proposed rRNA conformational change and, because of its high concentration, remains bound to the assembling subunit, leading to the 45S particle. The bound R331A protein may also block the conformational change from occurring spontaneously. Presumably the normal 50S subunits observed in the R331A cells arise from the successful binding and action of the low concentrations of endogenous active DbpA. The 50S subunits could also mature by using an alternative assembly pathway, similar to that presumably used in Δ*dbpA* strains. The accumulation of 45S particles is not observed when wild type DbpA is overproduced because it is fully active and thereby can catalyze the conformational change that allows assembly to continue.

The 45S particles that accumulate in cells overexpressing the R331A mutant contain

reduced levels of four L-proteins (L16, L25, L28, and L33) and significantly reduced amounts of L35. Therefore, on average they are missing 1-2 proteins and are not homogeneous. The small difference in mass that would result from losing 1-2 proteins indicates that the faster sedimentation of the 45S particle is due to it being in a more open conformation. Large sedimentation shifts due to conformational differences has been observed in natural precursors and reconstitution intermediates and is consistent with the compaction of the large subunit during the final stages of 50S subunit assembly (Dohme and Nierhaus 1976). The five proteins reduced in the 45S particles bind late in proposed ribosome assembly pathways (Herold and Nierhaus 1987) and most lie near the peptidyl transferase center of the 50S subunit (Figure 3.10). Of particular interest is L16, which contacts helices from two 23S rRNA domains and 5S rRNA. Additionally, L16, has been shown to induce a large conformational change upon binding to a core particle *in vitro* (Teraoka, H. and Nierhaus, K. H. 1978), suggesting that it acts as "molecular glue", to hold the 50S subunit in its compact structure (Nishimura et al. 2004). It is striking that one of the helices that L16 binds to is helix 89, which has been identified as the DbpA-ATP binding site and has been suggested as a site of DbpA action (Polach and Uhlenbeck 2002; Karginov and Uhlenbeck 2004). Therefore, the presence of the inactive R331A mutant on the maturing ribosome may prevent the conformational change needed for the binding of L16 and possibly other nearby late assembly proteins.

If 45S particles accumulate because they require action of DbpA before assembly can continue, they should be substrates for for DbpA as long as the inhibitory inactive R331A protein can be removed. Western blots show that the majority of the R331A protein dissociates after two successive sucrose gradients, and therefore does not interfere with activity assays. These purified 45S particles are very good substrates for DbpA, which is consistent with them being

Figure 3.10 Crystal structure of the 50S subunit

The crystal structure of the 50S *E. coli* subunit (PDB: 2AW4) highlighting the DbpA binding site, yellow, and four of the L-proteins that are reduced in the 45S particle, L16, L25, L33, and L35, red. The 23S rRNA is in grey and the other L-proteins are not shown.

intermediates that accumulated because DbpA failed to act. However, efforts to convert 45S particles to 50S subunits by the addition of active DbpA either in the presence or absence of cell lysates were not successful. This raises the possibility that the inactive R331A mutant blocks the conformational rearrangement at an earlier stage, but assembly proceeds with other regions of the 23S rRNA continuing to fold and L-proteins continuing to bind. At a certain point, the pre-ribosome can no longer continue to assemble and the resulting 45S particle accumulates in the cell. This scenario may explain why the 45S particles are heterogeneous. It is not known at this point whether the R331A 45S particle could completely assemble if the R331A protein was removed or whether it represents a dead-end misfolded particle that results from the incorrect order of rRNA folding or protein binding.

An alternative model is that the R331A protein does not block assembly by preventing an rRNA conformational change, but by preventing the methylation of U2552 in hairpin 92 by RrmJ. In some way the 2'-O-methyl at U2552 may be required for the final maturation of the 50S subunit. Therefore, when the overproduced R331A protein blocks RrmJ methyltransferase it also blocks assembly. This model is supported by the observation that the 2'-O-methylation at U2552 is absent in R331A 45S particles and by the fact that Δ*rrmJ* strains also accumulate 40S particles that are very similar to those obtained by overproducing the R331A mutant. However, since RrmJ methylates 50S particles and not 40S particles from Δ*rrmJ* strains, it has been proposed to act late in assembly after the 50S subunit is nearly complete (Bügl et al. 2000; Caldas et al. 2000a). Therefore, the unmethylated U2552 in 45S particles would presumably not be recognized as a substrate for RrmJ and would not be modified, until later. For these reasons, this model seems less able to explain the phenotype of the R331A mutant.

In summary, we have presented evidence that DbpA is involved in the assembly of the

50S ribosomal subunit. The absence of DbpA does not affect ribosome assembly but the inactivity of DbpA mutants causes a block in assembly resulting in slow growth due to an accumulation of incomplete 50S subunits. These 45S particles contain reduced amounts of L-proteins that are found near the same region that DbpA binds to, which is consistent with the absence of a conformational rearrangement necessary for their binding at this site. However, similar to other factors implicated in ribosome assembly, the point at which DbpA acts is not precisely defined. Although, the new data presented here taken together with previous extensive biochemical experiments, strongly suggests that DbpA is promoting a conformational change that is essential for complete folding of the 50S subunit. Future studies will be important in determining the nature of the conformational change and the stage in assembly at which it occurs.

REFERENCES

Agarwalla, S., Kealey, J. T., Santi, D. V. and Stroud, R. M. (2002) Characterization of the 23 S Ribosomal RNA m5U1939 Methyltransferase from Escherichia coli. *J Biol Chem*, **277**, 8835-8840.

Alix, J. H. and Guerin, M. F. (1993) Mutant DnaK chaperones cause ribosome assembly defects in Escherichia coli. *Proc Natl Acad Sci U S A*, **90**, 9725-9.

Andersen, T. E., Porse, B. T. and Kirpekar, F. (2004) A novel partial modification at C2501 in Escherichia coli 23S ribosomal RNA. *RNA*, **10**, 907-913.

Arigoni, F., Talabot, F., Peitsch, M., Edgerton, M. D., Meldrum, E., Allet, E., Fish, R., Jamotte, T., Curchod, M. L. and Loferer, H. (1998) A genome-based approach for the identification of essential bacterial genes. *Nat Biotech*, **16**, 851-6.

Awano, N., Xu, C., Ke, H., Inoue, K., Inouye, M. and Phadtare, S. (2007) Complementation analysis of the cold-sensitive phenotype of the Escherichia coli csdA deletion strain. *J Bacteriol*, **189**, 5808-15.

Baba, T., Ara, T., Hasegawa, M., Takai, Y., Okumura, Y., Baba, M., Datsenko, K. A., Tomita, M., Wanner, B. L. and Mori, H. (2006) Construction of Escherichia coli K-12 in-frame, single-gene knockout mutants: the Keio collection. *Mol Syst Biol*, **2**,

Bakin, A. and Ofengand, J. (1993) Four newly located pseudouridylate residues in Escherichia coli 23S ribosomal RNA are all at the peptidyltransferase center: analysis by the application of a new sequencing technique. *Biochemistry*, **32**, 9754-62.

Ban, N., Nissen, P., Hansen, J., Moore, P. B. and Steitz, T. A. (2000) The Complete Atomic Structure of the Large Ribosomal Subunit at 2.4 A Resolution. *Science*, **289**, 905-920.

Benz, J., Trachsel, H. and Baumann, U. (1999) Crystal structure of the ATPase domain of translation initiation factor 4A from Saccharomyces cerevisiae--the prototype of the DEAD box protein family. *Structure*, **7**, 671-9.

Bharat, A., Jiang, M., Sullivan, S. M., Maddock, J. R. and Brown, E. D. (2006) Cooperative and critical roles for both G domains in the GTPase activity and cellular function of ribosome-associated Escherichia coli EngA. *J Bacteriol*, **188**, 7992-6.

Bizebard, T., Ferlenghi, I., Iost, I. and Dreyfus, M. (2004) Studies on three E. coli DEAD-box helicases point to an unwinding mechanism different from that of model DNA helicases. *Biochemistry*, **43**, 7857-66.

Blattner, F. R., Plunkett, G., III, Bloch, C. A., Perna, N. T., Burland, V., Riley, M., Collado-Vides, J., Glasner, J. D., Rode, C. K., Mayhew, G. F., Gregor, J., Davis, N. W., Kirkpatrick, H. A., Goeden, M. A., Rose, D. J., Mau, B. and Shao, Y. (1997) The Complete Genome Sequence of Escherichia coli K-12. *Science*, **277**, 1453-1462.

Bourne, H. R., Sanders, D. A. and McCormick, F. (1991) The GTPase superfamily: conserved structure and molecular mechanism. *Nature*, **349**, 117-27.

Bram, R. J., Young, R. A. and Steitz, J. A. (1980) The ribonuclease III site flanking 23S sequences in the 30S ribosomal precursor RNA of E. coli. *Cell*, **19**, 393-401.

Brimacombe, R., Mitchell, P., Osswald, M., Stade, K. and Bochkariov, D. (1993) Clustering of modified nucleotides at the functional center of bacterial ribosomal RNA. *FASEB J*, **7**, 161-7.

Bryant, R. E. and Sypherd, P. S. (1974) Genetic analysis of cold-sensitive ribosome maturation mutants of Escherichia coli. *J Bacteriol*, **117**, 1082-92.

Bügl, H., Fauman, E. B., Staker, B. L., Zheng, F., Kushner, S. R., Saper, M. A., Bardwell, J. C. A. and Jakob, U. (2000) RNA Methylation under Heat Shock Control. *Mol Cell*, **6**, 349-360.

Bylund, G. O., Persson, B. C., Lundberg, L. A. and Wikström, P. M. (1997) A novel ribosome-associated protein is important for efficient translation in Escherichia coli. *J Bacteriol*, **179**, 4567-74.

Bylund, G. O., Wipemo, L. C., Lundberg, L. A. and Wikström, P. M. (1998) RimM and RbfA are essential for efficient processing of 16S rRNA in Escherichia coli. *J Bacteriol*, **180**, 73-82.

Caldas, T., Binet, E., Bouloc, P., Costa, A., Desgres, J. and Richarme, G. (2000a) The FtsJ/RrmJ Heat Shock Protein of Escherichia coli Is a 23 S Ribosomal RNA Methyltransferase. *J Biol Chem*, **275**, 16414-16419.

Caldas, T., Binet, E., Bouloc, P. and Richarme, G. (2000b) Translational Defects of Escherichia coli Mutants Deficient in the Um2552 23S Ribosomal RNA Methyltransferase RrmJ/FTSJ. *Biochem Biophys Res Commun*, **271**, 714-718.

Caldon, C. E., Yoong, P. and March, P. E. (2001) Evolution of a molecular switch: universal bacterial GTPases regulate ribosome function. *Mol Microbiol*, **41**, 289-97.

Carmel, A. B. and Matthews, B. W. (2004) Crystal structure of the BstDEAD N-terminal domain: a novel DEAD protein from Bacillus stearothermophilus. *RNA*, **10**, 66-74.

Caruthers, J. M., Johnson, E. R. and McKay, D. B. (2000) Crystal structure of yeast initiation factor 4A, a DEAD-box RNA helicase. *Proc Natl Acad Sci U S A*, **97**, 13080-5.

Caruthers, J. M. and McKay, D. B. (2002) Helicase structure and mechanism. *Curr Opin Struct Biol*, **12**, 123-133.

Chang, T. H., Latus, L. J., Liu, Z. and Abbott, J. M. (1997) Genetic interactions of conserved regions in the DEAD-box protein Prp28p. *Nucleic Acids Res.*, **25**, 5033-5040.

Charollais, J., Dreyfus, M. and Iost, I. (2004) CsdA, a cold-shock RNA helicase from Escherichia coli, is involved in the biogenesis of 50S ribosomal subunit. *Nucleic Acids Res*, **32**, 2751-9.

Charollais, J., Pflieger, D., Vinh, J., Dreyfus, M. and Iost, I. (2003) The DEAD-box RNA helicase SrmB is involved in the assembly of 50S ribosomal subunits in Escherichia coli. *Mol Microbiol*, **48**, 1253-65.

Chen-Schmeisser, U. and Garrett, R. (1976) Distribution of Protein Assembly Sites along the 23-S Ribosomal RNA of Escherichia coli. *FEBS Lett*, **69**, 401-410.

Cheng, Z., Coller, J., Parker, R. and Song, H. (2005) Crystal structure and functional analysis of DEAD-box protein Dhh1p. *RNA*, **11**, 1258-70.

Cordin, O., Banroques, J., Tanner, N. K. and Linder, P. (2006) The DEAD-box protein family of RNA helicases. *Gene*, **367**, 17-37.

Cordin, O., Tanner, N. K., Doere, M., Linder, P. and Banroques, J. (2004) The newly discovered Q motif of DEAD-box RNA helicases regulates RNA-binding and helicase activity. *EMBO J*, **23**, 2478-87.

Culver, G. M. (2003) Assembly of the 30S ribosomal subunit. *Biopolymers*, **68**, 234-249.

Culver, G. M. and Noller, H. F. (1999) Efficient reconstitution of functional Escherichia coli 30S ribosomal subunits from a complete set of recombinant small subunit ribosomal proteins. *RNA*, **5**, 832-843.

Daga, R. R. and Jimenez, J. (1999) Translational control of the cdc25 cell cycle phosphatase: a molecular mechanism coupling mitosis to cell growth. *J Cell Sci*, **112 Pt 18**, 3137-46.

Dahlberg, A. E., Dahlberg, J. E., Lund, E., Tokimatsu, H., Rabson, A. B., Calvert, P. C., Reynolds, F. and Zahalak, M. (1978) Processing of the 5' end of Escherichia coli 16S ribosomal RNA. *Proc Natl Acad Sci U S A*, **75**, 3598-602.

Dammel, C. S. and Noller, H. F. (1995) Suppression of a cold-sensitive mutation in 16S rRNA by overexpression of a novel ribosome-binding factor, RbfA. *Genes Dev*, **9**, 626-37.

Daugeron, M.-C. and Linder, P. (2001) Characterization and mutational analysis of yeast Dbp8p, a putative RNA helicase involved in ribosome biogenesis. *Nucleic Acids Res.*, **29**, 1144-1155.

Decatur, W. A. and Fournier, M. J. (2002) rRNA modifications and ribosome function. *Trends Biochem Sci*, **27**, 344-51.

Diges, C. M. and Uhlenbeck, O. C. (2005) Escherichia coli DbpA Is a 3' --> 5' RNA Helicase. *Biochemistry*, **44**, 7903-7911.

Diges, C. M., Uhlenbeck, O.C. (2001) Escherichia coli DbpA is an RNA helicase that requires hairpin 92 of 23S rRNA. *EMBO J*, **20**, 5503-5512.

Dittrich, M., Hayashi, S. and Schulten, K. (2004) ATP hydrolysis in the betaTP and betaDP catalytic sites of F1-ATPase. *Biophys J*, **87**, 2954-67.

Dohme, F. and Nierhaus, K. H. (1976) Total reconstitution and assembly of 50 S subunits from Escherichia coli Ribosomes in vitro. *J Mol Biol*, **107**, 585-99.

Dunn, J. J. and Studier, F. W. (1973) T7 early RNAs and Escherichia coli ribosomal RNAs are cut from large precursor RNAs in vivo by ribonuclease 3. *Proc Natl Acad Sci U S A*, **70**, 3296-3300.

El Hage, A. and Alix, J. H. (2004) Authentic precursors to ribosomal subunits accumulate in Escherichia coli in the absence of functional DnaK chaperone. *Mol Microbiol*, **51**, 189-201.

El Hage, A., Sbai, M. and Alix, J. H. (2001) The chaperonin GroEL and other heat-shock proteins, besides DnaK, participate in ribosome biogenesis in Escherichia coli. *Mol Gen Genet*, **264**, 796-808.

El Hage, A. and Tollervey, D. (2004) A surfeit of factors: why is ribosome assembly so much more complicated in eukaryotes than bacteria? *RNA Biol*, **1**, 10-5.

Fahlman, R. P., Dale, T. and Uhlenbeck, O. C. (2004) Uniform Binding of Aminoacylated Transfer RNAs to the Ribosomal A and P Sites. *Molecular Cell*, **16**, 799-805.

Forget, B. G. and Varricchio, F. (1970) A naturally occurring 43 s ribosomal precursor particle in Escherichia coli: nature and ribonucleic acid composition. *J Mol Biol*, **48**, 409-19.

Fuller-Pace, F. V., Nicol, S. M., Reid, A. D. and Lane, D. P. (1993) DbpA: a DEAD box protein specifically activated by 23s rRNA. *EMBO J*, **12**, 3619-26.

Gorbalenya, A. E. and Koonin, E. V. (1993) Helicases: amino acid sequence comparisons and structure-function relationships. *Curr Opin Struct Biol*, **3**, 419-429.

Gotta, S. L., Miller, O. L., Jr. and French, S. L. (1991) rRNA transcription rate in Escherichia coli. *J Bacteriol*, **173**, 6647-9.

Green, R. and Noller, H. F. (1996) In vitro complementation analysis localizes 23S rRNA posttranscriptional modifications that are required for Escherichia coli 50S ribosomal subunit assembly and function. *RNA*, **2**, 1011-1021.

Gustafsson, C. and Persson, B. C. (1998) Identification of the rrmA Gene Encoding the 23S rRNA m1G745 Methyltransferase in Escherichia coli and Characterization of an m1G745-Deficient Mutant. *J Bacteriol*, **180**, 359-365.

Gutgsell, N. S., Del Campo, M., Raychaudhuri, S. and Ofengand, J. (2001) A second function for pseudouridine synthases: A point mutant of RluD unable to form pseudouridines 1911, 1915, and 1917 in Escherichia coli 23S ribosomal RNA restores normal growth to an RluD-minus strain. *RNA*, **7**, 990-8.

Gutgsell, N. S., Deutscher, M. P. and Ofengand, J. (2005) The pseudouridine synthase RluD is required for normal ribosome assembly and function in Escherichia coli. *RNA*, **11**, 1141-52.

Guthrie, C., Nashimoto, H. and Nomura, M. (1969) Studies on the assembly of ribosomes in vivo. *Cold Spring Harb Symp Quant Biol*, **34**, 69-75.

Hager, J., Staker, B. L., Bügl, H. and Jakob, U. (2002) Active site in RrmJ, a heat shock-induced methyltransferase. *J Biol Chem*, **277**, 41978-86.

Hansen, J. L., Moore, P. B. and Steitz, T. A. (2003) Structures of Five Antibiotics Bound at the Peptidyl Transferase Center of the Large Ribosomal Subunit. *J Mol Biol*, **330**, 1061-1075.

Hansen, L. H., Kirpekar, F. and Douthwaite, S. (2001) Recognition of nucleotide G745 in 23 S ribosomal RNA by the rrmA methyltransferase. *J Mol Biol*, **310**, 1001-10.

Harms, J., Schluenzen, F., Zarivach, R., Bashan, A., Gat, S., Agmon, I., Bartels, H., Franceschi, F. and Yonath, A. (2001) High Resolution Structure of the Large Ribosomal Subunit from a Mesophilic Eubacterium. *Cell*, **107**, 679-688.

Hayes, F. and Hayes, D. H. (1971) Biosynthesis of ribosomes in E. coli. I. Properties of ribosomal precursor particles and their RNA components. *Biochimie*, **53**, 369-82.

Hayes, F. and Vasseur, M. (1976) Processing of the 17-S Escherichia coli precursor RNA in the 27-S pre-ribosomal particle. *Eur J Biochem*, **61**, 433-42.

Held, W. A., Ballou, B., Mizushima, S. and Nomura, M. (1974) Assembly mapping of 30 S ribosomal proteins from Escherichia coli. Further studies. *J Biol Chem*, **249**, 3103-11.

Held, W. A. and Nomura, M. (1973) Rate determining step in the reconstitution of Escherichia coli 30S ribosomal subunits. *Biochemistry*, **12**, 3273-81.

Henn, A., Cao, W., Hackney, D. D. and De La Cruz, E. M. (2008) The ATPase cycle mechanism of the DEAD-box rRNA helicase, DbpA. *J Mol Biol*, **377**, 193-205.

Henn, A., Shi, S.-P., Zarivach, R., Ben-Zeev, E. and Sagi, I. (2002) The RNA Helicase DbpA Exhibits a Markedly Different Conformation in the ADP-bound State When Compared with the ATP- or RNA-Bound States. *J Biol Chem*, **277**, 46559-46565.

Herold, M. and Nierhaus, K. H. (1987) Incorporation of six additional proteins to complete the assembly map of the 50 S subunit from Escherichia coli ribosomes. *J Biol Chem*, **262**, 8826-33.

Herschlag, D. (1995) RNA chaperones and the RNA folding problem. *J Biol Chem*, **270**, 20871-4.

Himeno, H., Hanawa-Suetsugu, K., Kimura, T., Takagi, K., Sugiyama, W., Shirata, S., Mikami, T., Odagiri, F., Osanai, Y., Watanabe, D., Goto, S., Kalachnyuk, L., Ushida, C. and Muto, A. (2004) A novel GTPase activated by the small subunit of ribosome. *Nucleic Acids Res*, **32**, 5303-9.

Homann, H. E. and Nierhaus, K. H. (1971) Ribosomal proteins. Protein compositions of biosynthetic precursors and artifical subparticles from ribosomal subunits in Escherichia coli K 12. *Eur J Biochem*, **20**, 249-57.

Hosokawa, K., Fujimura, R. K. and Nomura, M. (1966) Reconstitution of functionally active ribosomes from inactive subparticles and proteins. *Proc Natl Acad Sci U S A*, **55**, 198-204.

Hotz, H.-R. and Schwer, B. (1998) Mutational Analysis of the Yeast DEAH-Box Splicing Factor Prp16. *Genetics*, **149**, 807-815.

Huang, L., Ku, J., Pookanjanatavip, M., Gu, X., Wang, D., Greene, P. J. and Santi, D. V. (1998) Identification of Two Escherichia coli Pseudouridine Synthases That Show Multisite Specificity for 23S RNA. *Biochemistry*, **37**, 15951-15957.

Hwang, J. and Inouye, M. (2006) The tandem GTPase, Der, is essential for the biogenesis of 50S ribosomal subunits in Escherichia coli. *Mol Microbiol*, **61**, 1660-1672.

Inoue, K., Alsina, J., Chen, J. and Inouye, M. (2003) Suppression of defective ribosome assembly in a rbfA deletion mutant by overexpression of Era, an essential GTPase in Escherichia coli. *Mol Microbiol*, **48**, 1005-16.

Inoue, K., Chen, J., Tan, Q. and Inouye, M. (2006) Era and RbfA have overlapping function in ribosome biogenesis in Escherichia coli. *J Mol Microbiol Biotechnol*, **11**, 41-52.

Iost, I. and Dreyfus, M. (2006) DEAD-box RNA helicases in Escherichia coli. *Nucleic Acids Res*, **34**, 4189-97.

Iost, I., Dreyfus, M. and Linder, P. (1999) Ded1p, a DEAD-box Protein Required for Translation Initiation in Saccharomyces cerevisiae, Is an RNA Helicase. *J Biol Chem*, **274**, 17677-17683.

Jain, C. (2008) The E. coli RhlE RNA helicase regulates the function of related RNA helicases during ribosome assembly. *RNA*, **14**, 381-9.

Jiang, M., Datta, K., Walker, A., Strahler, J., Bagamasbad, P., Andrews, P. C. and Maddock, J. R. (2006) The Escherichia coli GTPase CgtAE Is Involved in Late Steps of Large Ribosome Assembly. *J Bacteriol*, **188**, 6757-6770.

Jiang, M., Sullivan, S. M., Walker, A. K., Strahler, J. R., Andrews, P. C. and Maddock, J. R. (2007) Identification of novel Escherichia coli ribosome-associated proteins using isobaric tags and multidimensional protein identification techniques. *J Bacteriol*, **189**, 3434-44.

Johnson, S. C., Watson, N. and Apirion, D. (1976) A lethal mutation which affects the maturation of ribosomes. *Mol Gen Genet*, **147**, 29-37.

Kaczanowska, M. and Ryden-Aulin, M. (2004) Temperature sensitivity caused by mutant release factor 1 is suppressed by mutations that affect 16S rRNA maturation. *J Bacteriol*, **186**, 3046-55.

Kaczanowska, M. and Rydén-Aulin, M. (2005) The YrdC protein--a putative ribosome maturation factor. *Biochim Biophys Acta*, **1727**, 87-96.

Kaczanowska, M. and Rydén-Aulin, M. (2007) Ribosome biogenesis and the translation process in Escherichia coli. *Microbiol Mol Biol Rev*, **71**, 477-94.

Karbstein, K. (2007) Role of GTPases in ribosome assembly. *Biopolymers*, **87**, 1-11.

Karginov, F. V., Caruthers, J. M., Hu, Y., McKay, D. B. and Uhlenbeck, O. C. (2005) YxiN is a modular protein combining a DEx(D/H) core and a specific RNA-binding domain. *J Biol Chem*, **280**, 35499-505.

Karginov, F. V. and Uhlenbeck, O. C. (2004) Interaction of Escherichia coli DbpA with 23S rRNA in different functional states of the enzyme. *Nucleic Acids Res*, **32**, 3028-3032.

Khemici, V., Toesca, I., Poljak, L., Vanzo, N. F. and Carpousis, A. J. (2004) The RNase E of Escherichia coli has at least two binding sites for DEAD-box RNA helicases: functional replacement of RhlB by RhlE. *Mol Microbiol*, **54**, 1422-30.

Kim, D. W., Kim, J., Gwack, Y., Han, J. H. and Choe, J. (1997) Mutational analysis of the hepatitis C virus RNA helicase. *J Virol*, **71**, 9400-9409.

King, T. C. and Schlessinger, D. (1983) S1 nuclease mapping analysis of ribosomal RNA processing in wild type and processing deficient Escherichia coli. *J Biol Chem*, **258**, 12034-42.

King, T. C., Sirdeshmukh, R. and Schlessinger, D. (1984) RNase III Cleavage is Obligate for Maturation but not for Function of Escherichia coli Pre-23S rRNA. *Proc Natl Acad Sci U S A*, **81**, 185-188.

Kossen, K., Karginov, F. V. and Uhlenbeck, O. C. (2002) The carboxy-terminal domain of the DExDH protein YxiN is sufficient to confer specificity for 23S rRNA. *J Mol Biol*, **324**, 625-36.

Kossen, K. and Uhlenbeck, O. C. (1999) Cloning and biochemical characterization of Bacillus subtilis YxiN, a DEAD protein specifically activated by 23S rRNA: delineation of a novel sub-family of bacterial DEAD proteins. *Nucleic Acids Research*, **27**, 3811-3820.

Krzyzosiak, W., Denman, R., Nurse, K., Hellmann, W., Boublik, M., Gehrke, C. W., Agris, P. F. and Ofengand, J. (1987) In vitro synthesis of 16S ribosomal RNA containing single base changes and assembly into a functional 30S ribosome. *Biochemistry*, **26**, 2353-2364.

Leipe, D. D., Wolf, Y. I., Koonin, E. V. and Aravind, L. (2002) Classification and evolution of P-loop GTPases and related ATPases. *J Mol Biol*, **317**, 41-72.

Li, Z. and Deutscher, M. P. (1995) The tRNA processing enzyme RNase T is essential for maturation of 5S RNA. *Proc Natl Acad Sci U S A*, **92**, 6883-6.

Li, Z., Pandit, S. and Deutscher, M. P. (1999a) Maturation of 23S ribosomal RNA requires the exoribonuclease RNase T. *RNA*, **5**, 139-46.

Li, Z., Pandit, S. and Deutscher, M. P. (1999b) RNase G (CafA protein) and RNase E are both required for the 5' maturation of 16S ribosomal RNA. *EMBO J*, **18**, 2878-85.

Lindahl, L. (1975) Intermediates and time kinetics of the in vivo assembly of Escherichia coli ribosomes. *J Mol Biol*, **92**, 15-37.

Linder, P., Lasko, P. F., Ashburner, M., Leroy, P., Nielsen, P. J., Nishi, K., Schnier, J. and Slonimski, P. P. (1989) Birth of the D-E-A-D box. *Nature*, **337**, 121-2.

Liu, M., Novotny, G. W. and Douthwaite, S. (2004) Methylation of 23S rRNA nucleotide G745 is a secondary function of the $RlmA^{I}$ methyltransferase. *RNA*, **10**, 1713-20.

Lorsch, J. R. (2002) RNA Chaperones Exist and DEAD Box Proteins Get a Life. *Cell*, **109**, 797-800.

Lövgren, J. M., Bylund, G. O., Srivastava, M. K., Lundberg, L. A., Persson, O. P., Wingsle, G. and Wikström, P. M. (2004) The PRC-barrel domain of the ribosome maturation protein RimM mediates binding to ribosomal protein S19 in the 30S ribosomal subunits. *RNA*, **10**, 1798-812.

Lowe, T. M. and Eddy, S. R. (1999) A computational screen for methylation guide snoRNAs in yeast. *Science*, **283**, 1168-71.

Maki, J. A. and Culver, G. M. (2005) Recent developments in factor-facilitated ribosome assembly. *Methods*, **36**, 313-20.

Maki, J. A., Schnobrich, D. J. and Culver, G. M. (2002) The DnaK chaperone system facilitates 30S ribosomal subunit assembly. *Mol Cell*, **10**, 129-38.

Maki, J. A., Southworth, D. R. and Culver, G. M. (2003) Demonstration of the role of the DnaK chaperone system in assembly of 30S ribosomal subunits using a purified in vitro system. *RNA*, **9**, 1418-21.

Mangiarotti, G., Apirion, D., Schlessinger, D. and Silengo, L. (1968) Biosynthetic precursors of 30S and 50S ribosomal particles in Escherichia coli. *Biochemistry*, **7**, 456-72.

Mangiarotti, G., Turco, E., Ponzetto, A. and Altruda, F. (1974) Precursor 16S RNA in active 30S ribosomes. *Nature*, **247**, 147-8.

Martin, A., Schneider, S. and Schwer, B. (2002) Prp43 Is an Essential RNA-dependent ATPase Required for Release of Lariat-Intron from the Spliceosome. *J Biol Chem*, **277**, 17743-17750.

McCarthy, B. J., Britten, R. J. and Roberts, R. B. (1962) The Synthesis of Ribosomes in E. coli: III. Synthesis of Ribosomal RNA. *Biophys J*, **2**, 57-82.

Misra, T. K. and Apirion, D. (1979) RNase E, an RNA processing enzyme from Escherichia coli. *J Biol Chem*, **254**, 11154-9.

Mizushima, S. and Nomura, M. (1970) Assembly mapping of 30S ribosomal proteins from E. coli. *Nature*, **226**, 1214.

Moazed, D., Stern, S. and Noller, H. F. (1986) Rapid chemical probing of conformation in 16 S ribosomal RNA and 30 S ribosomal subunits using primer extension. *J Mol Biol*, **187**, 399-416.

Nicol, S. M. and Fuller-Pace, F. V. (1995) The "DEAD box" protein DbpA interacts specifically with the peptidyltransferase center in 23S rRNA. *Proc Natl Acad Sci U S A*, **92**, 11681-5.

Nierhaus, K. H. (1991) The assembly of prokaryotic ribosomes. *Biochimie*, **73**, 739-755.

Nierhaus, K. H., Bordasch, K. and Homann, H. E. (1973) In vivo assembly of Escherichia coli ribosomal proteins. *J Mol Biol*, **74**, 587-97.

Nierhaus, K. H. and Dohme, F. (1974) Total reconstitution of functionally active 50S ribosomal subunits from Escherichia coli. *Proc Natl Acad Sci U S A*, **71**, 4713-7.

Nierhaus, K. H. and Montejo, V. (1973) A protein involved in the peptidyltransferase activity of Escherichia coli ribosomes. *Proc Natl Acad Sci U S A*, **70**, 1931-5.

Nikolaev, N., Silengo, L. and Schlessinger, D. (1973) Synthesis of a large precursor to ribosomal RNA in a mutant of Escherichia coli. *Proc Natl Acad Sci U S A*, **70**, 3361-5.

Nishi, K., Morel-Deville, F., Hershey, J. W. B., Leighton, T. and Schnier, J. (1988) An eIF-4A-like protein is a suppressor of an Escherichia coli mutant defective in 50S ribosomal subunit assembly. *Nature*, **336**, 496-498.

Nishimura, M., Yoshida, T., Shirouzu, M., Terada, T., Kuramitsu, S., Yokoyama, S., Ohkubo, T. and Kobayashi, Y. (2004) Solution structure of ribosomal protein L16 from Thermus thermophilus HB8. *J Mol Biol*, **344**, 1369-83.

Noble, S. M. and Guthrie, C. (1996) Identification of novel genes required for yeast pre-mRNA splicing by means of cold-sensitive mutations. *Genetics*, **143**, 67-80.

Ofengand, J. and del Campo, M. 29 December 2004, posting date. Chapter 4.6.1, Modified nucleosides of *Escherichia coli* ribosomal RNA. *In* G. R. Björk (ed.), EcoSal—*Escherichia coli* and *Salmonella*: cellular and molecuclar biology. ASM Press, Washington, DC. http://www.ecosal.org.

Oh, J. Y. and Kim, J. (1999) ATP hydrolysis activity of the DEAD box protein Rok1p is required for in vivo ROK1 function. *Nucleic Acids Res.*, **27**, 2753-2759.

Osawa, S., Otaka, E., Itoh, T. and Fukui, T. (1969) Biosynthesis of 50 s ribosomal subunit in Escherichia coli. *J Mol Biol*, **40**, 321-351.

Pan, J., Thirumalai, D. and Woodson, S. A. (1997) Folding of RNA involves parallel pathways. *J Mol Biol*, **273**, 7-13.

Pardo, D. and Rosset, R. (1977) A new ribosomal mutation which affects the two ribosomal subunits in Escherichia coli. *Mol Gen Genet*, **153**, 199-204.

Pause, A., Methot, N., Svitkin, Y., Merrick, W. C. and Sonenberg, N. (1994) Dominant negative mutants of mammalian translation initiation factor eIF-4A define a critical role for eIF-4F in cap-dependent and cap-independent initiation of translation. *EMBO J*, **13**, 1205-15.

Pause, A. and Sonenberg, N. (1992) Mutational analysis of a DEAD box RNA helicase: the mammalian translation initiation factor eIF-4A. *EMBO J*, **11**, 2643-2654.

Pichon, J., Marvaldi, J. and Marchis-Mouren, G. (1975) The in vivo order of protein addition in the course of Escherichia coli 30 S and 50 S subunit biogenesis. *J Mol Biol*, **96**, 125-130.

Polach, K. J. and Uhlenbeck, O. C. (2002) Cooperative Binding of ATP and RNA Substrates to the DEAD/H Protein DbpA. *Biochemistry*, **41**, 3693-3702.

Powers, T., Daubresse, G. and Noller, H. F. (1993) Dynamics of in vitro assembly of 16 S rRNA into 30 S ribosomal subunits. *J Mol Biol*, **232**, 362-74.

Prud'homme-Genereux, A., Beran, R. K., Iost, I., Ramey, C. S., Mackie, G. A. and Simons, R. W. (2004) Physical and functional interactions among RNase E, polynucleotide phosphorylase and the cold-shock protein, CsdA: evidence for a 'cold shock degradosome'. *Mol Microbiol*, **54**, 1409-1421.

Pugh, G. E., Nicol, S. M. and Fuller-Pace, F. V. (1999) Interaction of the Escherichia coli DEAD box protein DbpA with 23 S ribosomal RNA. *J Mol Biol*, **292**, 771-8.

Raychaudhuri, S., Conrad, J., Hall, B. G. and Ofengand, J. (1998) A pseudouridine synthase required for the formation of two universally conserved pseudouridines in ribosomal RNA is essential for normal growth of Escherichia coli. *RNA*, **4**, 1407-1417.

Rocak, S. and Linder, P. (2004) DEAD-box proteins: the driving forces behind RNA metabolism. *Nat Rev Mol Cell Biol*, **5**, 232-41.

Rohl, R. and Nierhaus, K. H. (1982) Assembly map of the large subunit (50S) of Escherichia coli ribosomes. *Proc Natl Acad Sci U S A*, **79**, 729-33.

Roth, H. E. and Nierhaus, K. H. (1980) Assembly map of the 50-S subunit from Escherichia coli ribosomes, covering the proteins present in the first reconstitution intermediate particle. *Eur J Biochem*, **103**, 95-8.

Roy, M. K., Singh, B., Ray, B. K. and Apirion, D. (1983) Maturation of 5-S rRNA: ribonuclease E cleavages and their dependence on precursor sequences. *Eur J Biochem*, **131**, 119-27.

Sato, A., Kobayashi, G., Hayashi, H., Yoshida, H., Wada, A., Maeda, M., Hiraga, S., Takeyasu, K. and Wada, C. (2005) The GTP binding protein Obg homolog ObgE is involved in ribosome maturation. *Genes Cells*, **10**, 393-408.

Schaefer, L., Uicker, W. C., Wicker-Planquart, C., Foucher, A.-E., Jault, J.-M. and Britton, R. A. (2006) Multiple GTPases Participate in the Assembly of the Large Ribosomal Subunit in Bacillus subtilis. *J Bacteriol*, **188**, 8252-8258.

Schluenzen, F., Tocilj, A., Zarivach, R., Harms, J., Gluehmann, M., Janell, D., Bashan, A., Bartels, H., Agmon, I., Franceschi, F. and Yonath, A. (2000) Structure of Functionally Activated Small Ribosomal Subunit at 3.3 A Resolution. *Cell*, **102**, 615-623.

Schlünzen, F., Zarivach, R., Harms, J., Bashan, A., Tocilj, A., Albrecht, R., Yonath, A. and Franceschi, F. (2001) Structural basis for the interaction of antibiotics with the peptidyl transferase centre in eubacteria. *Nature*, **413**, 814-821.

Schmid, S. R. and Linder, P. (1991) Translation initiation factor 4A from Saccharomyces cerevisiae: analysis of residues conserved in the D-E-A-D family of RNA helicases. *Mol Cell Biol*, **11**, 3463-3471.

Schneider, S., Hotz, H.-R. and Schwer, B. (2002) Characterization of Dominant-negative Mutants of the DEAH-box Splicing Factors Prp22 and Prp16. *J Biol Chem*, **277**, 15452-15458.

Schuwirth, B. S., Borovinskaya, M. A., Hau, C. W., Zhang, W., Vila-Sanjurjo, A., Holton, J. M. and Cate, J. H. D. (2005) Structures of the Bacterial Ribosome at 3.5 A Resolution. *Science*, **310**, 827-834.

Schwer, B. and Meszaros, T. (2000) RNA helicase dynamics in pre-mRNA splicing. *EMBO J*, **19**, 6582-6591.

Semrad, K. and Green, R. (2002) Osmolytes stimulate the reconstitution of functional 50S ribosomes from in vitro transcripts of Escherichia coli 23S rRNA. *RNA*, **8**, 401-11.

Sengoku, T., Nureki, O., Nakamura, A., Kobayashi, S. and Yokoyama, S. (2006) Structural Basis for RNA Unwinding by the DEAD-Box Protein Drosophila Vasa. *Cell*, **125**, 287-300.

Sergiev, P. V., Serebryakova, M. V., Bogdanov, A. A. and Dontsova, O. A. (2008) The ybiN Gene of Escherichia coli Encodes Adenine-N6 Methyltransferase Specific for Modification of A1618 of 23 S Ribosomal RNA, a Methylated Residue Located Close to the Ribosomal Exit Tunnel. *Journal of Molecular Biology*, **375**, 291-300.

Sharpe Elles, L. M. and Uhlenbeck, O. C. (2008) Mutation of the arginine finger in the active site of Escherichia coli DbpA abolishes ATPase and helicase activity and confers a dominant slow growth phenotype. *Nucleic Acids Res*, **36**, 41-50.

Shi, H., Cordin, O., Minder, C. M., Linder, P. and Xu, R. M. (2004) Crystal structure of the human ATP-dependent splicing and export factor UAP56. *Proc Natl Acad Sci U S A*, **101**, 17628-33.

Sieber, G. and Nierhaus, K. H. (1978) Kinetic and thermodynamic parameters of the assembly in vitro of the large subunit from Escherichia coli ribosomes. *Biochemistry*, **17**, 3505-11.

Silverman, E., Edwalds-Gilbert, G. and Lin, R.-J. (2003) DExD/H-box proteins and their partners: helping RNA helicases unwind. *Gene*, **312**, 1-16.

Singh, B. and Apirion, D. (1982) Primary and secondary structure in a precursor of 5 S rRNA. *Biochim Biophys Acta*, **698**, 252-9.

Sirdeshmukh, R. and Schlessinger, D. (1985a) Ordered processing of Escherichia coli 23S rRNA in vitro. *Nucleic Acids Res*, **13**, 5041-54.

Sirdeshmukh, R. and Schlessinger, D. (1985b) Why is processing of 23 S ribosomal RNA in Escherichia coli not obligate for its function? *J Mol Biol*, **186**, 669-72.

Smith, J. E., Cooperman, B. S. and Mitchell, P. (1992) Methylation sites in Escherichia coli ribosomal RNA: localization and identification of four new sites of methylation in 23S rRNA. *Biochemistry*, **31**, 10825-34.

Spierer, P., Wang, C. C., Marsh, T. L. and Zimmermann, R. A. (1979) Cooperative interactions among protein and RNA components of the 50S ribosomal subunit of Escherichia coli. *Nucleic Acids Res*, **6**, 1669-82.

Spierer, P. and Zimmermann, R. A. (1976) RNA-protein interactions in the ribosome. Binding of proteins L1, L3, L6, L13 and L23 to specific fragments of the 23S RNA. *FEBS Lett*, **68**, 71-5.

Spillmann, S., Dohme, F. and Nierhaus, K. H. (1977) Assembly in vitro of the 50 S subunit from Escherichia coli ribosomes: proteins essential for the first heat-dependent conformational change. *J Mol Biol*, **115**, 513-23.

Srivastava, A. K. and Schlessinger, D. (1988) Coregulation of processing and translation: mature 5' termini of Escherichia coli 23S ribosomal RNA form in polysomes. *Proc Natl Acad Sci U S A*, **85**, 7144-8.

Srivastava, A. K. and Schlessinger, D. (1990) Mechanism and Regulation of Bacterial Ribosomal RNA Processing. *Ann Rev Microbio*, **44**, 105-129.

Story, R. M., Li, H. and Abelson, J. N. (2001) Crystal structure of a DEAD box protein from the hyperthermophile Methanococcus jannaschii. *Proc Natl Acad Sci U S A*, **98**, 1465-70.

Story, R. M. and Steitz, T. A. (1992) Structure of the recA protein-ADP complex. *Nature*, **355**, 374-6.

Studier, F. W. (1991) Use of bacteriophage T7 lysozyme to improve an inducible T7 expression system. *J Mol Biol*, **219**, 37-44.

Studier, F. W. and Moffatt, B. A. (1986) Use of bacteriophage T7 RNA polymerase to direct selective high-level expression of cloned genes. *J Mol Biol*, **189**, 113-130.

Svitkin, Y. V., Herdy, B., Costa-Mattioli, M., Gingras, A. C., Raught, B. and Sonenberg, N. (2005) Eukaryotic translation initiation factor 4E availability controls the switch between cap-dependent and internal ribosomal entry site-mediated translation. *Mol Cell Biol*, **25**, 10556-65.

Talavera, M. A., Matthews, E. E., Eliason, W. K., Sagi, I., Wang, J., Henn, A. and De La Cruz, E. M. (2006) Hydrodynamic Characterization of the DEAD-box RNA Helicase DbpA. *J Mol Biol*, **355**, 697-707.

Talkington, M. W., Siuzdak, G. and Williamson, J. R. (2005) An assembly landscape for the 30S ribosomal subunit. *Nature*, **438**, 628-32.

Tan, J., Jakob, U. and Bardwell, J. C. A. (2002) Overexpression of Two Different GTPases Rescues a Null Mutation in a Heat-Induced rRNA Methyltransferase. *J Bacteriol*, **184**, 2692-2698.

Theissen, B., Karow, A. R., Kohler, J., Gubaev, A. and Klostermeier, D. (2008) Cooperative binding of ATP and RNA induces a closed conformation in a DEAD box RNA helicase. *Proc Natl Acad Sci U S A*, **105**, 548-53.

Toh, S.-M., Xiong, L., Bae, T. and Mankin, A. S. (2008) The methyltransferase YfgB/RlmN is responsible for modification of adenosine 2503 in 23S rRNA. *RNA*, **14**, 98-106.

Toone, W. M., Rudd, K. E. and Friesen, J. D. (1991) deaD, a new Escherichia coli gene encoding a presumed ATP-dependent RNA helicase, can suppress a mutation in rpsB, the gene encoding ribosomal protein S2. *J Bacteriol*, **173**, 3291-3302.

Traub, P. and Nomura, M. (1968) Reconstitution of functionally active 30S ribosomal particles from RNA and proteins. *Proc Natl Acad Sci U S A*, **59**, 777-84.

Traub, P. and Nomura, M. (1969) Mechanism of assembly of 30 s ribosomes studied in vitro. *J Mol Biol*, **40**, 391-404.

Tscherne, J. S., Nurse, K., Popienick, P. and Ofengand, J. (1999) Purification, Cloning, and Characterization of the 16 S RNA m2G1207 Methyltransferase from Escherichia coli. *J Biol Chem*, **274**, 924-929.

Tsu, C. A., Kossen, K. and Uhlenbeck, O. C. (2001) The Escherichia coli DEAD protein DbpA recognizes a small RNA hairpin in 23S rRNA. *RNA*, **7**, 702-709.

Tsu, C. A. and Uhlenbeck, O. C. (1998) Kinetic Analysis of the RNA-Dependent Adenosinetriphosphatase Activity of DbpA, an Escherichia coli DEAD Protein Specific for 23S Ribosomal RNA. *Biochemistry*, **37**, 16989-16996.

Vaidyanathan, P. P., Deutscher, M. P. and Malhotra, A. (2007) RluD, a highly conserved pseudouridine synthase, modifies 50S subunits more specifically and efficiently than free 23S rRNA. *RNA*, **13**, 1868-1876.

Wang, S., Hu, Y., Overgaard, M. T., Karginov, F. V., Uhlenbeck, O. C. and McKay, D. B. (2006) The domain of the Bacillus subtilis DEAD-box helicase YxiN that is responsible for specific binding of 23S rRNA has an RNA recognition motif fold. *RNA*, **12**, 959-967.

Weeks, K. M. (1997) Protein-facilitated RNA folding. *Curr Opin Struct Biol*, **7**, 336-42.

Williamson, J. R. (2003) After the ribosome structures: How are the subunits assembled? *RNA*, **9**, 165-167.

Williamson, J. R. (2005) Assembly of the 30S ribosomal subunit. *Q Rev Biophys*, **38**, 397-403.

Wilson, D. N. and Nierhaus, K. H. (2007) The Weird and Wonderful World of Bacterial Ribosome Regulation. *Crit Rev Biochem Mol Biol*, **42**, 187 - 219.

Wimberly, B. T., Brodersen, D. E., Clemons, W. M., Morgan-Warren, R. J., Carter, A. P., Vonrhein, C., Hartsch, T. and Ramakrishnan, V. (2000) Structure of the 30S ribosomal subunit. *Nature*, **407**, 327-339.

Wireman, J. W. and Sypherd, P. S. (1974) Properties of 30S ribosomal particles reconstituted from precursor 16S ribonucleic acid. *Biochemistry*, **13**, 1215-21.

Woodson, S. A. (2000) Recent insights on RNA folding mechanisms from catalytic RNA. *Cell Mol Life Sci*, **57**, 796-808.

Wrzesinski, J., Nurse, K., Bakin, A., Lane, B. G. and Ofengand, J. (1995) A dual-specificity pseudouridine synthase: an Escherichia coli synthase purified and cloned on the basis of its specificity for Ψ746 in 23S RNA is also specific for Ψ32 in tRNA(phe). *RNA*, **1**, 437-448.

Yang, Q., Del Campo, M., Lambowitz, A. M. and Jankowsky, E. (2007) DEAD-Box Proteins Unwind Duplexes by Local Strand Separation. *Mol Cell*, **28**, 253-263.

Yao, N., Hesson, T., Cable, M., Hong, Z., Kwong, A. D., Le, H. V. and Weber, P. C. (1997) Structure of the hepatitis C virus RNA helicase domain. *Nat Struct Biol*, **4**, 463-7.

Young, R. A. and Steitz, J. A. (1978) Complementary sequences 1700 nucleotides apart form a ribonuclease III cleavage site in Escherichia coli ribosomal precursor RNA. *Proc Natl Acad Sci U S A*, **75**, 3593-7.

Yusupov, M. M., Yusupova, G. Z., Baucom, A., Lieberman, K., Earnest, T. N., Cate, J. H. D. and Noller, H. F. (2001) Crystal Structure of the Ribosome at 5.5 A Resolution. *Science*, **292**, 883-896.

Zhang, M. and Green, M. R. (2001) Identification and characterization of yUAP/Sub2p, a yeast homolog of the essential human pre-mRNA splicing factor hUAP56. *Genes Dev*, **15**, 30-35.

Zhang, Y., Buchholz, F., Muyrers, J. P. P. and Stewart, A. F. (1998) A new logic for DNA engineering using recombination in Escherichia coli. *Nat Genet*, **20**, 123-128.

Zhao, R., Shen, J., Green, M. R., MacMorris, M. and Blumenthal, T. (2004) Crystal structure of UAP56, a DExD/H-box protein involved in pre-mRNA splicing and mRNA export. *Structure*, **12**, 1373-81.